SPECIAL PUBLICATION SJ2007-SP7

CHARACTERIZATION OF SANDHILL LAKE SOILS: IN SUPPORT OF ST. JOHNS RIVER WATER MANAGEMENT DISTRICT'S MINIMUM FLOWS AND LEVELS PROGRAM

CHARACTERIZATION OF SANDHILL LAKE SOILS:
In Support of St. Johns River Water Management District's Minimum Flows and Levels Program

Contract No. SI32012

FINAL REPORT

Peter Nkedi-Kizza[1]

AND

Travis C. Richardson[1,2]

[1]Soil and Water Science Department
University of Florida
2169 McCarty Hall, PO Box 110290 Gainesville, FL 32611-0290
(352) 392-1952/236

and

[2]St. Johns River Water Management District
PO Box 1429 Palatka, FL 32178-1429

July 18, 2007

EXECUTIVE SUMMARY

Sandhill lakes often exhibit ephemeral wetland plant communities that shift in location and species abundance according to widely fluctuating water levels (SJRWMD 2006a). Consequently, short-lived herbaceous wetland species associated with sandhill lakes can be poor indicators of long-term hydrology and may be insufficient to support the determination of Minimum Flows and Levels (MFLs). The widely fluctuating water levels and nutrient poor conditions inhibit the formation of organic soils, which also results in difficulty for the determination of MFLs. Because of the inadequacy of long-lived wetland community hydrologic indicators at sandhill lakes, unique soil morphologies were identified at specific long-term lake stage statistics at numerous sandhill lakes (SJRWMD 2006a). These unique soil morphologies, termed lake stage indicators (LSIs), are intended to support the determination of MFLs at sandhill lakes.

MFLs must consider existing changes and structural alterations to watersheds, surface waters, and aquifers [Section 373.042(1)(a) and (b) *Florida Statutes (*F.S.)] and non-consumptive uses, including navigation, recreation, fish and wildlife habitat, and other natural resource values [Section 62-40.473, Florida Administrative Code (F.A.C.)]. The LSIs are indicative of long-term hydrology and thus are applicable in the determination of MFLs. A threshold offset establishing the maximum allowable change in hydrology from the LSIs without causing unacceptable harm was needed.

Jones Edmunds (2006) developed a threshold concept allowing for an elevation offset from the LSIs. The basis of the thresholds associated with LSIs is to protect the ecological functions and values associated with high and low water levels. High and low water level thresholds can allow for a small change from historic hydrology, while protecting the ecological structure, functions, and values associated with sandhill lakes. Jones Edmunds (2006) investigated literature regarding the capillary fringe (CF) in soils as one potential threshold for maintaining wetlands vegetation and soils at sandhill lakes while allowing for some change from historic hydrology, but observed highly variable results in the literature. Jones Edmunds (2006) also reviewed literature regarding soil oxidation-reduction potential (ORP). Based on the review Jones Edmunds (2006) concluded that anaerobic conditions resulting from saturation or inundation are necessary to maintain wetland vegetation, eliminate upland vegetation species that encroach into the lake bed during low water, and maintain organic materials that accumulate in the soil.

The threshold presented by Jones Edmunds (2006) states that, by maintaining anaerobic conditions near the soil surface at the LSIs, at the same frequency and duration as expected due to surface water saturation or inundation should protect the ecological functions and values associated with high and low water levels. This threshold would allow for a reduction in long-term hydrology equal to the height of anaerobic conditions (HAC) above a water table in soils associated with LSIs. Based on Jones Edmunds' conclusions, St. Johns River Water Management District (SJRWMD) funded this study to investigate the physical properties of sandhill lake soils to support the determination of MFLs at sandhill lakes.

This study revealed that the CF was measurable and typically extended 3.3 – 11.8 cm above the water table. Anaerobic conditions persisted through and slightly above the upper extent of the CF (5.4 – 16.5 cm). Multiple regressions were developed to estimate the capillary fringe height (CFH) and HAC from easily determined physical soil characteristics (e.g., particle-size distribution, bulk density, particle density, etc.), as well as soil characteristics that integrate soil properties (e.g., air entry values, AEVs).

The CFH was best predicted by the physical soil characteristics: percent sand, silt, and clay (adjusted R^2=0.6943). However, due to extreme multicollinearity (the condition when one or more variables are linear functions of other variables, StatSoft, Inc. 2005) this model was not recommended for use. A more robust model to estimate the CFH incorporates the physical soil characteristics: percent clay (cl) and percent very coarse (vc), coarse (c), fine (fi), and very fine (vf) sand fractions (Equation ES1, adjusted R^2=0.6279).

$$\text{Predicted CFH (cm)} = 2.60(cl) + 9.22(vc) - 1.90(c) - 0.37(fi) - 0.60(vf) + 28.15 \quad \text{(ES1)}$$

The HAC was best predicted by the physical soil characteristics: percent clay and percent very coarse, coarse, fine, and very fine sand fractions (adjusted R^2=0.4601). Because of the relatively low adjusted R^2, additional regression models were investigated to provide a better estimate of the HAC. The best predictor of the HAC was the CFH (Equation ES2, adjusted R^2=0.6869).

$$\text{HAC (cm)} = 1.17(\text{CFH}) + 2.06 \quad \text{(ES2)}$$

The CFH is a measure of the near saturated zone above the water table and should provide a better estimate of the HAC over a larger range of sandhill lake soils.

The air entry values (AEVs), based on the Brooks and Corey equation (Brooks and Corey 1964) were similar in magnitude to the CFHs and the HACs but were too variable to result in a strong relationship with either parameter. Poor fit between the AEVs and the CFHs or HACs was likely the result of the different methods of determination (i.e., drainage of a soil for AEV determinations and wetting a soil for determination of CFHs and HACs). In addition, the AEVs were estimated for 0-18 cm depth by averaging individual 3-cm short core measurements across the 0-18 cm depth, which may not adequately represent the pore connectivity in an intact 18 cm soil core. The narrow data range also contributes to the poor fit of these parameters.

The CFH and HAC provide the corner stone for establishing MFLs at sandhill lakes with LSIs. Jones Edmunds (2006) recommended a static threshold based on preliminary CFH and HAC data collected in the study reported herein, which may not be applicable to all sandhill lakes. Analysis of the physical soil characteristics at Lake Brooklyn, Clay County, and Swan Lake and Two Mile Pond in Putnam County, shows significant differences in particle-size classes ($p<0.0001$) for all classes except coarse sand. Because the CFHs and HACs are strongly related to the particle-size distribution, threshold offsets should be developed at individual sandhill lakes based on the regression equations developed herein.

The regression equations to predict the CFH and HAC are based on small data sets because of the time and level of effort required to determine the CFH by wetting soil columns. These regression equations should be revised as additional data are collected. Data collection can be expedited by using only one water table depth that fully covers the range of the CF zone and not excessively air drying the soil cores (resulting in long wetting times) prior to rewetting them.

ACKNOWLEDGEMENTS

We would like to thank Drs. Jim Jawitz, Mary Collins, and Robert Epting and Wade Hurt for their guidance and invaluable input to this project. We sincerely appreciate the assistance of Dr. Bob Epting and Jodi Slater with statistical analyses. We would also like to thank Kafui Awuma, Tripp Tibbetts, Gabriel Kasozi, Kamal Mahmoud, John Wasswa, Jane Mace, and Sophie Namugenyi for assistance with field sampling and laboratory analyses. Finally, we would like to thank St. Johns River Water Management District for funding this research.

TABLE OF CONTENTS

LIST OF TABLES

LIST OF FIGURES

ABBREVIATIONS

AEV	Air Entry Value
BRK	Lake Brooklyn
CF	Capillary Fringe
CFH	Capillary Fringe Height
DI	Deionized (water)
DNAPL	Dense Non-aqueous Phase Liquids
DNR	Department of Natural Resources
Eh	Electric Potential
F.A.C.	Florida Administrative Code
FH	Frequent High
FL	Frequent Low
FNAI	Florida Natural Areas Inventory
F.S.	Florida Statutes
HAC	Height of anaerobic conditions
Ksat	Saturated Hydraulic Conductivity
LNAPL	Light Non-aqueous Phase Liquids
LOI	Weight Loss on Ignition
LSIs	Lake Stage Indicators
MFLs	Minimum Flows and Levels
NRCS	Natural Resource Conservation Commission
OC	Organic Carbon
OM	Organic Matter
ORP	Oxidation-Reduction Potential
PC	Principal Component
PCA	Principle Components Analysis
SCS	Soil Conservation Service
SJRWMD	St. Johns River Water Management District
SMP	Sodium Metaphosphate
SMRC	Soil Moisture Release Curve
SW	Swan Lake
TCE	Trichloroethane
TM	Two Mile Pond
USDA	U.S. Department of Agriculture
WMDs	Water Management Districts

INTRODUCTION

Florida has experienced tremendous population growth over the past decades, resulting in an increased demand for water and other resources. This increased water demand has caused impacts to natural ecosystems and helped shape the missions of Florida's five water management districts (Figure 1). The original goal of water management in Florida was to provide flood control (Purdum et al. 1998). Implementation of the Water Resources Act of 1972 (Chapter 373, Florida Statutes [F.S.]) resulted in formation of the five water management districts (WMDs) and the Department of Natural Resources (now the Department of Environmental Protection). Additionally, water management goals were altered to include broader objectives, such as water supply planning, resource management, environmental restoration, and conservation (Purdum et al. 1998). Providing water sources for a growing population, while protecting natural resources is a challenge. This goal is, in part, achieved through the development and implementation of minimum flows and levels (MFLs). The MFLs designate an environmentally protective hydrologic regime and identify water levels and/or flows above which water is available for consumptive use.

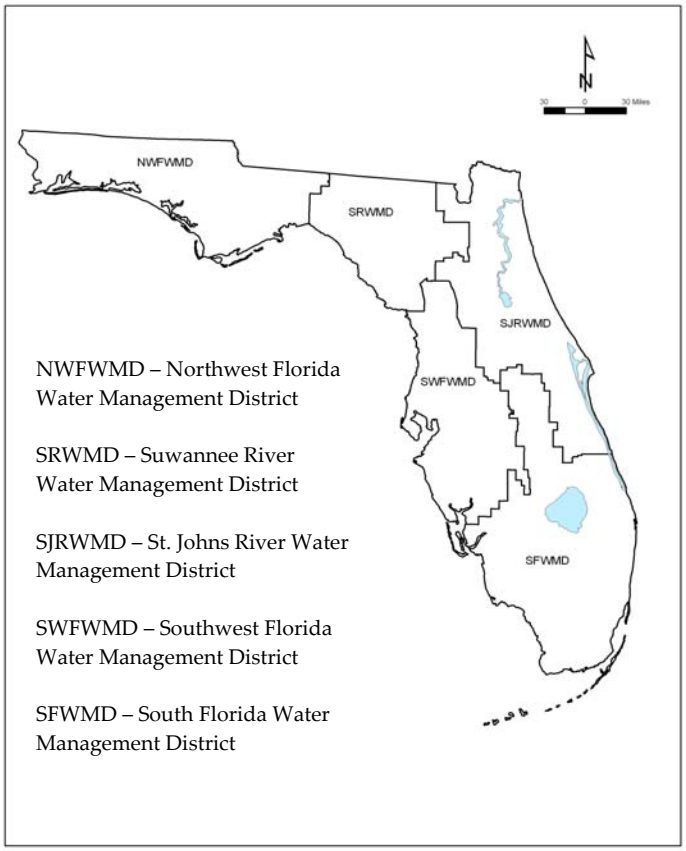

Figure 1. Florida's five water management districts

The WMDs establish MFLs for lakes, streams and rivers, wetlands, springs, and aquifers, based on the requirements of Section 373.042 and 373.0421, F.S. The St. Johns River Water Management

District's (SJRWMD) MFLs Program is also subject to the provisions of Chapter 40C-8, Florida Administrative Code (F.A.C.) and provides technical support to the regional water supply planning process (Section 373.0361, F.S.) and the consumptive use-permitting programs (Chapter 40C-2, F.A.C.). Based on the provisions of Section 40C-8.011 (3), F.A.C., "the Governing Board shall use the best information and methods available to establish limits which prevent significant harm to the water resources or ecology." Significant harm, or the environmental effects resulting from the reduction of long-term water levels and/or flows below MFLs, is prohibited by Section 373.042(1a)(1b), F.S. Additionally, MFLs should be expressed as multiple flows or levels defining a minimum hydrologic regime, to the extent practical and necessary to establish the limit beyond which further withdrawals would be significantly harmful to the water resources or the ecology of the area (Section 62-40.473(2), F.A.C.).

Each WMD has developed a methodology to determine MFLs. The MFLs established by SJRWMD's MFLs Program are based on ecological data and implemented with water budget models that account for cumulative water withdrawals. The SJRWMD's MFLs are primarily based on the protection of vegetation communities and organic soils, where present, and are supported with literature regarding the hydrology and functions associated with specific vegetation communities and soil characteristics (SJRWMD 2006b). The SJRWMD's typical approach for establishing MFLs is effective for most systems; however, the development of criteria for determining minimum levels for sandhill lakes has been difficult.

Sandhill lakes are typically sinkhole features in sandy landscapes that contain deep sandy soils. Florida Natural Areas Inventory (FNAI) and Florida Department of Natural Resources (DNR) provide a thorough description of sandhill lakes:

> Sandhill lakes are shallow, rounded solution depressions that occur in sandy upland communities. The open water tends to be permanent, but levels may fluctuate dramatically with complete drying during extreme drought. Typically, these lakes are lentic with no significant surface inflows or outflows. The substrate is primarily sand with organic deposits that may increase with depth. In general, the water is clear, circumneutral to slightly acidic, and moderately soft, with variable mineral content. These lakes are seldom eutrophic unless artificially fertilized through human activity (FNAI and DNR 1990).

Sandhill lakes have ephemeral wetland vegetation that changes location because of widely fluctuating water levels (SJRWMD 2006a). Consequently, the emergent communities adjacent to sandhill lakes can be poor indicators of long-term hydrology and may be insufficient to support the determination of MFLs. The widely fluctuating water levels and nutrient poor conditions inhibit the formation of organic soils, which also results in difficulty for the determination of minimum levels. Because of the inconsistency of hydrologic indicators at sandhill lakes, Ellis (2002) recommended that unique soil morphologies be identified, tied to lake stage, and termed lake stage indicators (LSIs) to support the determination of minimum levels at sandhill lakes.

Morphological features develop in soils as a result of oxidation-reduction chemical reactions that occur when soils become anaerobic and chemically reduced (Vepraskas 2001). These soil morphologies that develop due to anaerobic processes can persist through both wet and dry periods (Hurt et al. 2000). Soils subject to frequent inundation and dewatering were investigated at two sandhill lakes in northeast Florida by Ellis (2002), who identified unique soil morphologies within the lakes' fluctuation range. Following this investigation SJRWMD, in cooperation with U.S. Department of Agriculture, Natural Resources Conservation Service (USDA, NRCS) and Jones, Edmunds, and Associates (Jones Edmunds), investigated soils within the stage fluctuation ranges of 27 sandhill lakes in northeast Florida, resulting in the identification of multiple unique soil morphologies (SJRWMD 2006a). Several of the unique soil morphologies were determined to be reliable indicators of 20% and 80% stage exceedance. In addition, specific site selection criteria were identified by SJRWMD (2006a) to facilitate identification of LSIs at sandhill lakes.

The LSIs identified by Ellis (2002) and SJRWMD (2006a) indicate long-term high and low lake stages (20 and 80% stage exceedence, respectively). Existing changes and structural alterations to watersheds, surface waters, and aquifers (Section 373.042(1)(a) and (b) F.S.) and non-consumptive uses, including navigation, recreation, fish and wildlife habitat, and other natural resource values (Section 62-40.473, F.A.C.) must be considered in determining MFLs. Therefore, LSIs cannot be directly applied as the elevation component of a MFLs determination. A threshold establishing the maximum allowable change from the LSIs without causing unacceptable impacts to the ecological functions and values was needed.

Jones Edmunds (2006) developed a threshold concept that allows for an offset from the LSIs. The basis of the thresholds offset associated with

LSIs is to protect the ecological functions and values associated with high and low water levels. High water levels are needed for biologically relevant durations and frequencies to maximize aquatic habitat, maintain shoreline communities, provide connectivity of surface waters, and allow redistribution of fauna/flora that may have been extirpated during drought conditions (CH2M Hill 2003). Low water levels are ecologically necessary to facilitate decomposition of accumulated organic materials, which in turn releases nutrient for plant growth, enable germination from the seedbank, and possibly trigger the reproductive cycles of some species (CH2M Hill 2003). The magnitude, duration, and frequency of low water events should not be exacerbated by anthropogenic activities to the extent that organic soil materials completely oxidize and alter the nutrient and energy cycles within the system. High and low water threshold offsets may allow for some change from historic hydrology while protecting the ecological functions and values associated with both, high and low levels.

Jones Edmunds (2006) investigated literature regarding the capillary fringe (CF) in soils as one potential threshold for maintaining wetlands vegetation and soils at sandhill lakes while allowing for some change from historic hydrology. The CF would maintain near-saturated conditions at the soil surface for approximately the same duration and frequency as historically observed for surface water. Based on results in the literature, Jones Edmunds (2006) could not conclude with a high degree of certainty that saturation from the CF would protect the functions and values associated with sandhill lakes.

Jones Edmunds (2006) also reviewed literature regarding oxidation-reduction potential (ORP) and concluded that anaerobic conditions are necessary to eliminate upland vegetation species that encroach into the lakebed during low water, and maintain organic materials that accumulate in the soil. A direct link between the CFH and ORP could not be made based on review of the literature, therefore, Jones Edmunds (2006) suggested that, by maintaining anaerobic conditions, rather than saturation from the CF, near the soil surface at the LSIs, for the same frequency and duration as expected due to surface water flooding, should protect the ecological functions and values associated with high and low water levels. Based on Jones Edmunds' conclusions, SJRWMD funded this study to investigate the physical properties of sandhill lake soils to support the determination of MFLs at sandhill lakes.

RESEARCH GOALS AND OBJECTIVES

The first goal of this research was to quantify the offsets from LSIs of high and low water levels at sandhill lakes based on the thresholds developed by Jones Edmunds (2006). The second goal of this research was to develop predictive models to estimate the offsets based on easily measured soil characteristics. To accomplish these goals, four research objectives were established:

1. Determine if a capillary fringe (CF) exists in soils where high and low LSIs have been identified

2. Determine if anaerobic conditions develop within the CF

3. Develop a model to estimate the capillary fringe height (CFH) based on the physical properties of soils where high and low LSIs have been identified

4. Develop a model to estimate the height of anaerobic conditions (HAC) above a fixed water table in soils where high and low LSIs have been identified.

LITERATURE REVIEW

CAPILLARY FRINGE (CF)

The CF is generally considered to be the near-saturated zone above the water table that is held under a slight tension. The CF is the interface between the free water table and the unsaturated zone above, and because of the high moisture content, mix of aerobic and anaerobic conditions, and available carbon near the soil surface this is a biologically and chemically reactive region (Ronen et al. 2000). The presence of large quantities of water and air makes the CF a suitable environment for biodegradation processes as well as other important chemical reactions (Affek et al. 1998, Sinke et al. 1998). In addition to movement and degradation of solutes and pollutants, the CF is important for the success of created wetlands, to wetlands maintenance, for heat transport in soils, for the determination of a soil's mechanical properties, and in the determination of soil water storage (Berkowitz et al. 2004, Boufadel et al. 1999, Gerla 1992, Hunt et al. 1999, Nachabe et al. 2004, Price et al. 2002, Tokunaga et al. 2004).

The CF is created by adhesion and cohesion of water molecules and the CFH above a free water table is directly affected by the radius of the soil pores. Richards (1928) observed the rise of water in cylindrical capillary tubes and derived the capillary function (Equation 1), where, h is the height of capillary rise (cm), T is the surface tension of the liquid (dyne/cm), α is the contact angle between the liquid and the solid surface, ρ is the density of the liquid (g/cm^3), r = tube radius (cm), and g = acceleration due to gravity (cm/s^2).

$$h = 2T\cos\alpha / \rho r g \quad (1)$$

Richards (1928) simplified Equation 1 by assuming pure water with a density of 1 and a contact angle of 0°. Equation 1 can further be simplified with a known or assumed constant for the surface tension of the liquid and the acceleration due to gravity. If water at 25°C is the liquid of interest, then the capillary function can be reduced to Equation 2.

$$h = 0.15/r \quad (2)$$

Although the definition of the CF is generally accepted, review of the literature shows that water content within the CF is not constant among scientific studies (Slaymaker 2000, Williams et al. 2002). Numerous studies have verified that there is sufficient water in the CF to support

hydrophytic vegetation (Duever 1988, Rosenberry and Winter 1997, Hunt et al. 1999, Heuperman 1999, Veneklaas and Poot 2003, Kacimov 2004, Kim and Eltahir 2004). In addition to supporting wetland vegetation, Stephens (1984) reported that by maintaining a water table 10 cm below an organic soil in the Everglades, no organic soil was lost. This suggests that the CF was saturated, such that anaerobic conditions dominated the zone above the water table and inhibited soil oxidation. Morris et al. (2004) provided further support for Stephens (1984) by reporting a CF of 16 cm in a south Florida muck soil that was sufficiently saturated to prevent any loss of organic matter.

Studies of solute transport have shown varied results with respect to the degree of saturation in the CF. In a ground water contamination study Miller et al. (2004) concluded that the CF had to be saturated to prevent diffusion of light non-aqueous phase liquids (LNAPL). Simmons et al. (2002), reported that the observed flow of dense non-aqueous phase liquids (DNAPL) in the CF required full saturation. In a dye study by Silliman et al. (2002), saturated flow was observed within the CF of homogenous sand.

Conversely, a recent study of hysteresis in soil pore water suggested that the CF may not be saturated (Lehmann et al. 1998). Jellali et al. (2003) and Klenk and Grathwohl (2002) reported that diffusion of trichloroethane (TCE) through the CF in entrained air bubbles suggested that the CF was not fully saturated. Boufadel et al. (1999) concluded that the degree of saturation within the CF on seepage slopes was highly variable and that implications for unsaturated flow in the CF existed.

Several biogeochemical studies of the CF have also shown varied results. In studies of ammonia nitrification and ORP within the CF it was reported that sufficient oxygen was present to raise the ORP, which implies an unsaturated CF (Zilberbrand et al. 2001, Marrin and Adriany 1999). Conversely, Cirmo and McDonnell (1997) reported the CF to be anaerobic based on measured levels of nitrate reduction. Blodau et al. (2004) observed significant methane production in the CF at a very low ORP. The later two studies mentioned both show that the CF was saturated or nearly saturated, resulting in anaerobic conditions.

Bovan et al. (2003) reported that the density of the CF was indiscernible from the free water table when using ground-penetrating radar to measure water table depth. Further analyses led Bovan et al. (2003) to conclude that there was a saturated CF that became unsaturated with increasing height above the water table. The contrasting conclusions of

numerous studies regarding the degree of saturation, and whether aerobic or anaerobic conditions exist within the CF, suggests that the CF may not be consistently identified among studies. Soils characteristics likely varied among studies (different textures, mineralogy, organic carbon content, particle size, shape, coating, porosity, pore size, etc.), which would result in different CFHs, but one would expect general agreement regarding the degree of saturation and aerobic/anaerobic conditions in the CF.

The CFH is often discussed in the literature but how the CF is identified in a particular study is seldom directly stated. It is assumed herein that the CFH is typically based on the air entry value (AEV) or calculated with Equation 1 and an estimation of the mean pore radius, based on particle-size distribution. The AEV is the suction at which air first enters a saturated soil and provides an estimate of how tightly the water is held by the soil. AEVs are typically determined from soil moisture tension data. A soil with smaller pore radii would hold water with a greater tension (larger CF) and would have a larger AEV. However, the AEV varies depending on whether the soil is being wetted or drained and the wetting/draining history (Gillham 1984). The AEV for drainage of a soil sample is up to twice that of the AEV determined for wetting a soil sample (Haines 1927). The AEVs reported for sands or sandy soils for drainage and wetting and the CFH from numerous studies range from 1 to 140 cm (Table 1).

Table 1. Summary of air entry values (AEVs) and height of capillary fringe (CFH) reported in the literature for sands or sandy soils

Texture	AEV – drainage (cm)	AEV – wetting (cm)	CFH (cm)	Method	Source
Sand	51.41			Brooks and Corey equation	Bumb et al. 1992
Sand	37.79			Fermi Distribution	
Sand	49.19			Boltzmann Distribution	
Medium – fine grained sand	25	3		Visually estimated from SMRC data	Gillham 1984
Coarse sand – fine sand			1-60	CF equation and mean pore radii	
Sand	23-44			Visually estimated from SMRC data	Haines 1927
Various sands	18.59-41.29	5-20		Determined via a power fitting equation applied to SMRC data from multiple sources	Haverkamp and Parlange 1986
Sand (2 mm)			3.4	Determined by measuring pore pressure under drainage	Keihn 1992
Sand (0.37 mm)			14.26		
Sand (0.13 mm)			34.34		
Sand	9.1-14.0		6-12	AEV –Brooks and Corey equation Capillary Fringe –wetting soil cores and determining water content gravimetrically	Nkedi-Kizza and Richardson 2005
Sand (104-125 μm)	40	10		Visually estimated from SMRC data	Klute and Wilkinson 1958
Sand (125-149 μm)	40	15			
Sand (149-177 μm)	45	25			

Table 1. (cont.)

Texture	AEV – drainage (cm)	AEV – wetting (cm)	CFH (cm)	Method	Source
Sand (177-210 μm)	55	35		Visually estimated from SMRC data	Klute and Wilkinson 1958
Sand (210-250 μm)	65	35			
Coarse sand	24.5	13.6		Brooks and Corey equation	Lehman et al. 1998
Sand			1-9	Based on personal communication with Otto Bauer, 1990	Mausbach 1990
Fine sand			3-10		
Medium – fine grained sand	30			Visually estimated from SMRC data	Novakowski and Gillham 1988
Sand	7.26-15.98			Brooks and Corey equation	Rawls et al. 1982
Medium sand			15	CF equation and mean pore radius of (0.01cm)	Richardson et al. 2001
Sand			Up to 140	Reported value based on measurement of soil water content above and below the water table	Ronen et al. 2000
Sand	20			Predicted SMRC based on centroid texture for sand	Saxton et al. 1986
Accusand grade 12/20	5.42			Brooks and Corey equation	Schroth et al. 1996
Accusand grade 20/30	8.66				
Accusand grade 30/40	13.03				
Accusand grade 40/50	40				
Hanford sand (0.2mm)		10		Visually estimated from SMRC data	Tokunaga et al. 2004

OXIDATION-REDUCTION POTENTIAL (ORP)

The occurrence of anaerobic conditions can be verified by measuring the ORP and the pH of the soil (Reddy and D'Angelo 1994). ORP is a measure of electron pressure or activity present in soils related to microbial respiration and oxidation of organic substrates. ORP ranges from highly reduced or anaerobic (-250 mV) to highly oxidized or aerobic (+500 mV). The level of electron potential in the soil is measured with a millivolt (mV) meter equipped with a standard reference electrode corrected to a standard hydrogen electrode, and a platinum tipped electrode inserted into the soil. The electrical resistance between the electrodes is translated into an electrical potential (Eh) with a mV meter. At a soil pH of 7, Eh values greater than +300 mV occur in the presence of oxygen and Eh values below +300 mV are generally considered to be anaerobic (Delaune and Reddy 2004), meaning that oxygen is no longer available as an electron acceptor.

Microbial activity is a function of numerous environmental factors including, temperature, pH, moisture content, and carbon availability. As microbes deplete oxygen as the primary electron acceptor during respiration and metabolism, secondary electron acceptors are utilized. This allows microbial communities to continue to metabolize organic substrates, although the energy gained by the microbes is lessened. Lower energy gain by the microbes is the result of increasing energy needed for respiration and transfer of electrons. Obligate anaerobic microbes typically dominate the microbial community when the ORP potential is below that required to reduce Mn^{+4}, approximately 180 mV (Schlesinger 1997). Further, much research in this area has demonstrated a highly predictable sequence of electron acceptors when soils become anoxic, typically due to high moisture content which decreases the diffusion rate of air into the soil (Ponnamperuma 1972, Patrick and Jugsujinda 1992, Achtnich et al. 1995, Peters and Conrad 1996). This sequence of electron acceptors is closely linked to discrete ranges of ORPs (Table 2).

Anaerobic conditions are often assumed to occur in saturated or flooded soils because the oxygen dissolved in water is rapidly consumed by microorganisms and oxygen diffuses very slowly into water (Brady and Weil 2002, Faulkner et al. 1989). This is often true, but can be an invalid assumption. Since microbial decomposition plays a paramount role in the cycling of carbon (Cebrian 2004) and thus the electron pressure and aerobic/anaerobic status of the soil it is important to measure ORP. Numerous studies have reported increased oxidation rates with increased soil drainage, suggesting aerobic conditions, or decreased oxidation rates with high water tables (Schothorst 1977, Browder and Volk 1978, Stephens

1984, Ingebritsen et al. 1999). However, flooding does not always indicate anaerobic conditions. For example, Lockaby et al. (1996) reported greater decomposition rates (though not statistically significant) under flooded conditions as compared to drained conditions and ORP greater than 300 mV, indicating that aerobic conditions can persist under flooded conditions for some duration or when the water source is oxygen rich.

Measurement of soil Eh can aid in determining the level of reduction and the general chemical species dominating the reduction pathway at a given depth or soil condition (Reddy and D'Angelo 1994). It is important to note that as ORP decreases below 300 mV, anaerobic conditions dominate and the decomposition rate of organic substrates (organic matter oxidation) decreases as energetic costs to microbes increase. A near saturated or inundated soil with highly reducing conditions predictably loses organic matter at a much slower rate than aerobic soils where oxidizing conditions prevail. In addition, upland plant species are generally less tolerant of anaerobic conditions as compared to wetland vegetation species and can be eliminated from the lake bed when anaerobic conditions persist for a sufficient duration.

Table 2. Typical sequence of electron acceptors and oxidation-reduction potential ranges (Ponnamperuma 1972, Patrick and Jugsujinda 1992, Achtnich et al. 1995, Peters and Conrad 1996)

Electron Acceptor (oxidized to reduced)	**Redox Potential Range (mV)**
O_2 to H_2O	+300 to +700 mV
NO_3^- to N_2	+240 to +300 mV
Mn^{+4} to Mn^{+2}	+180 to +240 mV
Fe^{+3} to Fe^{+2}	+50 to +90 mV
SO_4^{-2} to S^{-2}	-180 to -100 mV
CO_2 to CH_4	-250 to –200 mV

GENERAL DESCRIPTION OF STUDY AREA

Three lakes were selected for study along the central ridge of Florida: Lake Brooklyn, Swan Lake, and Two Mile Pond (Figure 2). These lakes are located in southwestern Clay County and northwestern Putnam County and are located within the Interlachen Sand Hills subdistrict of the Central Lakes District (Brooks 1982). The Central Lakes District consists of surficial sands underlain by uplifted limestones of the Floridan aquifer. This region has active collapse sinkhole development and is a principle recharge area for the Floridan aquifer (Brooks 1982). The Interlachen Sand Hills subdistrict is described as having a direct hydraulic connection through thick sand and gravel to the Floridan aquifer, which results in lake levels in the region being at or slightly above the potentiometric surface of the aquifer (Brooks 1982). Because of the physiography of the region there are many small lakes and few streams. Water is maintained in these lakes because of a small surplus of precipitation, which recharges the aquifer and maintains the potentiometric surface of the aquifer.

The average rainfall for the study area is approximately 135 cm/year with about 60% of this rainfall occurring from June through October (Rao et al. 1990). The evapotranspiration can range from approximately 102 to 113 cm/year (Motz and Heaney 1991). Because lake levels in this region are tied to the potentiometric surface of the Floridan aquifer, small deficits in rainfall can result in wide stage fluctuations. The large ground water and surface water fluctuations associated with this region affect the vegetation and soils.

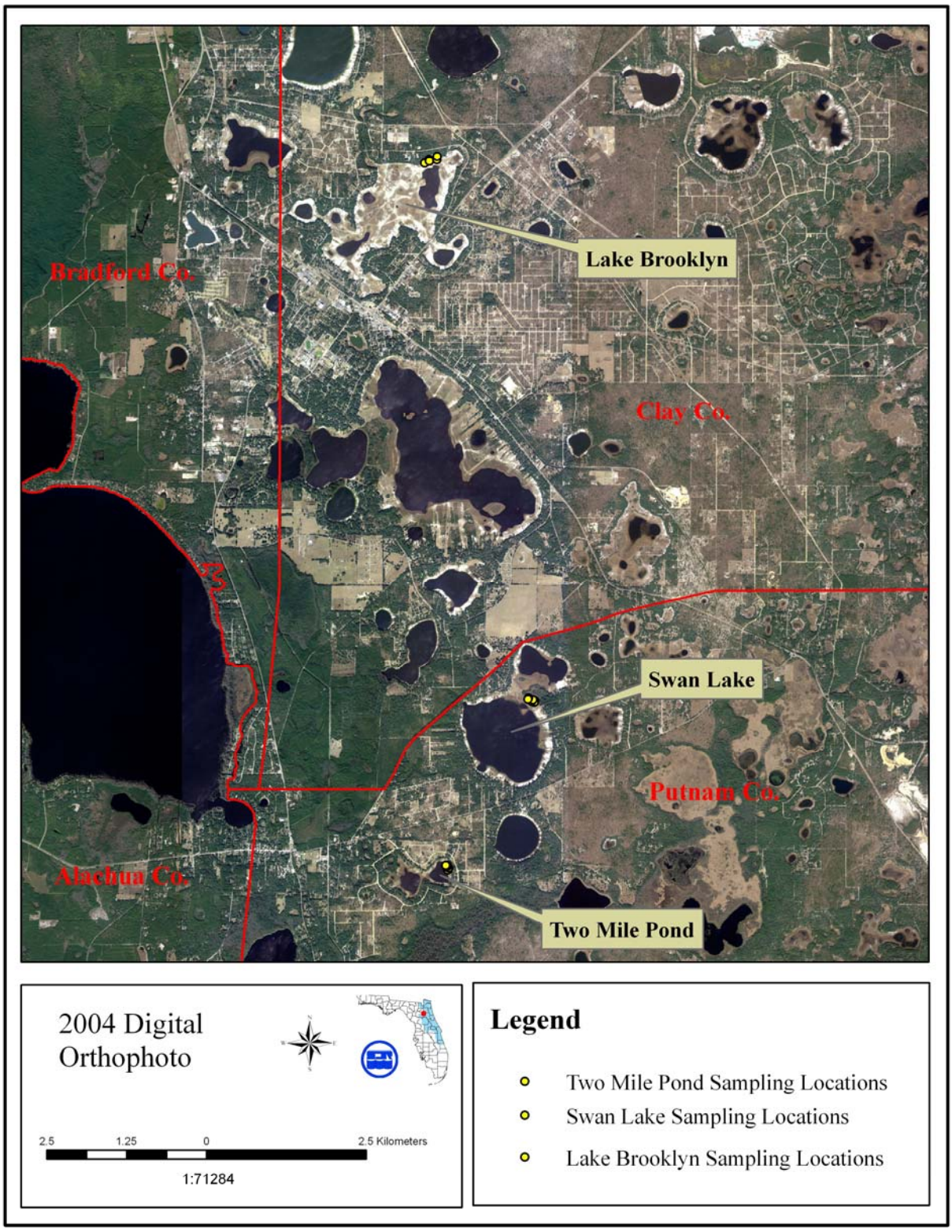

Figure 2. Sampling locations: Lake Brooklyn, Clay County and Swan Lake and Two Mile Pond, Putnam County

SOILS

Soils were mapped adjacent to Lake Brooklyn, Swan Lake, and Two Mile Pond (USDA Soil Conservation Service 1990 and 1989, Figures 3, 4, and 5, and Table 3). The mapped soil series and their associated Orders and taxonomic classification are listed in Table 3. Entisols (Penney and Osier series) and Inceptisols (Placid series) dominate the areas directly adjacent to these lakes. Ultisols and Spodosols are common in the surrounding areas. Entisols are common in the excessively and very poorly drained area, Spodosols are common in the poorly drained areas, and Inceptisols and Ultisols are common in the intermediately drained areas. Entisols are soils that do not meet the diagnostic characteristics of the other soil orders and are typically considered to be genetically young mineral soils with little horizon development. Some soils in this region, although classified as Entisols, are highly weathered but lack any substantial horizons within the upper 2 m, from which soils are classified based on Soil Taxonomy (Soil Survey Staff 1999). Inceptisols are considered to be developmentally older than Entisols because these soils display some diagnostic features, including inception or weak formation of a B horizon (a horizon associated with illuvial accumulation of silicate clays, aluminum, organic acids, and/or iron). Ultisols are well developed soils that contain an argillic horizon (illuvial accumulation of clay) with low base saturation (<35%). Spodosols in this region occur in coarse textured soils with a seasonal high water table that is near the soil surface and acid producing vegetation. Spodosols contain a spodic horizon, which is an alluvial accumulation of organic matter and aluminum and/or iron oxides. The surface horizons of each of these soils are dominated by quartz sand and contain a small percentage of clay, silt, and organic carbon (USDA Soil Conservation Service 1990 and 1989).

Soils at each of the sampling locations typically had an A horizon at the surface, underlain by multiple E or C horizons (depending on one's interpretation). An A horizon is a mineral horizon that formed at the surface or below an O (organic) horizon where organic material is accumulating (USDA, NRCS 2002). An E horizon is a mineral horizon in which the dominant process is loss of silicate clay, aluminum, and/or iron, leaving a concentration of sand and silt particles (USDA, NRCS 2002). A C horizon is a mineral horizon which is relatively unaffected by biological activity or pedogenesis and lacks properties diagnostic of A or B horizons (Brady and Weil 2002).

Soils at each of the sampling locations were classified to the subgroup level as Typic Psammaquents. Typic Psammaqu**ent**s (interpreted right to left) are **Ent**isols, which have little or no evidence of soil formation. Entisols are either young soils or their parent materials have not reacted to soil forming factors (Brady and Weil 2002). These soils have an **aqu**ic moisture regime, which, indicates that they are saturated with water and virtually free of oxygen for sufficient periods for poor aeration to occur. Psammaquents are those Entisols that have sandy material in all horizons to a depth of 100 cm or more (**psamm**). **Typic** Psammaquents are typical of the great group, Psammaquent. They do not have contact with bedrock within the upper 50 cm, have a spodic horizon, or have an exchangeable sodium content of 15% or more within 100 cm of the surface, but are saturated for part of the year (Soil Survey Staff 1999).

Soil series identified based on field descriptions are the Osier series at Lake Brooklyn and the Pompano series at Swan Lake and Two Mile Pond. A different series was identified at Lake Brooklyn than at Swan Lake and Two Mile Pond because there is a change in soil temperature regime at the Clay/Putnam county line, with a thermic regime north of the line and hyperthermic to the south. The thermic temperature regime has mean annual soil temperatures of 15°C or higher, but less than 22°C and the hyperthermic temperature regime has mean annual soil temperatures of 22°C or higher, both at a depth of 50 cm or at densic, lithic, or paralithic contact, whichever is shallower (Soil Survey Staff 1999).

The Osier series is a very deep, poorly drained, rapidly permeable soil formed in sandy alluvium. These soils are frequently flooded for brief periods and have a water table within 30 cm of the surface for 3 to 6 months in most years (USDA, NRCS 2006).

The Pompano series is a very deep, very poorly drained, rapidly permeable soil formed in thick beds of marine sands. These soils have a water table within 25 cm of the soil surface for 2 to 6 months during most years. During drier months the water table remains within depths of 76 cm for more than 9 months each year. Depressional areas of Pompano soils have a water table above the surface for more than 3 months each year (USDA, NRCS 2006).

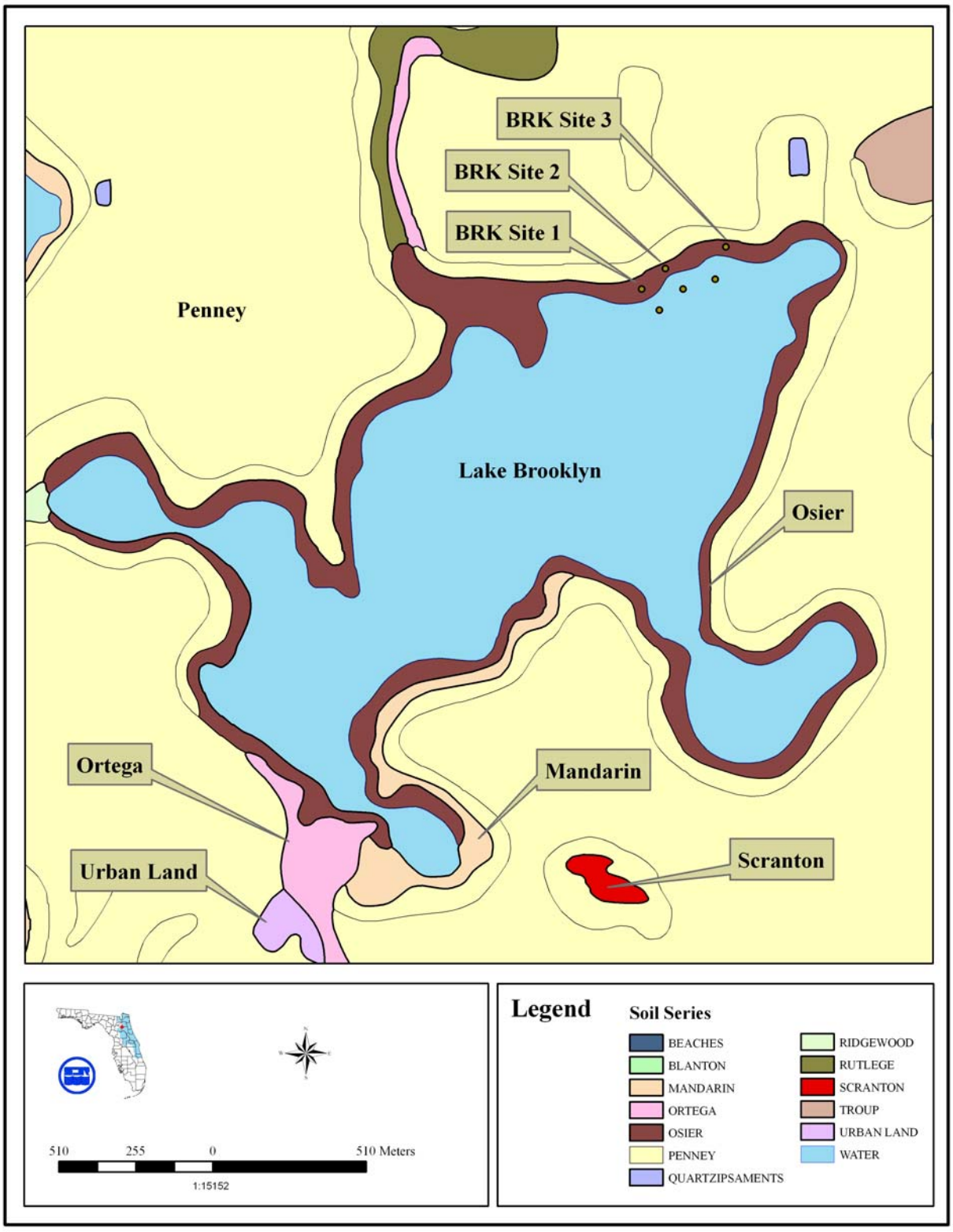

Figure 3. Soil series mapped adjacent to Lake Brooklyn

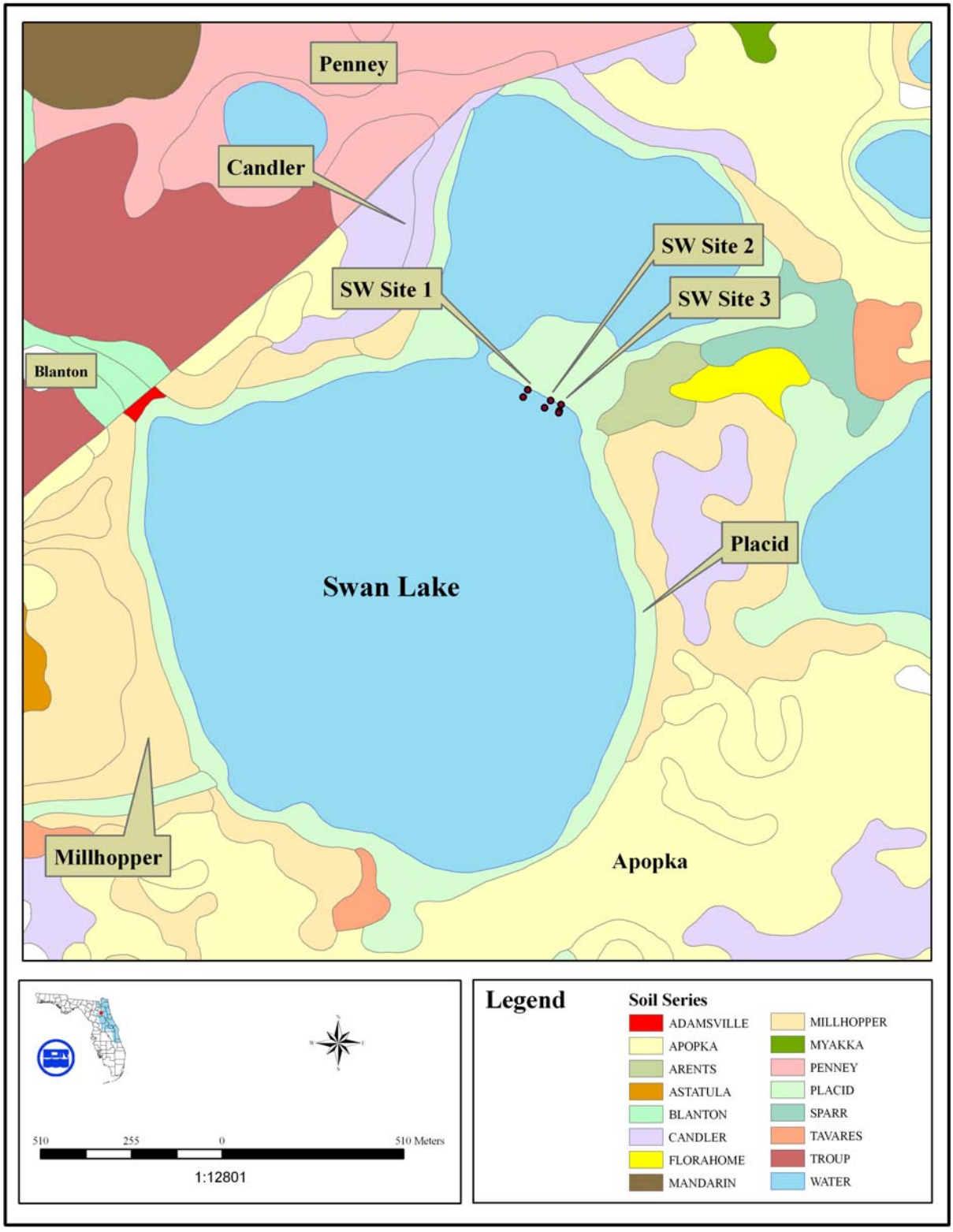

Figure 4. Soil series mapped adjacent to Swan Lake

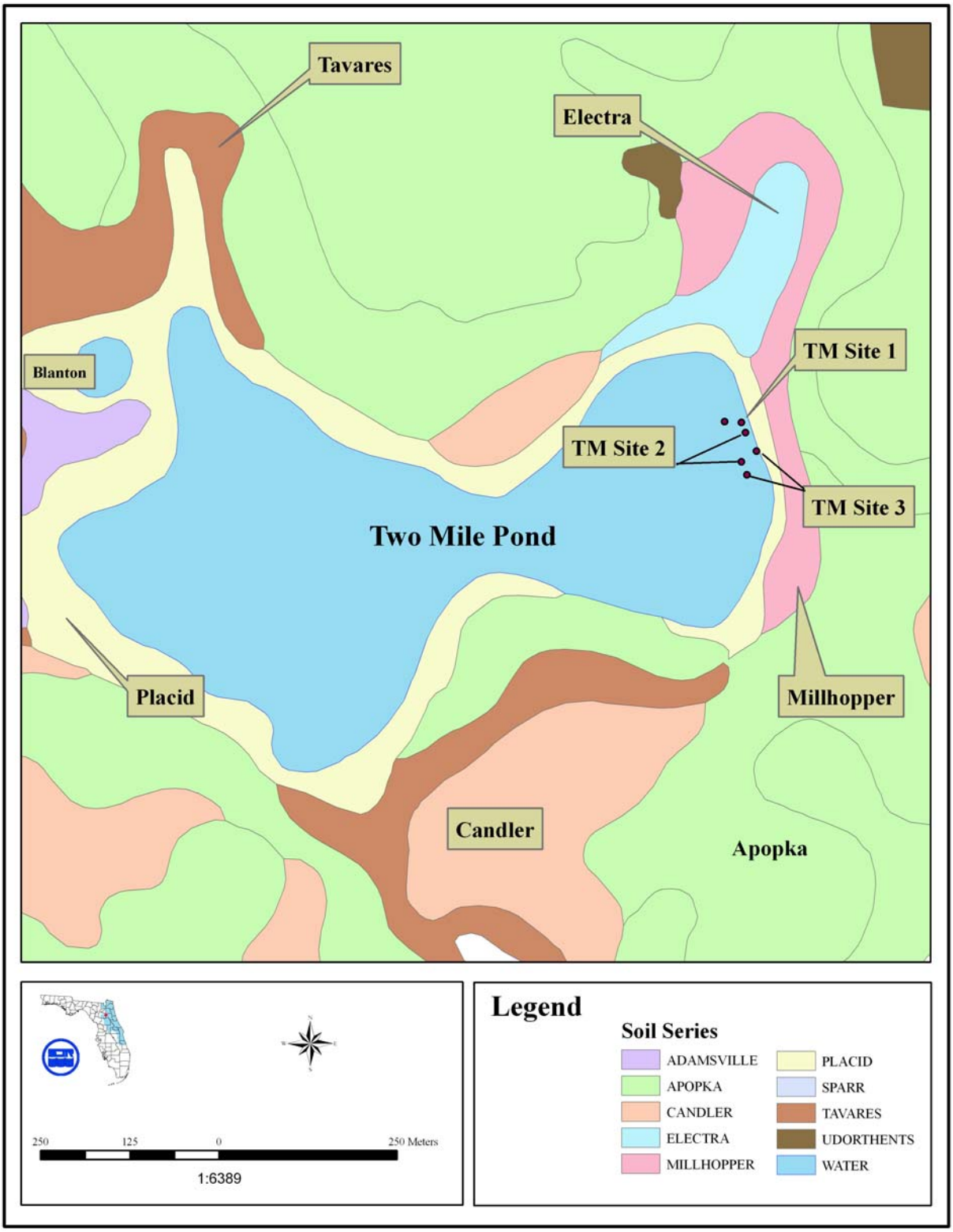

Figure 5. Soil series mapped adjacent to Two Mile Pond

Table 3. Soil Orders, taxonomic classification, and series mapped adjacent to study sites

Order	**Taxonomic Classification**	**Series Name**
Entisol	Hyperthermic, uncoated Aquic Quartzipsamments	Adamsville
Ultisol	Loamy, siliceous, subactive, hyperthermic Grossarenic Paleudults	Apopka
-	excavated material - 30% loamy, 50% sandy, and up to 35% clayey	Arents
Ultisol	Loamy, siliceous, semiactive, thermic Grossarenic Paleudults	Blanton
Entisol	Hyperthermic, uncoated Lamellic Quartzipsamments	Candler
Spodosol	Sandy, siliceous, hyperthermic Oxyaquic Alothods	Electra
Inceptisol	Siliceous, hyperthermic Humic Psammentic Dystrudepts	Florahome
Spodosol	Sandy, siliceous, thermic Oxyaquic Alorthods	Mandarin
Ultisol	Loamy, siliceous, semiactive, hyperthermic Grossarenic Paleudults	Millhopper
Entisol	Thermic, uncoated Typic Quartzipsamments	Ortega
Entisol	Siliceous, thermic Typic Psammaquent	Osier
Entisol	Thermic, uncoated Lamellic Quartzipsamments	Penney
Inceptisol	Sandy, siliceous, hyperthermic Typic Humaquepts	Placid
Ultisol	Loamy, siliceous, subactive, hyperthermic Grossarenic Paleudults	Sparr
Entisol	Hyperthermic, uncoated Typic Quartzipsamments	Tavares

VEGETATION

Vegetation communities were mapped by SJRWMD, based on interpretation of aerial imagery. Mapped vegetation communities adjacent to Lake Brooklyn, Swan Lake, and Two Mile Pond include upland, deep marsh, shallow marsh, wet prairie, transitional shrub, and barren areas (Figure 6). The upland community dominates the aerial extent of this region and is typically composed of various hardwood species. The deep and shallow marshes may be ephemeral communities that move up and down slope based on the water level in the lake or may completely die-off during low water periods and reestablish from the seedbank during periods of higher water. Deep marshes are often dominated by a mixture of water lilies (*Nymphaea odorata*) and deep-water emergent species (Kinser 1996). Water lilies are intolerant of desiccation and require inundation for seed germination (David 1996; Conti and Gunther 1984; Hagenbuck et al. 1974). Shallow marshes are typically dominated by species such as sawgrass (*Cladium jamaicense*), maidencane (*Panicum hemitomon*), pickerel weed (*Pontederia cordata*), arrowhead (*Sagittaria spp.*), or other grasses and broad leaved herbs (Kinser 1996). Many shallow marsh species often require drawdown conditions for reseeding and germination (Van der Valk 1981). The wet prairie and transitional shrub communities are typically located between the upland and wetter communities. Wet prairies are typically dominated by grasses, sedges, and herbs such as sand cordgrass (*Spartina bakeri*), maidencane, or a mixture of species (Kinser 1996) and are among the most species rich of Florida's marshes (Kushlan 1990). Transitional shrub communities are typically dominated by transitional shrubby vegetation such as wax myrtle (*Myrica cerifera*) and can form on wet prairies that have been protected from fire (Kinser 1996). Barren areas are common in sandhill lakes likely due to extended wet and dry periods resulting in conditions that are too wet for a vegetation community during high water and conditions that are too dry for a vegetation community during low water. This results in the majority of the zone within the lakes fluctuation range being sparsely covered by emergent species that germinate from the seedbank when conditions are favorable.

Vegetation communities at the Lake Brooklyn sampling locations consisted of upland, wet prairie, and barren areas. The upland was dominated by sand live oak (*Quercus geminata*) and saw palmetto (*Serenoa repens*). The wet prairie was dominated by sand cordgrass and blue maidencane (*Amphicarpum muhlenbergianum*). The barren areas contained scattered maidencane, blue maidencane, broom sedge (*Andropogon sp.*), and meadow beauty (*Rhexia spp.*) and other herbaceous species.

Vegetation communities at the Swan Lake sampling locations consisted of upland, wet prairie, and shallow marsh. The upland was dominated by sand live oak and also contained scattered slash pine (*Pinus elliottii*). The wet prairie was dominated by wax myrtle and sand cordgrass and also contained blue maidencane and scattered maidencane. The shallow marsh was dominated by rush-fuirena (*Fuirena scirpoidea*) and also contained maidencane, broom sedge, meadow beauty, and St. John's wort (*Hypericum spp.*). The shallow marsh appeared to be a stable community, but is likely present because of the extended period of low water levels. This community would likely be eliminated during an extended period of high water which would result in approximately 1 m of water overtop the tallest shallow marsh vegetation.

Vegetation communities at the Two Mile Pond sampling locations consisted of upland, wet prairie, and shallow marsh. The upland was dominated by sand live oak. The wet prairie was dominated by wax myrtle and sand cordgrass and also contained blue maidencane. The shallow marsh was dominated by rush-fuirena and American cupscale (*Sacciolepis striata*) and also contained maidencane, broom sedge, meadow beauty, golden-rod (*Solidago spp.*) and yellow-eyed grass (*Xyris spp.*). The shallow marsh appeared to be a stable community, but is likely present because of the extended period of low water levels. This community would likely be eliminated during an extended period of high water which would result in approximately 1 – 2 m of water overtop the tallest shallow marsh vegetation.

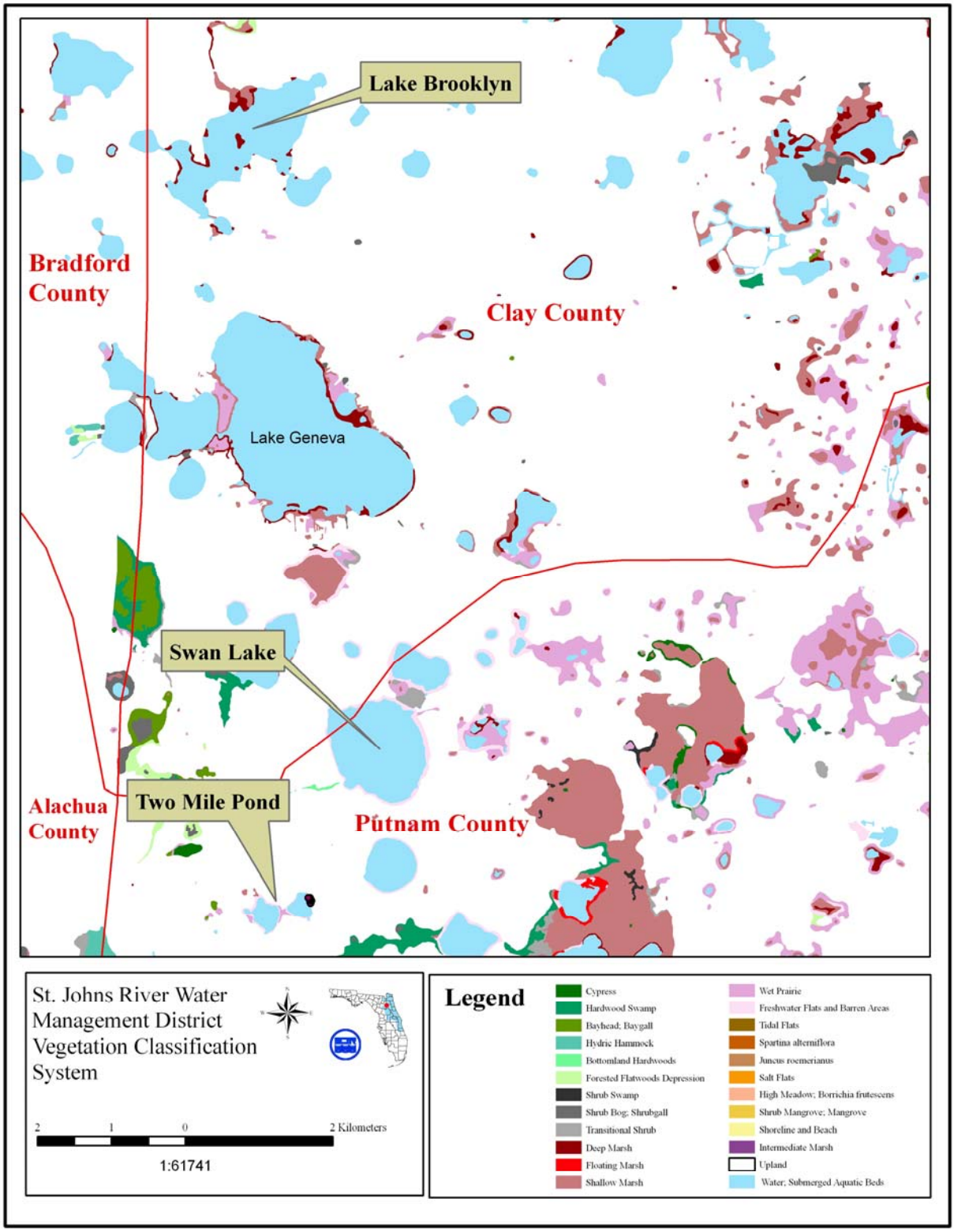

Figure 6. Vegetation communities mapped adjacent to study sites

METHODS

SITE SELECTION

Six sampling sites (Table 4) were established at each lake based upon the site selection criteria discussed in *Soil Indicators of Frequent High and Frequent Low Water Levels in Sandhill Lakes in St. Johns River Water Management District* (SJRWMD 2006a). These criteria include selecting sites that are undisturbed, along low energy shorelines, have a short slope from open water to upland, are not strongly affected by seepage, are not dominated by pines, and are not in areas with more than a few cm of muck on the soil surface. These criteria were developed to enhance the identification of frequent high (FH) and frequent low (FL) LSIs (20% and 80% stage exceedance, respectively). The FH LSI, stripped matrix, was identified at three sites along the perimeter of each lake (Figures 3, 4, and 5). The FL LSI, dark splotches, was identified at three sites, downslope from the FH sites, at each lake. FL sites 2 and 3 at Two Mile Pond were shifted to the south because the shoreline directly downslope from the FH site 2 was disturbed.

The physical soil properties and the resulting hydrologic properties of the soil are of primary interest in this study. An accurate measure of moisture content is necessary to determine the hydrologic characteristics of the soil, in particular, the water content distribution near and above the free water surface (water table). In addition, manipulating the water table in the field was not feasible in these sandy soils; therefore, soil cores were collected in the field and studied in a controlled setting.

Table 4. Soil sampling locations

Lake	Location	Latitude	Longitude
Brooklyn	FH1	29° 48′ 27.349″	82° 01′ 24.845″
	FH2	29° 48′ 28.471″	82° 01′ 21.651″
	FH3	29° 48′ 29.929″	82° 01′ 16.920″
	FL1	29° 48′ 26.506″	82° 01′ 24.143″
	FL2	29° 48′ 27.594″	82° 01′ 21.420″
	FL3	29° 48′ 28.371″	82° 01′ 17.168″
Swan	FH1	29° 43′ 52.894″	82° 00′ 17.319″
	FH2	29° 43′ 53.252″	82° 00′ 18.410″
	FH3	29° 43′ 54.218″	82° 00′ 20.832″
	FL1	29° 43′ 52.151″	82° 00′ 17.558″
	FL2	29° 43′ 52.589″	82° 00′ 19.050″
	FL3	29° 43′ 53.559″	82° 00′ 21.291″
Two Mile	FH1	29° 42′ 28.282″	82° 01′ 07.348″
	FH2	29° 42′ 27.827″	82° 01′ 07.131″
	FH3	29° 42′ 26.985″	82° 01′ 06.553″
	FL1	29° 42′ 28.316″	82° 01′ 08.234″
	FL2	29° 42′ 26.495″	82° 01′ 07.327″
	FL3	29° 42′ 25.904″	82° 01′ 07.046″

FIELD PROCEDURES

Prior to collecting any soil samples, the surface vegetation was manually removed with the sharp edge of a shovel. Roots were left intact so that soil samples would be as representative of the natural soils as possible. Two types of cylinders were used to collect undisturbed soil core samples. The first type is a small brass cylinder [5.38 cm (ID) x 3.00 cm (L)], henceforth referred to as "short soil core" or "short core." The second type is a plastic cylinder [4.73 cm (ID) x 30.48 cm (L)], henceforth referred to as "long soil core" or "long core."

Short Soil Cores

Short soil cores were collected to develop soil moisture release curves, determine saturated hydraulic conductivity (Ksat), particle-size distribution, organic carbon (OC) content, and to calculate bulk density and particle density. One hundred and twenty short cores were collected at each lake with 20 collected at each site (3 FH and 3 FL sites per lake). Two sets of 10 short cores were collected at each site to characterize the upper 30 cm of the soil, with each core representing a 3-cm segment from the soil surface to a depth of 30 cm. Soil moisture tension data and saturated hydraulic conductivity were measured from one set of 10 short cores from each site. Bulk density, particle density, percent OC, and particle-size distribution were measured from the second set of 10 short cores from each site.

The soil was sampled with the short core sampling apparatus (Figure 7). The assembly consists of the following:

- Chamber with sharp cutting edge
- Vented cap
- Weighted hammer
- Hollow barrel with handle
- Core extraction tool
- Two small (1 cm) rings
- Two short cores
- One small (1 cm) notched ring

The short cores and rings are aligned as shown (Figure 7). The notched ring is placed into the chamber first with the notches toward the cutting edge, followed by a short core, a small ring, another short core, and topped with another small ring. The hollow barrel is threaded onto the chamber to complete the assembly. The short core soil samples were collected by

placing the cutting edge of the chamber on the prepared soil surface and sliding the hammer into the hollow barrel. The hammer was repeatedly raised and then dropped, gently driving the chamber into the soil by the weight of the hammer. The barrel was maintained perpendicular to the soil surface so that the chamber filled evenly with soil. The chamber was not driven into the soil beyond the cap to limit compaction of the soil samples.

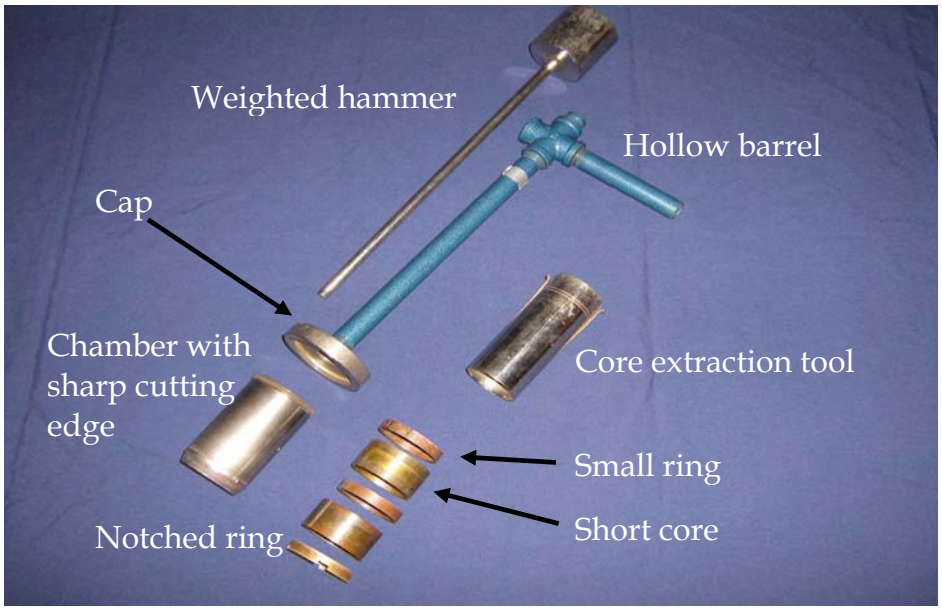

Figure 7. Short soil core sampling apparatus

The soil adjacent to the chamber was excavated with a shovel, enabling the hollow barrel to be leaned to the side and the open end of the chamber cupped with ones hand to prevent excessively dry/wet soil from falling out of the chamber or the soil core. The device was disassembled and the soil was removed from the chamber with an extraction tool (Figure 7). The extraction tool was inserted into the chamber on the side with the cutting edge and rotated until it engaged the notches in the small ring. Pressure was applied to the small-notched ring to extract the rings, short cores, and soil from the chamber. The short cores were separated using a knife to cut any roots between them. Extra soil was left protruding from the short cores, which were placed in plastic bags and secured with rubber bands to prevent evaporation and prevent soil from falling out of the cores, during transport to the laboratory.

The short soil cores were removed from their bags in the laboratory and the excess soil and roots protruding beyond the edge of the cores were removed. This resulted in a soil sample with the same volume as the short core (68.23 cm^3).

Long Soil Cores

Long undisturbed soil cores were collected to measure the CFH and ORP within the CF. Sixty long soil cores were collected at each lake with 10 collected at each FH and FL site. Ten long cores were collected at each site to ensure enough cores were available for all analyses. The soil was sampled with the long cores sampling apparatus (Figure 8). The assembly consists of the following:

- One long core
- One chamber with sharp cutting edge
- One vented cap
- One slide hammer

Figure 8. Long soil core sampling apparatus

The long core was inserted into the chamber and the chamber, cap, and slide hammer were threaded together. The long core soil samples were collected by placing the cutting edge on the prepared soil surface and repeatedly raising and dropping the slide hammer to gently drive the chamber into the soil. The chamber and slide hammer were maintained perpendicular to the soil surface to evenly fill the chamber with soil. The chamber was not driven in beyond the lower edge of the cap to limit compaction of the soil samples.

Soil adjacent to the chamber was excavated with a shovel, enabling the chamber and slide hammer to be leaned to the side and the open end of the chamber cupped with one's hand to prevent excessively dry/wet soil from falling out. The device was disassembled and the soil was removed from the chamber by putting pressure on the soil from the cutting edge side. The long cores were capped on both ends with plastic caps for transport to the laboratory.

One long core from each site was cut into 3-cm segments to determine bulk density and initial moisture content. The remaining long cores were air dried so that they had similar moisture contents prior to determining the CFH. Any excess soil or roots protruding beyond the ends of the long cores were left intact until the cores were assembled for the determination of the CFH. At that time, the excess soil or protruding roots were carefully trimmed flush with the edge of the long core so that the volume of the soil was equivalent to the volume of the long core (536.15 cm^3).

LABORATORY PROCEDURES

Physical soil characteristics were determined from one set of short cores from each sampling location. Soil moisture tension was measured with the second set of short cores from each sampling location. The CFH was measured in duplicate long cores collected at each sampling location. The HAC was measured in duplicate long cores from one FH and FL location at each lake.

Bulk Density

Bulk density (ρ_b, g/cm^3) was measured from short soil cores collected at each sampling site (Equation 3).

$$\rho_b = M_s/V_t \quad (3)$$

Bulk density is a measure of the mass of the dry soil (M_s, g) per unit volume of the sample (V_t, cm^3). Dry soil or oven-dried soil is a relative term and is used herein as soil that was dried in an oven at 105°C for 24 h. These short soil cores were prepared upon arrival in the laboratory, by removing excess soil and protruding roots, allowing the total volume of the soil to be equivalent to the volume of the short core. The short soil cores were oven dried, cooled in a desiccator, and the mass of the dry soil was determined. This resulted in the determination of bulk density for each 3-cm segment, from the soil surface to 30 cm, at each site. These soil samples were placed in labeled bags for further analyses.

Particle Density

Upon completion of the bulk density determinations, particle density (ρ_s, g/cm^3) was measured from a 25 g sub-sample from each short soil core (Equation 4).

$$\rho_s = M_s/V_s \quad (4)$$

Particle density is a measure of the mass of the dry soil (M_s, g) per unit volume of soil particles (V_s, cm^3). The volume of soil particles excludes pore space within the soil sample. Particle density was measured with a variation of the pycnometer method described by Blake and Hartge (1986). The pycnometer method herein, draws on the concept of Archimedes Principle to determine the volume of soil particles. Archimedes Principle states that a body immersed in a fluid is buoyed up by a force equal to the weight of the displaced fluid (Hillel 1998).

The volume of soil particles was determined with volumetric flasks (50 mL) rather than pycnometers (small volumetric flasks with beveled glass stoppers), which provide a very accurate and precise measure of volume, but are difficult to commercially obtain. The volume of soil particles in a sample was calculated by determining the mass of water displaced by a known mass of dry soil and then dividing by the density of water (ρ_w) to determine the volume of water displaced by the soil. This volume is equivalent to the volume of the soil particles.

Particle density was determined by the following process (Equation 5):

- Weigh a clean dry 50 mL volumetric flask (W_a, g)
- Weigh the 50 mL volumetric flask filled to volume with degassed deionized (DI) water (W_w)
- Dry the 50 mL volumetric flask, fill half full with dry soil and weigh (W_s, g)
- Fill flask containing soil (W_s) to volume with degassed DI water and weigh (W_{sw}, g)

$$\rho_s = \rho_w * [(W_s-W_a)/[(W_s-W_a) - (W_{sw}-W_w)]] \quad (5)$$

The expression in brackets is equal to M_s divided by the mass of water displaced by the soil. Multiplying by the density of water converts the mass of water to volume of water, which is equal to (V_s, mL).

Organic Carbon (OC) Content

The OC content was determined for short soil cores from Two Mile Pond and from each 3-cm segment from 0 to 30 cm in one long core from each FH and FL sampling location at Two Mile Pond (120 samples total) following the Walkley-Black method. This method has been described by Walkley and Black (1934) and Peech et al. (1947), and has been reprinted in numerous chemical soil analysis manuals (Nelson and Sommers 1986; Nelson and Sommers 1996; and USDA 1992). A general description of the Walkley-Black procedure follows.

Approximately 10 g of soil from one set of short cores and 10 g of soil from each 3-cm segment of a long core from each FH and FL site at Two Mile Pond (120 samples) were ground in a ball mill for 3 minutes. The ground samples were dried and a known mass of each sample (~0.5 g) was placed in a 250 mL Erlenmeyer flask. Ten mL of 1.0N potassium dichromate was added to each flask, which was swirled to wet the soil. Twenty mL of concentrated sulfuric acid was added to each flask, which was swirled for approximately 1 minute. The flasks were allowed to stand for 1 h at which time 200 mL of DI water was added to the flasks to virtually halt the reaction. Five drops of ferrous sulfate complex was added to each flask to facilitate identification of the titration end point. A stir bar was added to each flask, and the flasks were individually placed on a lighted stirrer and titrated with 0.5N ferrous sulfate. Upon titration the sample changed from orange to green to the reddish brown endpoint. Duplicates were analyzed for each sample and blank (containing no soil). The percent OC was calculated using Equation 6, where mL_{blank} is the volume of titrate for the blank, mL_{sample} is the volume of titrate for the sample, $M_{Fe^{2+}}$is the molarity of the ferrous sulfate, and f is a correction factor (1.30).

$$\%OC = [(mL_{blank} - mL_{sample})(M_{Fe^{2+}})(0.003)(100) / \text{mass (g) dry soil}]*f \qquad (6)$$

A correction factor of 1.30 was applied to more accurately estimate percent OC. A correction factor is necessary because the Walkley-Black procedure has been reported to recover, on average, 77% of OC with a range of 60% to greater than 95% (Nelson and Sommers 1996). Employing this correction factor does not result in a highly accurate percent OC determination for an individual soil sample, as compared with OC values determined for wet or dry combustion (Nelson and Sommers 1996). However, it does provide a reasonable OC estimate when the OC values for a number of soil samples are averaged.

Organic Matter (OM) Content

Organic matter (OM) content was determined by weight loss on ignition (LOI, Equation 7), where M_s is the mass of oven dry soil (g) and M_{550} is the mass of soil (g) after ignition at 550°C.

$$\% \text{ LOI} = [(M_s - M_{550})/M_s]*100 \quad (7)$$

Approximately 25 g of soil from one set of short cores and 25 g of soil from each 3-cm segment of the long cores used with the Walkley-Black method from each FH and FL site at Two Mile Pond (120 samples) were placed in 50-mL beakers, oven dried, and weighed to determine the mass of dry soil. These beakers were covered with aluminum weighing dishes and placed in a muffle furnace at 450°C for 8 h. The samples were removed from the muffle furnace and placed in a drying oven for 24 h to allow the sample to cool to 105°C at which point they were weighed to determine the LOI. This resulted in incomplete combustion of OM (Figure 9) and a poor relationship with percent OC determined via the Walkley-Black method for these samples. A smaller sample, higher temperature, and shorter time, 550°C for 3 h, as used by Howard and Howard (1990), was tested to obtain nearly complete combustion of the OM.

No soil remained from the Two Mile Pond short cores from which OC was determined with the Walkley-Black method. Soil moisture tension data collection for the duplicate set of short soil cores from Two Mile Pond was completed providing surrogate soil samples. Approximately 10 g of soil from these surrogate short cores and 10 g of soil from each 3-cm segment of the long cores were placed in 50-mL beakers, oven dried, and weighed to determine the mass of dry soil. The beakers were then covered with aluminum weighing dishes and placed in a muffle furnace at 550°C for 3 h. The samples were removed from the muffle furnace after 3 h and placed in a drying oven for 24 h to allow the samples to cool to 105°C and they were weighed to determine the LOI. This combination of temperature and time resulted in nearly complete combustion of the OM based on the color of the samples (Figure 9).

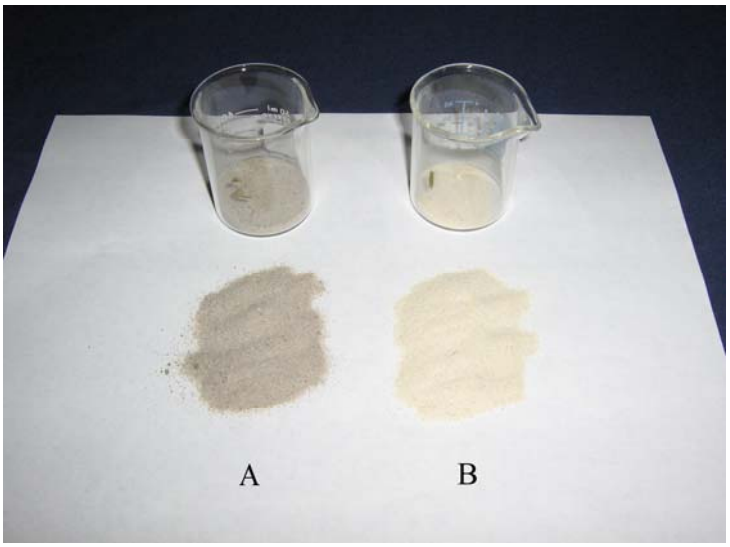

Figure 9. Soil sample combusted at 450°C for 8 h (A) and soil sample combusted at 550°C for 3 h (B)

Percent OM for the remaining short cores (Swan Lake and Lake Brooklyn) was determined with LOI at 550°C for 3 h. A relationship was developed between percent OM determined by LOI and percent OC determined with the Walkley-Black method for the short core and long core samples collected at Two Mile Pond (see Figure 16). Percent OM for Swan Lake and Lake Brooklyn was converted to percent OC based on the relationship developed.

Particle-size Analysis

Percent sand (2 mm to 45 μm), silt (45 to 2 μm), and clay (<2 μm) were determined with the pipette method (USDA 1992) and individual sand fractions were determined by dry sieving. Pretreatment of the soil is required to remove organic material and soluble salts; and to breakdown aggregates into individual particles (Gee and Bauder 1986). The soils being analyzed in this study are highly weathered and dominated by quartz, therefore, were only pretreated to remove organic matter and breakdown aggregates, following the pretreatment methods described by Gee and Bauder (1986).

A known mass of dry soil (approximately 50 g) from each of the short cores was placed in a 500-mL Erlenmeyer flask. The soils were moistened with DI water and approximately 10 mL of 30% hydrogen peroxide (H_2O_2) was added to the sample to begin oxidation of the organic matter as recommended by Day (1965). The reaction for these soils was weak, so approximately 100 mL of 30% H_2O_2 was added and the flasks were placed

on a hot plate and heated to 90°C to facilitate the reaction. When the reaction was assumed to be complete (light colored sample and evolution of few bubbles), the flasks were placed in the drying oven for 24 h at 105°C. The flasks were then weighed to determine the mass of the dry mineral fraction of the soil sample.

The next pretreatment step was the dispersion of aggregates. Chemical dispersion was accomplished utilizing a dispersing solution of sodium metaphosphate (SMP) made from a mixture of 50 g of SMP per 1L of DI water. One hundred mL of SMP solution was added to each sample. Samples were then shaken for 15 h to complete the pretreatment.

The samples were washed from the 500-mL flasks into 1-L graduated cylinders and filled to volume with DI water. Each graduated cylinder was covered and inverted 5 to 6 times to mix the sample and then placed in a water bath to maintain a constant temperature. Each remaining graduated cylinder was mixed and placed into the water bath at 3-minute intervals. After the settling time had elapsed, based on temperature and desired sampling depth (Table 5), a 25-mL aliquot was withdrawn from the first graduated cylinder at the appropriate depth with a pipette. The aliquot was discharged into a weighed and numbered aluminum weighing dish. Aliquots were removed from the remaining graduated cylinders at 3-minute intervals to continue sampling at the appropriate elapsed time.

Table 5. Settling times for particles less than 2 μm, with particle density of 2.65 g/cm^3 and 5g/L sodium metaphosphate (SMP, compiled from USDA 1992)

Temp. (°C)	Pipette Depth (cm)	Time (hh:min)	Temp. (°C)	Pipette Depth (cm)	Time (hh:min)
21	5	3:55	23	5	3:44
	6	4:41		6	4:28
	7	5:28		7	5:13
	8	6:15		8	5:58
22	5	3:49	24	5	3:38
	6	4:35		6	4:22
	7	5:20		7	5:06
	8	6:07		8	5:50

The aluminum weighing dishes, including a blank with SMP solution only, were placed in a drying oven for 24 h at 105°C and then weighed. Each sample remaining in the graduated cylinders was individually washed into

a 45 μm sieve (No. 325 sieve) on a ring stand, allowing the silt and clay to pass through and collecting the sand fraction. The sand fractions were washed back into the appropriately numbered 500-mL Erlenmeyer flasks, excess water was decanted, and the samples were placed in a drying oven for 24 h at 105°C and weighed. The oven dry sand fraction was then shaken in a nest of sieves (Nos. 18, 35, 60, 140, and 325) for 3 to 5 minutes to determine very coarse (1 to 2 mm), coarse (500 μm to 1 mm), medium (250 to 500 μm), fine (106 to 250 μm), and very fine (45 to 106 μm) sand fractions. Percent sand (Equation 8), silt (Equation 9), and clay (Equation 10) were calculated via the following equations, where sand = mass of dry sand; sample = mass of dry sample after removal of organic matter; $boat_s$ = mass of aluminum weighing dish and aliquot (dry); and $boat_b$ = mass of aluminum weighing dish and blank (dry). All masses are in grams (g).

$$\%sand = (sand*100)/\ sample \quad (8)$$

$$\%clay = ((boat_s - boat_b)*40*100)/sample \quad (9)$$

$$\%silt\ = 100\% - \%clay - \%sand \quad (10)$$

The particle settling times are determined following Stokes' Law. In this method, a small aliquot (25 mL in this case) is withdrawn from the graduated cylinder with a pipette at a specified depth (h), at a specified time (t), in which all particles coarser than (X) have settled below depth (h). The settling time for clay particles (<2 μm) can be calculated for a given depth and temperature with Stokes' Law in the form of Equation 11, where η = fluid viscosity (g cm^{-1} s^{-1}); g = acceleration due to gravity (cm s^{-2}), ρ_s = particle density (g cm^{-3}), ρ_1 = liquid density (g cm^{-3}), and X = particle diameter (cm) (Gee and Bauder, 1986).

$$t = 18\eta h/[g(\rho_s - \rho_1)X^2] \quad (11)$$

The settling time and sampling depth vary depending on the density and viscosity of the liquid, which vary depending on temperature. All sampling took place at either the 6 or 7 cm depth and followed the settling times in Table 5, based on an assumed particle density of 2.65 g/cm^3 and the maximum clay particle size, 2 μm. Particle density was assumed to equal 2.65 g/cm^3 because this value is the density of quartz (Hillel 1998). The samples were pretreated to remove organic material resulting in samples dominated by quartz sand.

Capillary Fringe

The CF, for the purposes of this study, was defined as the near saturated zone above the water table that has a water content similar to that determined below the water table. The existence of the CF was confirmed with long soil cores collected at the location of FH and FL LSIs at a sandhill lake by Nkedi-Kizza and Richardson (2005) and is further confirmed herein.

Long cores were prepared by carefully trimming soil and roots protruding beyond the ends of the cores, so that the volume of soil was equivalent to the volume of the core. A scale, from 0 to 30 cm, was attached to the length of the long core. An end cap, fitted with a porous frit and valve, was attached to the ends of the long core and sealed with silicon (Figure 10). A constant head of water within the long soil cores was established with Mariotte devices (Figures 11 and 12). The Mariotte devices were constructed from burettes and are described in detail (Appendix A). A constant head was applied to each long soil core by attaching a tube from the outlet of the Mariotte device to the valve at the bottom of the long soil core. This enabled a stable water table to be established at any desired point within the long soil core and the CF to stabilize. The water table was initially established in long soil cores at 5, 10, 15, 20, and 25 cm and in subsequent long cores at 6, 12, 18, and 24 cm. This enabled comparison of the CFH with water table depth. A change in the water table depths, from 5 cm intervals to multiples of 3 cm, was necessary to allow for better comparison with the short cores.

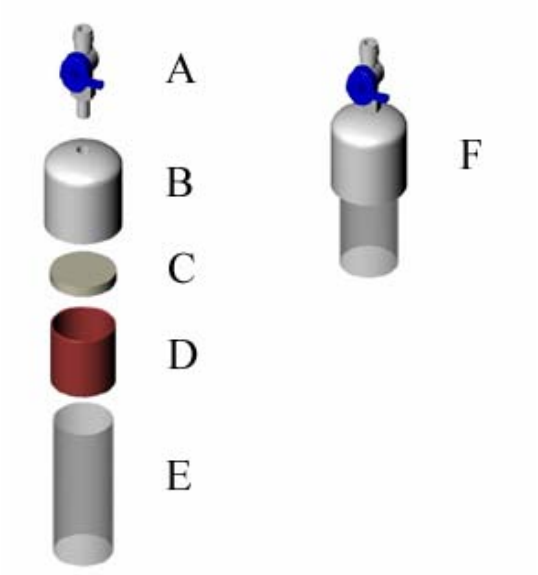

Figure 10. Long soil core assembly (from Nkedi-Kizza and Richardson 2005). A) Valve, B) End cap, C) Porous plate, D) Plastic end cap, E) Soil core, and F) Assembled soil core (Note – the plastic end cap (D) was open on both ends and used to provide a tighter fit between the soil core (E) and the end cap (B), when needed)

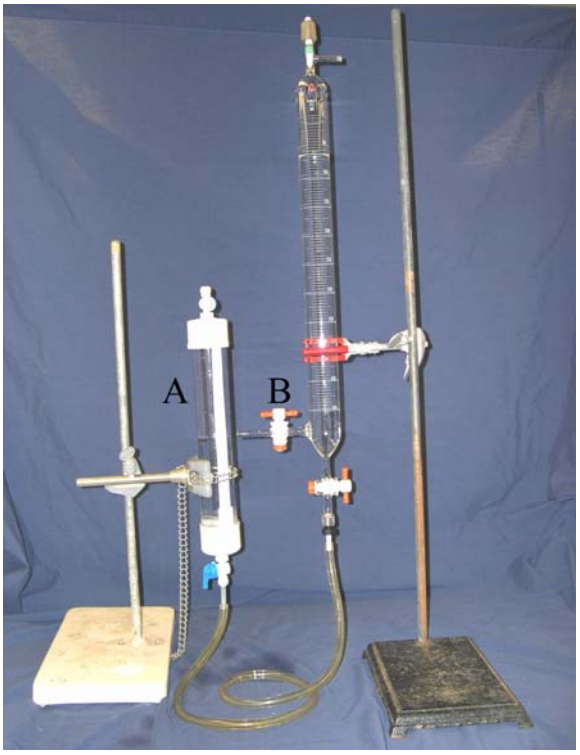

Figure 11. A long soil core with water only (A) and a Mariotte device with the air entry valve (B) set at 20 cm below the top of the soil core

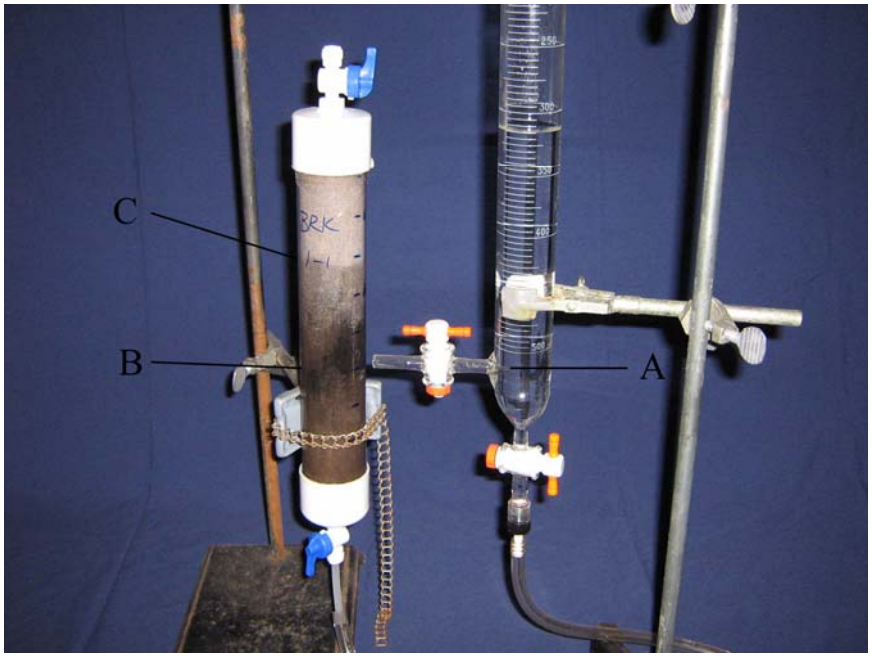

Figure 12. A soil core being wet with a Mariotte device. A) Air entry valve, B) Water table set at 18 cm, and C) Wetting front

The CF was assumed to be stable when the rate of water loss from the Mariotte devices was approximately 1 cm/24 h. This value is equivalent to the rate of water loss from a long soil core containing water only (i.e. evaporation rate) and measured with a Mariotte device. Upon stabilization of the CF within these long cores, the valves were closed on the top and bottom end caps, and the long cores were detached from the Mariotte devices, placed in the freezer in a vertical position, and allowed to freeze. The long cores were frozen to prevent water movement when the cores were cut into smaller segments. Within 1 week the long cores were removed from the freezer and cut into approximately 3-cm segments.

The long cores were typically cut into 3-cm segments, but occasionally, 2-cm segments were needed so that the water table was not located within a segment and to minimize the number of long core segments that did not exactly correspond to the short core 3-cm segments. For example, if the water table was at 20 cm the long core was cut into the following segments: 0 to 3 cm, 3 to 6 cm, 6 to 9 cm, 9 to 12 cm, 12 to 15 cm, 15 to 18 cm, 18 to 20 cm, 20 to 22 cm, 22 to 24 cm, 24 to 27 cm, and 27 to 30.5 cm. For analyses and comparisons the 20 to 22 and 22 to 24 cm segments would be compared with parameters determined for the 21 to 24 cm short core sample. Following initial analysis of the FH cores at Two Mile Pond, the water table was established at 6, 12, 18, and 24 cm in subsequent long soil cores so that the long cores could be sectioned into 3-cm segments without bisecting the water table and to allow better comparisons with the 3-cm short cores.

The bulk density and gravimetric moisture content were determined for each long core segment. These parameters were determined by removing the soil from the long core segment, obtaining the mass of the moist soil, obtaining the mass of oven dry soil (M_s), and determining the volume of each segment. The bulk density was calculated as described in Equation 3. The difference between the moist and dry soil provides the mass of water (M_w) that was in the segment allowing the moisture content to be determined on a gravimetric basis (Equation 12).

$$\theta_w = M_w/M_s \qquad (12)$$

The gravimetric moisture content (θ_w) was then converted to volumetric moisture content (θ_v) and then degree of saturation (s) via some simple relationships. Porosity (*f*), or the volume of pore space within the segment, was calculated based on the bulk density and particle density of each segment (Equation 13). The bulk density from each segment was calculated (Equation 3) and the particle density was assumed to be the same as determined for the short core segments. The mass of water was converted

to the volume of water (V_w) by assuming that the density of water (ρ_w) was one (Equation 14) to calculate the volumetric moisture content (θ_v). Degree of saturation (s) is a measure of the pore space filled with water and was calculated with Equation 15.

$$f = 1 - (\rho_b / \rho_s) \quad (13)$$

$$\theta_v = (\rho_b * \theta_w)/\rho_w \quad (14)$$

$$s = (\theta_v / f)*100 \quad (15)$$

The CFH was estimated for each long core from the profile of degree of saturation with depth from the soil surface. The degree of saturation in segments above the water table was expected to be equal to that below the water table for some distance and then begin to decrease. The CFH was estimated graphically as the distance between the water table and the point where the regression line fit to the data points where the degree of saturation began to decrease within the core segments intersected the calculated mean degree of saturation for all soil samples taken below the water table (s_b, Figure 13). If the percent saturation did not decrease with increasing height above the water table, the CFH was assumed to extend to at least the soil surface.

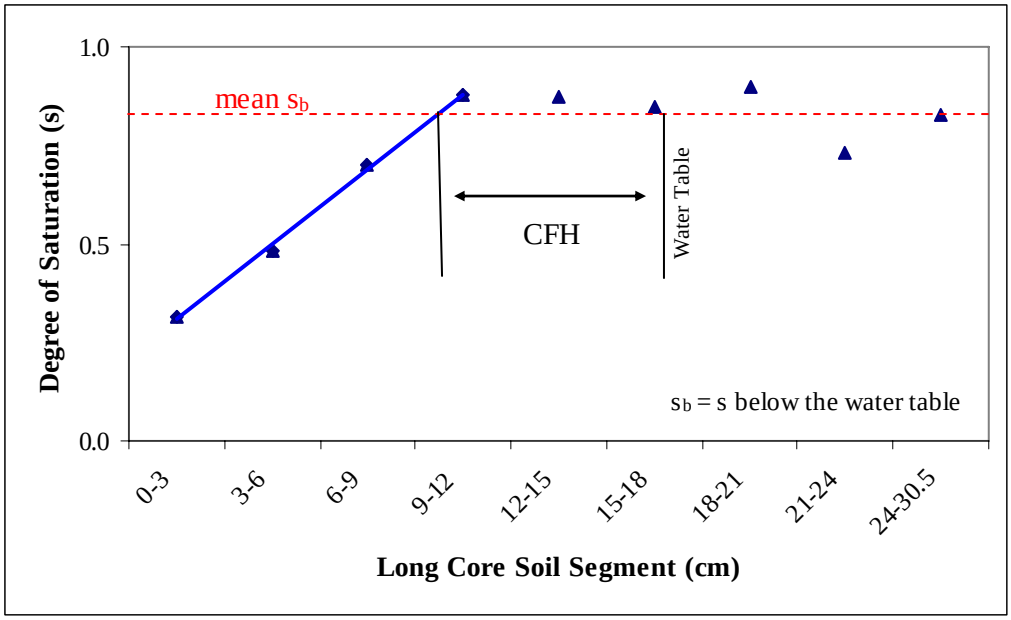

Figure 13. Example estimation of the capillary fringe height (CFH) from moisture content with depth

Oxidation-Reduction Potential (ORP)

The measurement of ORP followed the method presented by Faulkner et al. (1989). A 1.3-cm segment of platinum wire was soaked in a 1:1 mixture of concentrated nitric and hydrochloric acids for at least 4 h and then soaked in DI water for at least 12 h, to remove any surface contamination on the platinum wire. The 1.3-cm platinum wire was then welded onto an 18 gauge insulated copper wire. The welded area was covered with heat shrink tubing for insulation and then covered with epoxy to waterproof the connection. This resulted in 1 cm of the platinum wire being exposed for contact with the soil on each electrode.

Six platinum electrodes were installed in one FH and one FL long core from each lake sampled. A borehole in the soil that was just smaller than the diameter of the electrodes was created with a hollow glass tube. The boreholes were approximately 1 cm shallower than the depth of interest to ensure good contact between the platinum wire and the soil. The platinum electrodes were installed at 1, 3, 6, 9, 12, and 15 cm depths in each long core. Upon installation of the platinum electrodes, the long cores were suspended in a DI water bath resulting in a water table 18 cm below the soil surface of the long cores and 3 cm below the deepest electrode. The water table was established at 18 cm to enable comparison with the majority of the long cores in which the CFH was determined. The water bath was monitored regularly to maintain the water level at 18 cm in the long cores.

After 1 h ORP was measured with an Accumet AP71 pH/mV/C meter and an Accumet 13-620-258 standard reference electrode. The reference electrode was placed in the water bath and the Accumet AP71 was attached to the bare copper at the end of each platinum electrode. The Accumet AP71 corrects the ORP reading for the reference electrode and temperature so that the readings are comparable to the ORP that would have been measured with a standard hydrogen electrode. The readings were taken weekly for five weeks until the ORP readings were consistent with the readings from the previous week.

The degree of saturation at each platinum electrode was estimated as the median degree of saturation determined for the respective lake and 3-cm segments from duplicate long cores from which the CFH was determined. The HAC was estimated in each long soil core at the degree of saturation above which ORP was less than 0 mV. The degree of saturation was graphically estimated as the point where a regression line fit through the

ORP data plotted against degree of saturation intersected the ORP of 0 mV (Figure 14).

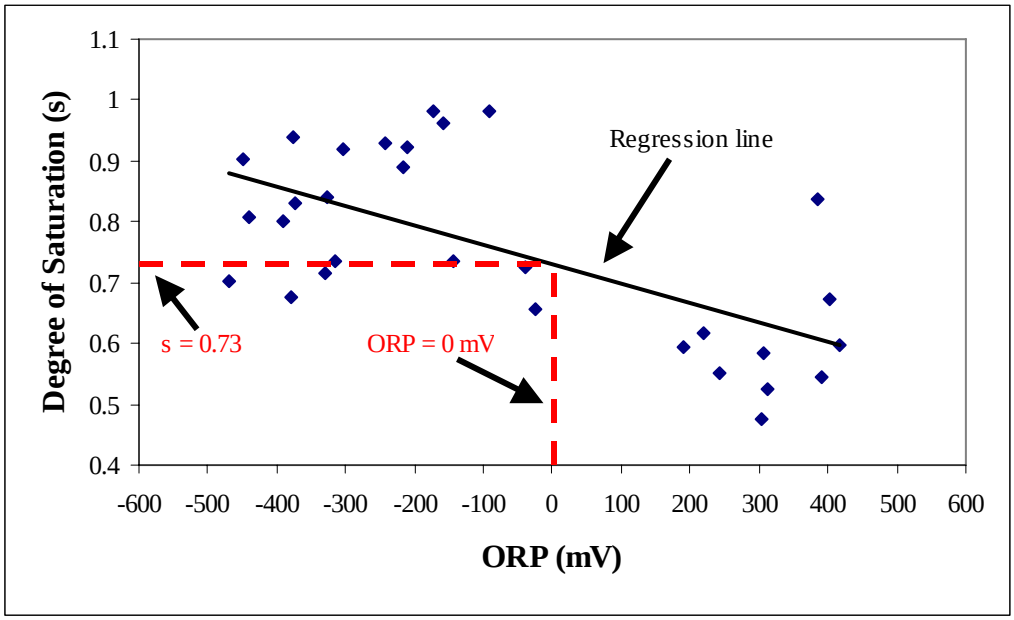

Figure 14. Example estimation of degree of saturation (s) above which the oxidation-reduction potential (ORP) is less than 0 mV

The HAC was then estimated in each long soil core where the degree of saturation equaled the degree of saturation above which the ORP was less than 0 mV. When the degree of saturation in adjacent long soil core segments encompassed this value then the degree of saturation was linearly interpolated between adjacent segments to estimate the HAC at the appropriate degree of saturation.

Soil pH

Soil pH was measured with an Accument 13-620-287 pH probe and an Accumet pH Meter 925 for each 3-cm short core. Soil pH was determined in a mixture of 10 g of soil and 30 mL of DI water. The pH electrode was thoroughly rinsed with DI water and dried between each pH measurement.

Soil Moisture Release Curves

The first 10 short cores from each site were delivered to the Soil Moisture Laboratory at the University of Florida, Soil and Water Science Department, for collection of soil moisture retention data under the supervision of Dr. Rao Mylavarapu. A soil moisture release curve (SMRC) is a plot of matric potential or suction versus soil water content of the sample. The SMRCs

were determined by applying known pressures to the short cores and determining the equilibrium water content. The equilibrium water content at each pressure applied is held in the soil by a suction equivalent to the pressure applied. Soil water contents were determined for pressures ranging from 0 to 345 cm of water (hereafter referred to as cm) following the procedures described in Tempe pressure cell operating instructions (Soil Moisture Equipment Corp.). Pressures of 5,000 and 15,000 cm were applied with a pressure plate.

Tempe pressure cells (Soil Moisture Equipment Corp.) are two-piece containers designed to hold short soil cores. The lower piece of the Tempe cell is fitted with a porous ceramic plate and the upper and lower pieces are fitted with o-rings. The porous ceramic plate in the lower part of the cell was saturated with degassed DI water. The short core was then pressed into the lower part of the cell so that the o-ring made a complete seal on the soil core and to ensure that the soil was in good contact with the porous ceramic plate. The short core was then saturated with degassed DI water and the upper portion of the cell was pressed onto the upper part of the short core. The upper and lower cell parts were bolted together and the initial mass was recorded to determine the water content at a suction of 0 cm. Next, hand pressure was applied to the Tempe cells at an estimated pressure of 3.5 cm . When no additional water exited the Tempe cell it was considered to be at equilibrium water content and its mass was recorded.

Subsequent pressures were applied using a pump to generate air pressure at the top of the Tempe cell through a tube. The air supply was passed through two regulator valves to minimize pressure fluctuations. Beyond the second regulator valve the air supply was attached to a rigid tube submersed in a column of water open to the atmosphere and to the tube supplying air to the Tempe cells. The air pressure was precisely controlled by the water level in the column. If the water level was 45 cm above the opening of the rigid tube, any pressure greater than 45 cm in the tube results in bubbles leaving the rigid tube. Slightly higher air pressures than desired were passed through the second regulation valve so that bubbles slowly exited the rigid tube and constant pressures were applied. Upon reaching equilibrium water content, the pressure applied and the mass of the Tempe cell with sample was recorded and the next desired pressure was applied up to 345 cm.

Pressures greater than 345 cm of water were applied using a pressure plate apparatus. This apparatus is composed of a chamber containing a porous plate. Soil cores were place on the porous plate, the chamber was sealed, and a pressure of 5,000 cm was applied until equilibrium water content was

reached. At the equilibrium water content the soil cores were weighed to determine the mass of water lost. The cores were placed back on the ceramic plate, the chamber was sealed, and a pressure of 15,000 cm was applied until equilibrium water content was again reached. At the equilibrium water content the soil cores were again weighed to determine the mass of water lost.

After all pressures were applied the short soil cores were oven dried to determine the bulk density (Equation 3) and the mass of dry soil. The mass of water lost was summed to determine the initial mass of water and the mass of water remaining in the soil subsequent to each pressure applied. The gravimetric water content (Equation 12) was calculated based on these data and converted to volumetric water content (Equation 14) to develop the SMRCs.

The suction and water content data were plotted and fitted with the Brooks and Corey equations (Brooks and Corey 1964; Equations 16 and 17), where θ = water content; θ_s = saturated water content; θ_r = residual water content; h = matric potential; h_A = air entry value matric potential; λ is a fitting parameter.

$$(\theta-\theta_r)/(\theta_s-\theta_r) = [h_A/h]\lambda \quad \text{when } h > h_A \tag{16}$$

$$(\theta-\theta_r)/(\theta_s-\theta_r) = 1 \quad \text{when } h < h_A \tag{17}$$

The AEV may be assumed to be equal to the CF under draining conditions (Berkowitz et al. 1999; Gillham 1984), and hence the AEV was the main component of the SMRCs of interest in this study. AEVs were calculated for the short cores at each FH and FL location at each lake based on Equation 17. The natural log of the suctions within the exponential range of the data (15-150 cm of suction for these soils) were plotted against the effective saturation (S_{eff}, Equation 18), with residual water content (θ_r) taken at 345 cm of suction, and provided a linear relationship between S_{eff} and ln h.

$$S_{eff} = (\theta-\theta_r)/(\theta_s-\theta_r) \tag{18}$$

The AEVs was estimated as the point where a regression line fit through these data points intersected an effective saturation equal to one (Figure 15).

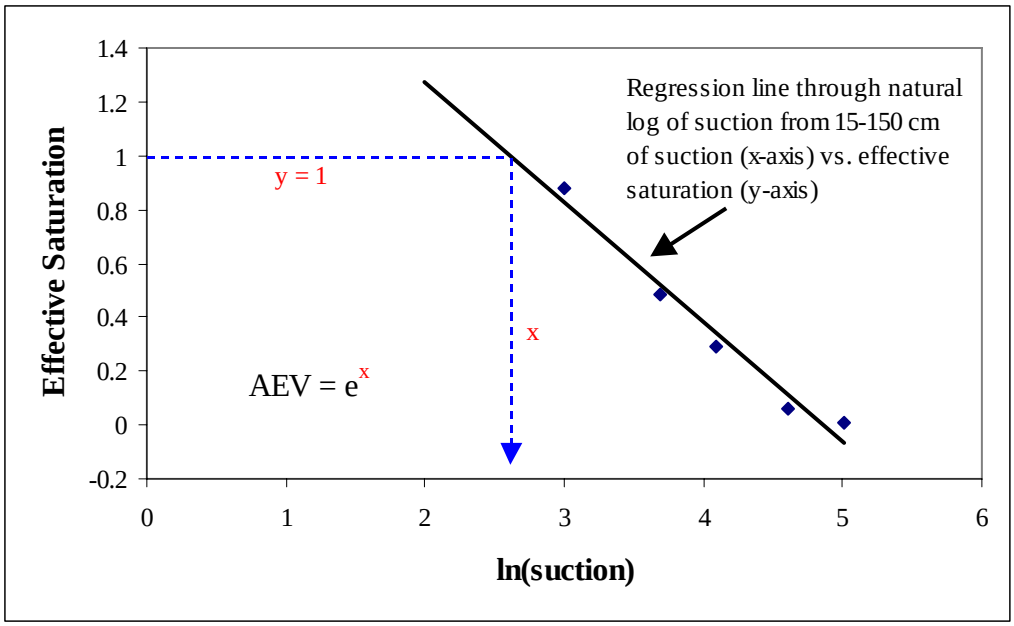

Figure 15. Example calculation of the air entry value (AEV) from suction data and effective saturation

STATISTICAL ANALYSIS PROCEDURES

Percent sand, silt, and clay, percent very coarse, coarse, medium, fine, and very fine sand fractions, and percent OC were initially reviewed for quality assurance with principal components analysis (PCA). PCA is a valuable tool for exploratory data analysis, identifying patterns in the data, reducing the number of variables in regression analysis, multivariate outlier detection, and reducing the number of dimensions without much loss of information (SAS Institute, Inc. 2003). One principal component (PC) is calculated for each variable based on the eigenvectors and eigenvalues generated from a correlation matrix of the original data. Eigenvectors are the coordinates that define the direction of the axes through the three-dimensional data cluster and eigenvalues are the length of the vectors. Each PC is a linear combination of the original variables, with coefficients equal to the eigenvectors of the correlation matrix. The first PC provides the best possible fit to the data points, and thus accounts for the largest portion of the variability in the data, followed by the second PC and so on.

Prior to comparisons of variable means, the particle-size classes, bulk density for the long and short cores, and percent OC were tested for normality (α=0.05, Shapiro-Wilkox normality test, SAS Institute Inc. 2003). These soil parameters were compared by lake, depth, and level with an ANOVA generated with the General Linear Model (GLM, SAS Institute, Inc.

2003). The Type III ANOVA in the GLM procedure was applicable because this method is robust when testing unbalanced samples. Bulk density from short and long soil cores were compared with a non-parametric two-sided t-test ($\alpha/2=0.025$, Wilcoxon Two-Sample Test – t approximation, SAS Institute, Inc. 2003).

Multiple linear regressions were developed to determine the best predictor of the CFH, HAC, and AEVs from the physical soil characteristics and PCs of the physical soil characteristics (SAS Institute, Inc. 2003, Hintze 2004). The final predictive models of CFH, HAC, and AEVs were confirmed with the 'RSQUARE' option for regression analysis (SAS Institute, Inc. 2003). The 'RSQUARE' procedure provided the best fit for a set of variables.

The predictive capability of the regression models was interpreted with an R^2-like statistic, calculated from the prediction sum of squares (PRESS, Equation 19, Hintze 2004), where y_i is the actual y value and $\hat{y}_{i,-i}$ is the predicted y value with the i^{th} observation deleted.

$$\text{PRESS} = \sum \left(y_i - \hat{y}_{i,-i} \right)^2 \qquad (19)$$

The PRESS R^2 (Equation 20) reflects the prediction ability of the model.

$$\text{PRESS } R^2 = 1 - \text{Press/Total Sum of Squares} \qquad (20)$$

If R^2 is high and PRESS R^2 is similar to the R^2, then the predictive capability of the regression model is validated (Hintz 2004).

RESULTS AND DISCUSSION

The goals of this study were to quantify the CFH and HAC in soil samples collected near the FH and FL LSIs at three sandhill lakes and develop models to estimate the CFH and HAC from the physical soil characteristics. In addition to these goals, the CFH and HAC were related to the AEVs, models to estimate the AEVs from the physical soil characteristics were developed, and an example of how this research might be applied to support the determination of minimum levels is presented.

The physical soil characteristics were determined and compared among lakes to accomplish these goals. The measured and calculated soil characteristics are summarized in Appendix B (Table B1 and B2) and were compared with the CFHs, AEVs, and HACs. Multiple linear regressions were developed to predict the CFH, AEV, and HAC from the physical soil characteristics to quantify offsets to support the determination of minimum levels at sandhill lakes. Linear regressions were also developed between the CFH and HAC and the AEVs in an attempt to provide an alternative method to predict the CFH and HAC.

DATA PROCESSING

Prior to data analysis, it was necessary to statistically compare sampling methods because multiple soil characteristics were determined from short and long soil cores with the intent of building a single data set. Sampling methods were compared by testing for significant differences in bulk density between short cores and each long core 3-cm segment for FH and FL sampling locations within each lake. Bulk density measures were not normally distributed (p<0.05) so differences in mean bulk density were tested with the non-parametric Wilcoxon Two-Sample Test – t approximation (SAS Institute, Inc. 2003). No statistically significant differences in mean bulk density were observed for 59 of 60 samples (Table 6). A statistically significant difference in mean bulk density between the short and long cores was observed for one 3-cm segment, the 9-12 cm segment at the Two Mile Pond FH location ($\alpha/2$=0.025, p=0.0329). This suggested that the short and long core sampling techniques did not result in differential compaction of the soil and allowed for further comparison of data from the long and short cores, within and among lakes. Compaction of the soil would alter the pore-size distribution by reducing the number of relatively large pores and increasing the number of relatively small and intermediate pores, which would then impact the measurement of the CFH, HAC, and AEVs.

Table 6. Wilcoxon scores (Rank Sums) for bulk density: Long core segments vs. short cores

Lake	Segment (cm)	Long Soil Cores		Short Soil Cores		$P^{£}$
		N[£]	Mean Score	N	Mean Score	
Swan (FH)	0-3	12	8.33	3	6.67	0.6213
	3-6	12	8.33	3	6.67	0.6213
	6-9	12	8.00	3	8.00	1.0000
	9-12	12	8.25	3	7.00	0.7236
	12-15	12	8.08	3	7.67	0.9435
	15-18	9	6.22	3	7.33	0.7186
	18-21	10	6.50	3	8.67	0.4616
	21-24	6	5.50	3	4.00	0.5367
	24-27	10	7.20	3	6.33	0.8041
	27-30	3	3.67	3	3.33	1.0000
Swan (FL)	0-3	9	5.78	3	8.67	0.2909
	3-6	9	6.00	3	8.00	0.4750
	6-9	9	7.33	3	4.00	0.2221
	9-12	9	7.00	3	5.00	0.4750
	12-15	9	6.67	3	6.00	0.8567
	15-18	7	5.43	3	5.67	1.0000
	18-21	9	6.67	3	6.00	0.8567
	21-24	5	4.40	3	4.67	1.0000
	24-27	9	6.00	3	8.00	0.4750
	27-30	2	4.50	3	2.00	0.2224
Brooklyn (FH)	0-3	5	5.20	3	3.33	0.4008
	3-6	5	5.00	3	3.67	0.5698
	6-9	5	5.20	3	3.33	0.4008
	9-12	5	4.60	3	4.33	1.0000
	12-15	5	5.00	3	3.67	0.5698
	15-18	5	5.40	3	3.00	0.2719
	18-21	5	5.60	3	2.67	0.1797
	21-24	5	5.60	3	2.67	0.1797
	24-27	5	5.40	3	3.00	0.2719
	27-30	-	-	-	-	-
Brooklyn (FL)	0-3	4	4.00	3	4.00	1.0000
	3-6	4	3.75	3	4.33	0.8655
	6-9	4	3.50	3	4.67	0.6149
	9-12	4	4.50	3	3.33	0.6149
	12-15	4	4.75	3	3.00	0.4108
	15-18	4	4.50	3	3.33	0.6149
	18-21	4	5.00	3	2.67	0.2622
	21-24	4	5.50	3	2.00	0.0998
	24-27	4	5.50	3	2.00	0.0998
	27-30	-	-	-	-	-

Table 6. Continued

Lake	Segment (cm)	Long Soil Cores		Short Soil Cores		*p*
		N	Mean Score	N	Mean Score	
Two Mile Pond (FH)	0-3	21	13.29	3	7.00	0.1759
	3-6	21	11.71	3	18.00	0.1759
	6-9	24	12.92	3	22.67	0.0599
	9-12	21	11.24	3	21.33	0.0329[a]
	12-15	20	11.90	3	12.67	0.8923
	15-18	19	10.95	3	15.00	0.3496
	18-21	19	11.26	3	13.00	0.7057
	21-24	19	12.42	3	5.67	0.1188
	24-27	20	12.80	3	6.67	0.1711
	27-30	9	7.00	3	5.00	0.4750
Two Mile Pond (FH)	0-3	12	6.75	3	13.00	0.0551
	3-6	12	7.17	3	11.33	0.1919
	6-9	12	8.25	3	7.00	0.7236
	9-12	12	6.92	3	12.33	0.0927
	12-15	12	7.17	3	11.33	0.1919
	15-18	10	6.60	3	8.33	0.5651
	18-21	12	7.25	3	11.00	0.2401
	21-24	8	5.50	3	7.33	0.4913
	24-27	11	6.64	1	5.00	0.7774
	27-30	3	3.00	1	1.00	0.4370

[£]N=sample size *p*=probability

[a]Statistically significant at $\alpha/2=0.05$

The relationship between percent OC and percent LOI was determined for soil samples at Two Mile Pond to estimate the percent OC for the remaining lake soil samples. These data were necessary to complete the soil core data set (Appendix B, Table B1). A regression between percent OC and percent LOI for Two Mile Pond was developed ($F=163.87$, $p<0.0001$, $R^2=0.5897$, Equation 21, Figure 16). The relationship between percent OC and percent LOI had a similar slope to those determined in numerous other studies (1.72 – 2.20), as summarized by Nelson and Sommers [1996]).

$$\text{Percent LOI} = 1.76(\text{percent OC}) + 0.23 \qquad (21)$$

The Walkley-Black method stipulates chromic acid for the measurement of oxidizable OC. The OM content was measured with an alternative method, LOI, because of concerns regarding the disposal of the chromic acid and hazards associated with its use. The LOI method relies on weight loss from an oven-dry soil sample during high temperature ignition to estimate OM content (Nelson and Sommers 1996 and Schulte

and Hopkins 1996). Temperatures ranging from 360 to 900°C and ignition times ranging from 0.5 to 28 h were reported to result in nearly complete combustion of OM and a high degree of fit with percent OC determined via Walkley-Black (Nelson and Sommers 1996 and Schulte and Hopkins 1996).

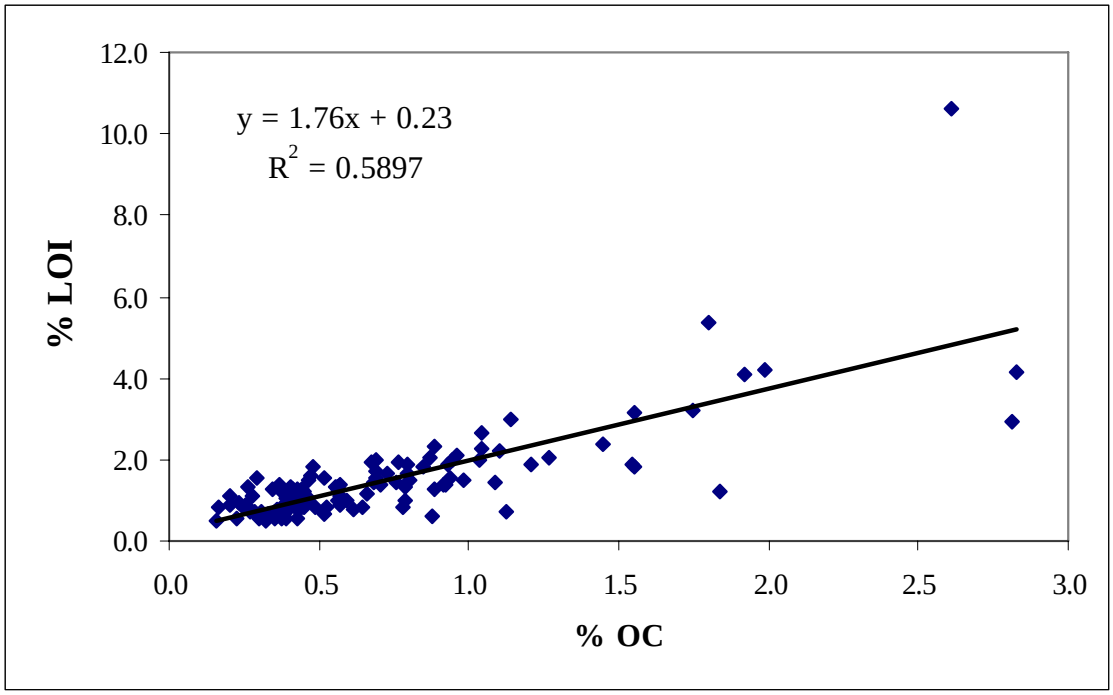

Figure 16. Relationship between percent organic carbon (OC) and percent weight loss on ignitions (LOI)

The relationship between percent OC and percent LOI had a reduced fit compared to the numerous other studies summarized by Nelson and Sommers (1996) and Schulte and Hopkins (1996). The reduced fit between percent OC and percent LOI has several causes. First, there were slight differences in estimation of the titration endpoint for the Walkley-Black method when determined by different technicians. Second, percent OC and percent LOI were not determined from the same samples for half of the samples in the regression equation reported (Equation 21). These samples were within 1 m of each other but likely have slightly different OC and OM contents and contribute to the reduced fit of the regression.

Percent sand, silt, and clay; percent very coarse, coarse, medium, fine, and very fine sand fractions; and percent organic carbon were reviewed with PCA, as a quality assurance step to identify outliers and unexpected data. The correlation matrix, eigenvectors, and eigenvalues are summarized in Tables 7, 8, and 9. The first two PCs of percent sand, silt, and clay; percent

very coarse, coarse, medium, fine, and very fine sand fractions; and percent organic carbon (Appendix C) account for approximately 57% of the variability observed for these characteristics (Table 9).

Scatter plots of the first two PCs were generated by 3-cm segments, by FH and FL levels, and by lake (Figures 17, 18, and 19). In general, the data were clustered, however, several data points were clearly outside of the cluster. These data points were tracked to the original data resulting in the correction or deletion of the data if errors were identified. Percent sand, silt, and clay were deleted for one sample (SW FH1 0-3 cm) due to an error during analysis. The Lake Brooklyn FH2 samples also plotted slightly outside of the cluster, suggesting a difference between this and the other sampling locations. This difference was not the result of an error during laboratory analysis, and is likely the result of a past disturbance or landscape position at this particular site. The Lake Brooklyn FH2 samples were retained for data analyses since the observed differences were not due to error and represent the potential variation that may be encountered.

Table 7. Correlation matrix for determination of principal components of percent sand, silt, and clay; percent very coarse, coarse, medium, fine, and very fine sand fractions; and percent organic carbon (OC)

	cl	sa	si	vc	c	m	fi	vf	oc
cl	1.000	-0.844	0.375	0.165	-0.058	-0.308	0.207	0.111	0.537
sa	-0.844	1.000	-0.806	-0.093	0.119	0.271	-0.086	-0.309	-0.580
si	0.375	-0.806	1.000	0.003	-0.144	-0.142	-0.064	0.401	0.421
vc	0.165	-0.093	0.003	1.000	0.622	-0.451	0.230	-0.125	0.192
c	-0.058	0.119	-0.144	0.622	1.000	0.241	-0.395	-0.201	0.005
m	-0.308	0.271	-0.142	-0.451	0.241	1.000	-0.803	-0.147	-0.162
fi	0.207	-0.086	-0.064	0.230	-0.395	-0.803	1.000	-0.375	0.189
vf	0.111	-0.309	0.401	-0.125	-0.201	-0.147	-0.375	1.000	-0.134
oc	0.537	-0.580	0.421	0.192	0.005	-0.162	0.189	-0.134	1.000

Table 8. Eigenvectors for determination of principal components of percent sand, silt, and clay; percent very coarse, coarse, medium, fine, and very fine sand fractions; and percent organic carbon (OC)

	PC1	PC2	PC3	PC4	PC5	PC6	PC7	PC8	PC9
cl	0.462	-0.347	0.103	-0.171	-0.709	-0.085	0.072	-0.037	0.480
sa	-0.520	0.220	-0.082	0.058	0.110	0.279	0.020	-0.049	0.761
si	0.401	-0.332	0.035	0.087	0.603	-0.414	-0.004	-0.038	0.429
vc	0.144	0.404	0.496	0.353	0.099	0.032	0.657	0.045	-0.032
c	-0.116	0.088	0.720	0.113	-0.035	-0.117	-0.632	0.178	0.041
m	-0.325	-0.430	0.221	-0.418	-0.021	-0.101	0.363	0.586	0.026
fi	0.223	0.556	-0.344	-0.063	0.086	-0.155	-0.147	0.681	0.051
vf	0.136	-0.419	-0.122	0.661	-0.120	0.426	-0.064	0.392	0.038
oc	0.384	0.023	0.189	-0.455	0.298	0.717	-0.078	0.016	0.009

Table 9. Eigenvalues and proportion of variance accounted for by each principal component of percent sand, silt, and clay; percent very coarse, coarse, medium, fine, and very fine sand fractions; and percent organic carbon (OC)

	Eigenvalue	Difference	Proportion	Cumulative
PC1	3.138	1.131	0.349	0.349
PC2	2.007	0.309	0.223	0.572
PC3	1.697	0.581	0.189	0.760
PC4	1.116	0.572	0.124	0.884
PC5	0.545	0.116	0.061	0.945
PC6	0.379	0.273	0.042	0.987
PC7	0.105	0.098	0.012	0.999
PC8	0.008	0.002	0.001	0.999
PC9	0.005	-	0.001	1.000

The first two PCs plotted by 3-cm segments show a fairly random distribution of the segments (Figure 17). This suggests that no differences in texture were detected from the soil surface to a depth of 30 cm. A random distribution of the PCs plotted by FH and FL level was also observed (Figure 18). This suggests that no differences in texture were detected between the FH and FL sampling locations. However, a random distribution was not observed for the PCs plotted by lake (Figure 19). The PCs plotted by lake form clusters for each individual lake. Some overlap exists due to the similarity in texture but the particle-size distribution among lakes is sufficiently different to be detected.

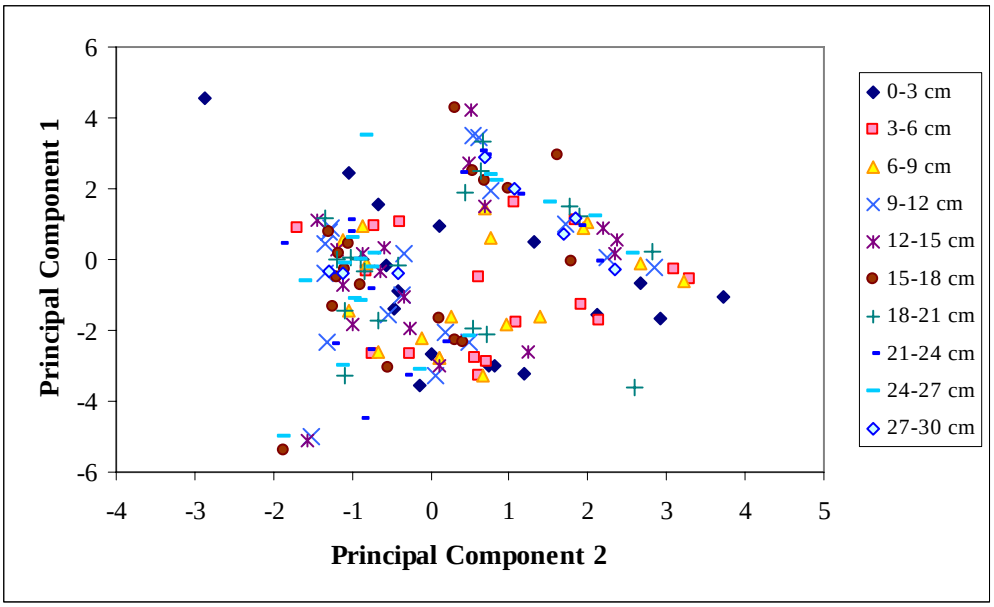

Figure 17. Scatter plot of principal components 1 and 2 labeled by 3-cm segment

Note – Principal components were generated from percent sand, silt, and clay; percent very coarse, coarse, medium, fine, and very fine sand fractions; and percent OC.

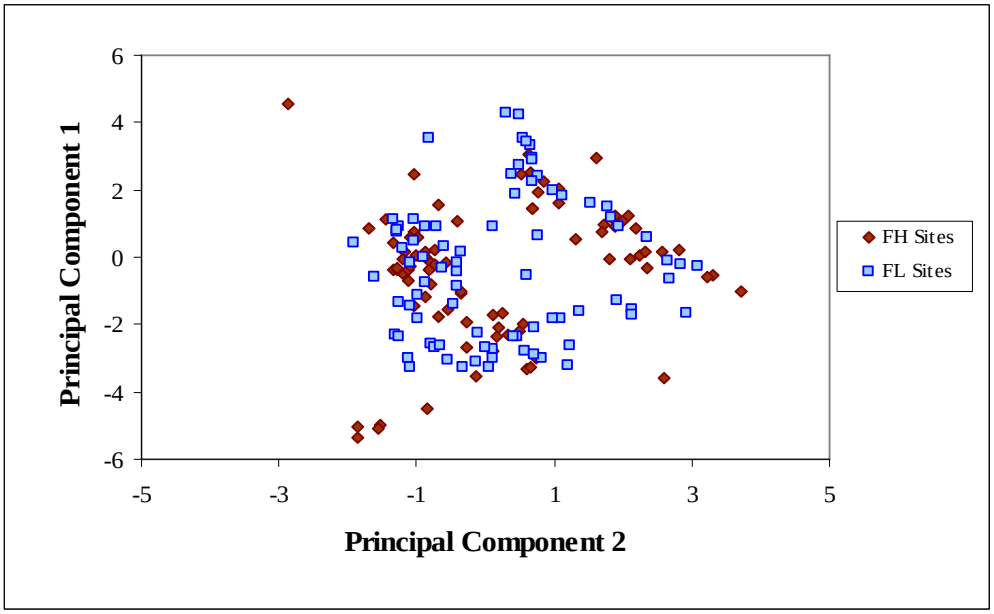

Figure 18. Scatter plot of principal components 1 and 2 labeled by frequent high (FH) and frequent low (FL) levels

Note – Principal components were generated from percent sand, silt, and clay; percent very coarse, coarse, medium, fine, and very fine sand fractions; and percent OC.

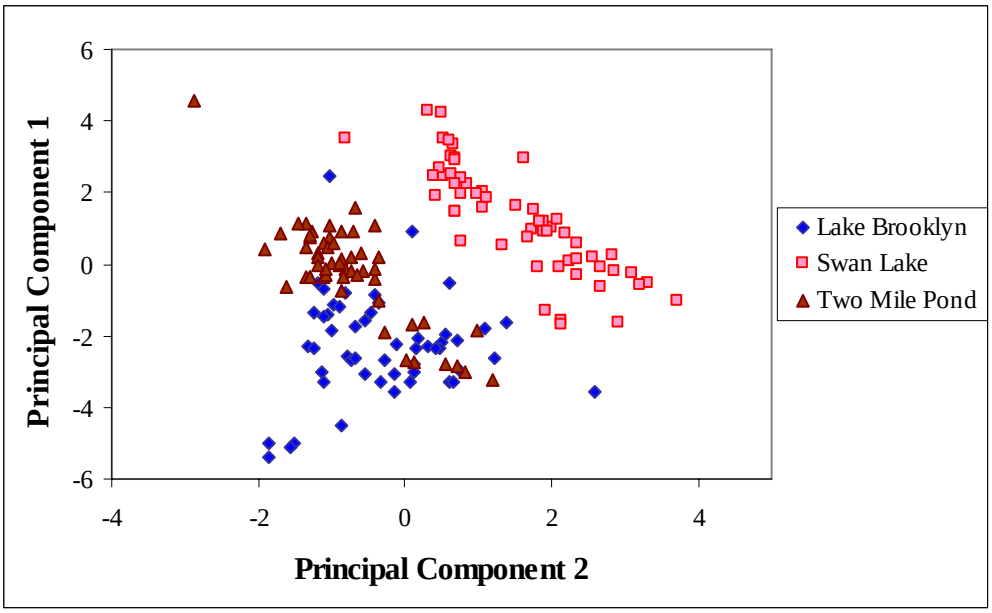

Figure 19. Scatter plot of principal components 1 and 2 labeled by lake

Note – Principal components were generated from percent sand, silt, and clay; percent very coarse, coarse, medium, fine, and very fine sand fractions; and percent OC.

PHYSICAL SOIL CHARACTERISTICS

Samples for all lakes had greater than 92.6% sand, less than 4.1% silt, and less than 4.2% clay (Figures 20, 21, and 22). Most 3-cm segments for all lakes had greater than 95% sand; a similar distribution of very coarse, coarse, medium, fine, and very fine sand fractions (dominated by medium and fine sand); and less than 1% organic carbon (Figures 20, and 23 – 28). Box plots of each particle-size class (Figure 20 – 27), percent OC (Figure 28), and bulk density (long and short cores, Figure 29) were generated resulting in the identification of several outliers. Outliers were tracked to original data and resulted in deletion of one data point:

- Bulk density from the 0-3 cm long core segment from the FL3 sampling location at Two Mile Pond (1.97 g/cm^3) was deleted due to a clear error in the recorded soil volume.

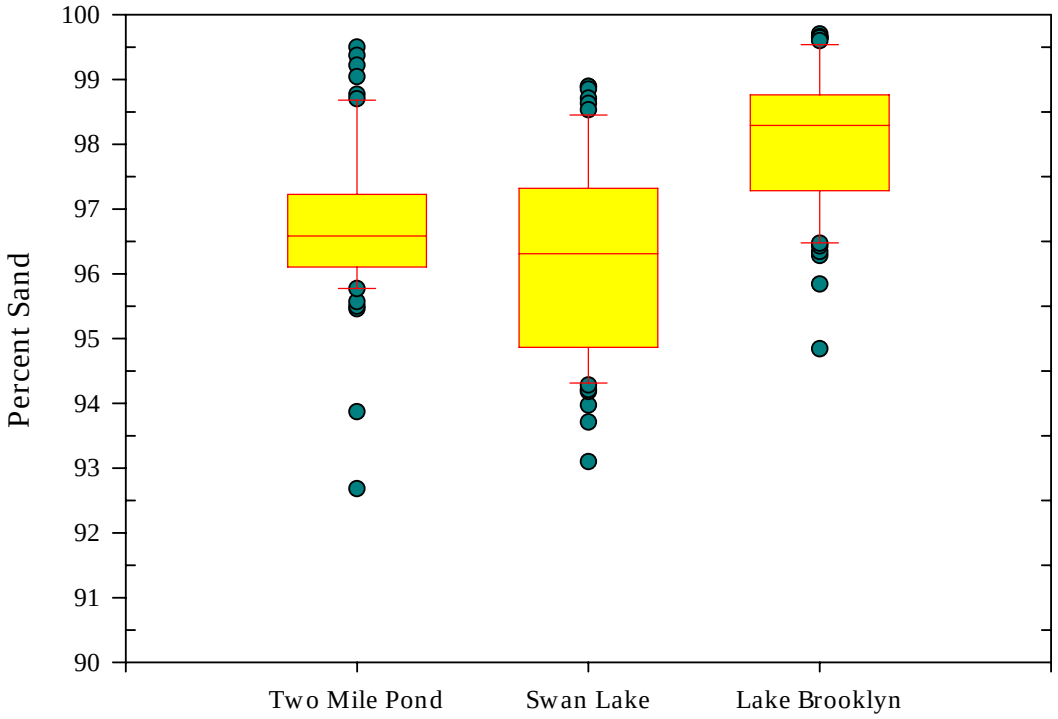

Figure 20. Comparison of percent sand among lakes

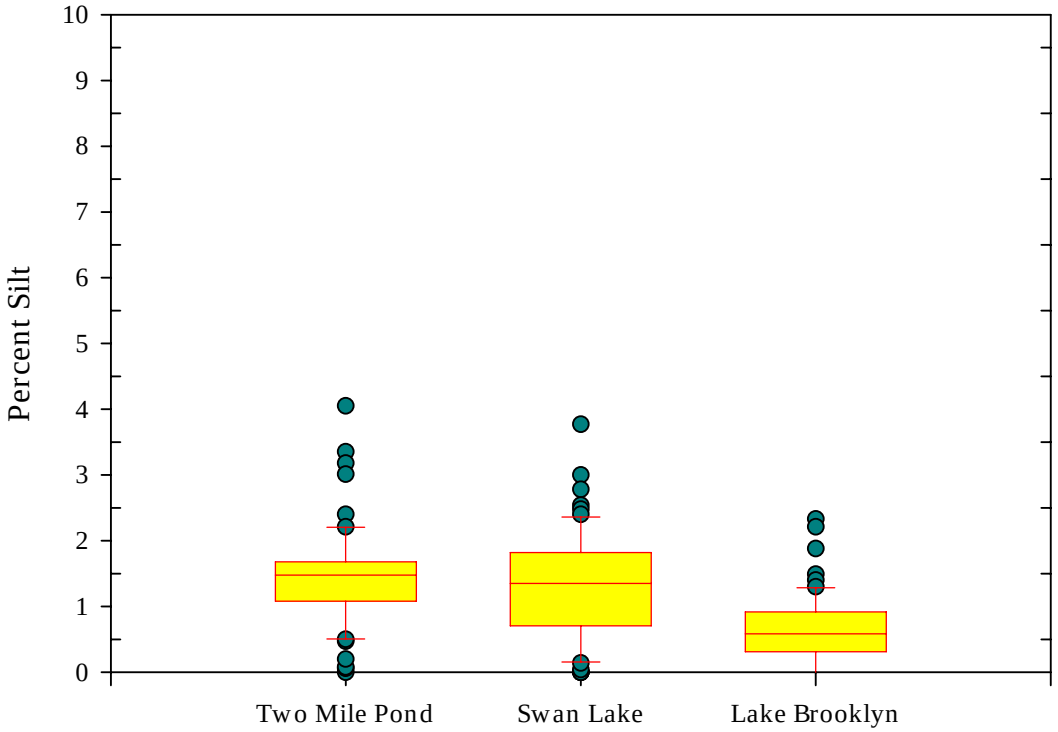

Figure 21. Comparison of percent silt among lakes

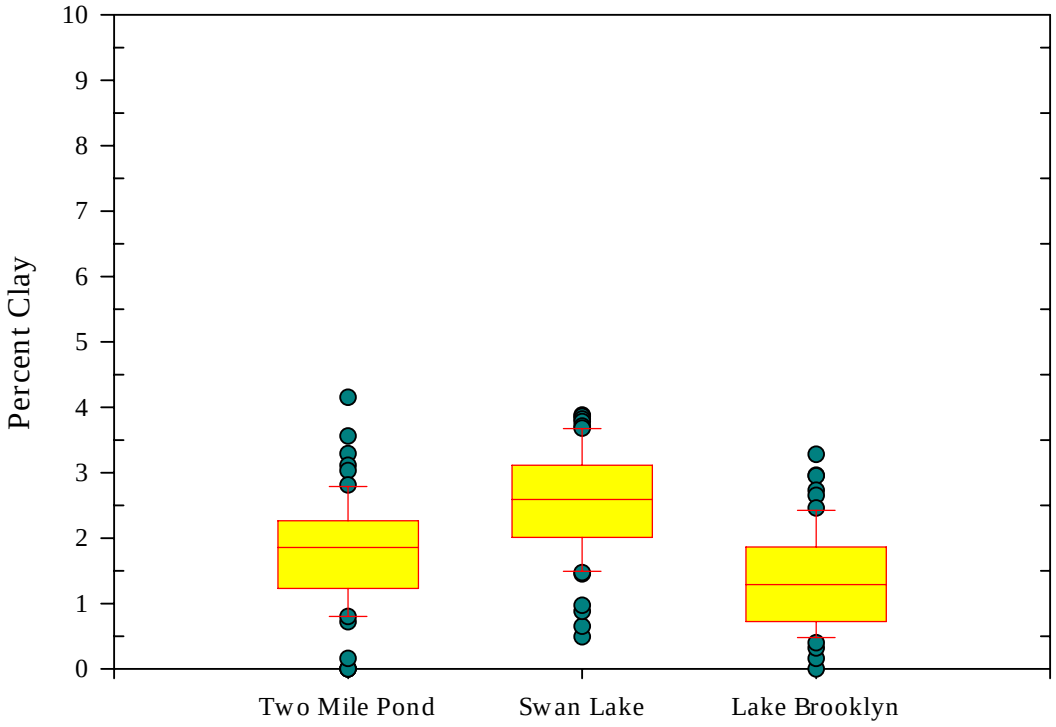

Figure 22. Comparison of percent clay among lakes

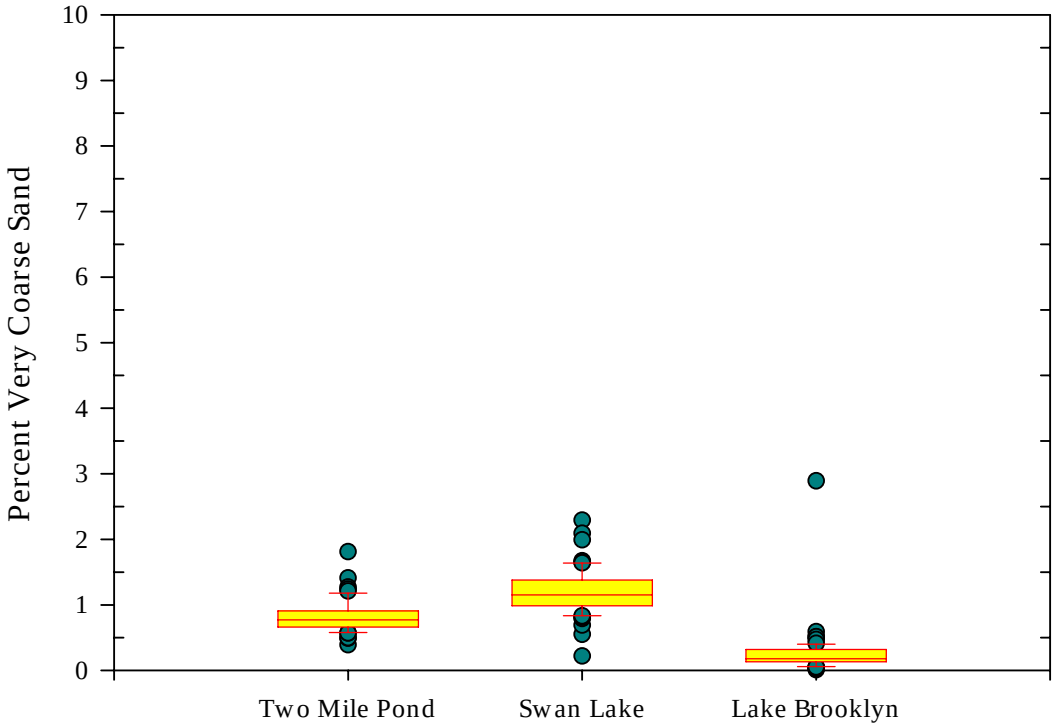

Figure 23. Comparison of percent very coarse sand among lakes

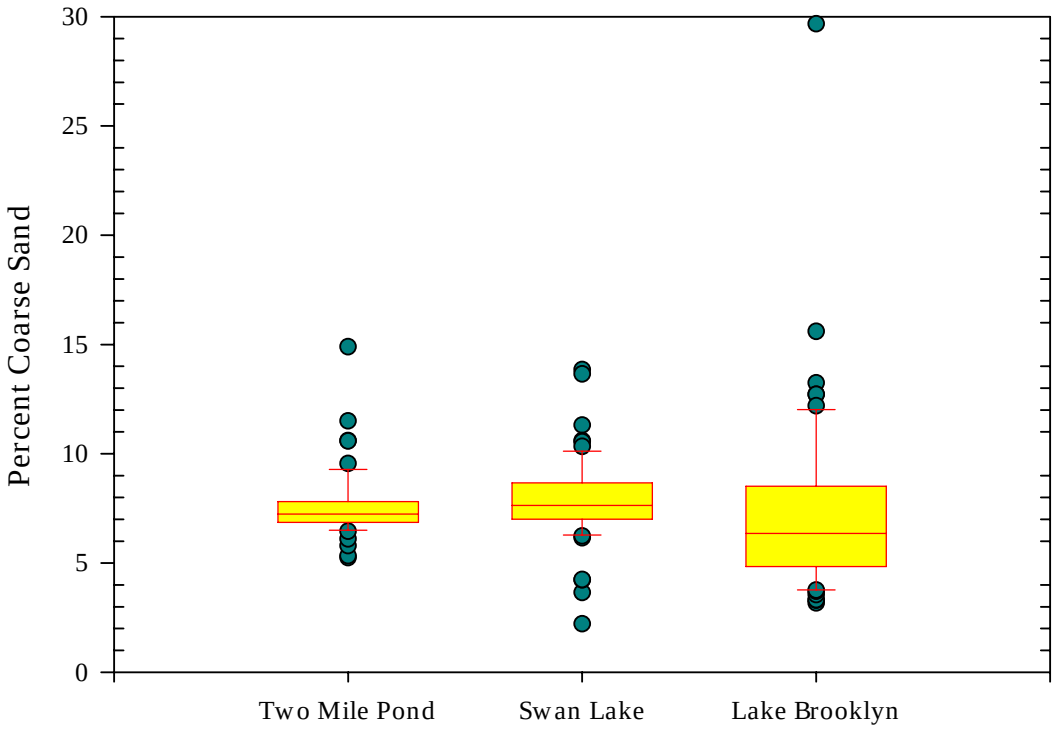

Figure 24. Comparison of percent coarse sand among lakes

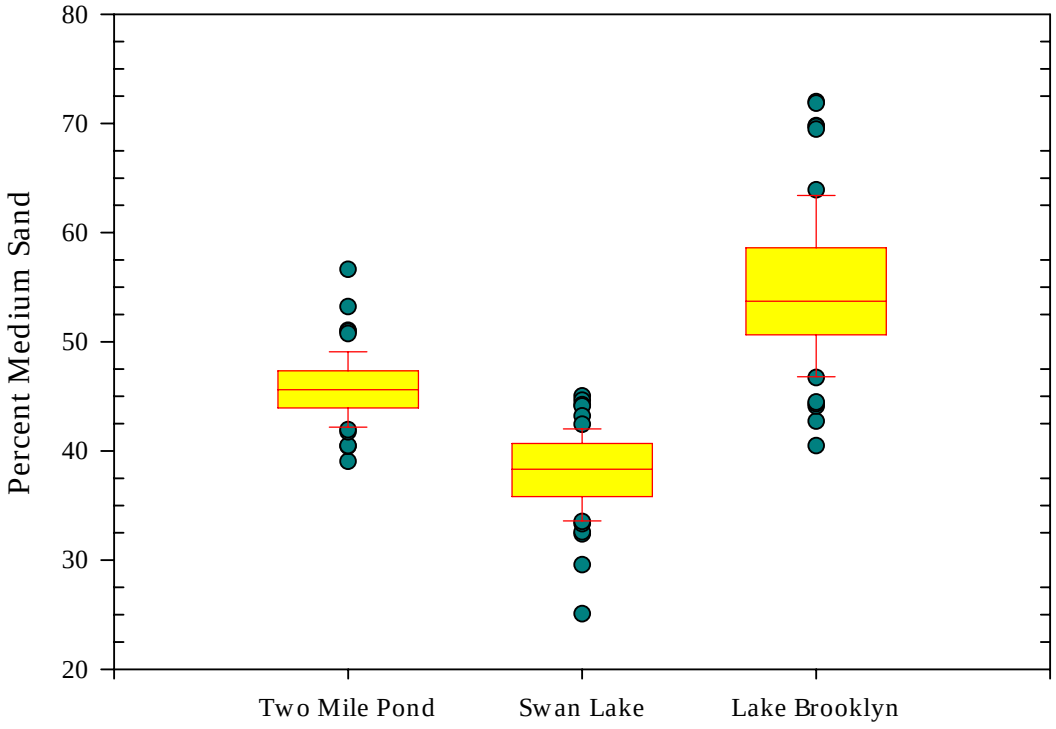

Figure 25. Comparison of percent medium sand among lakes

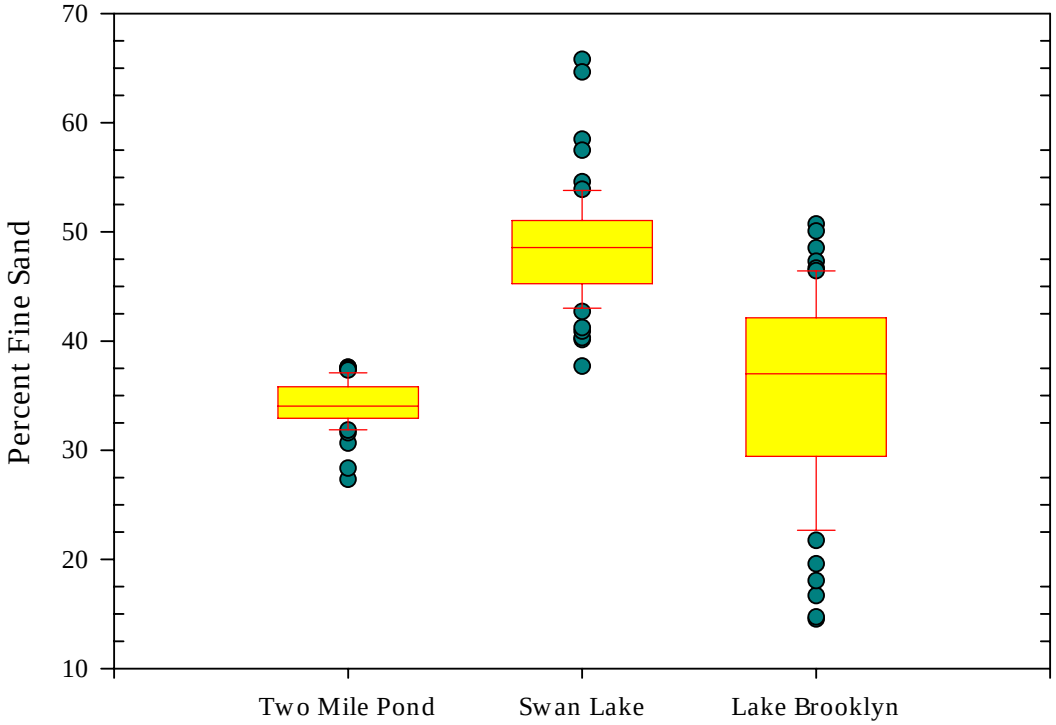

Figure 26. Comparison of percent fine sand among lakes

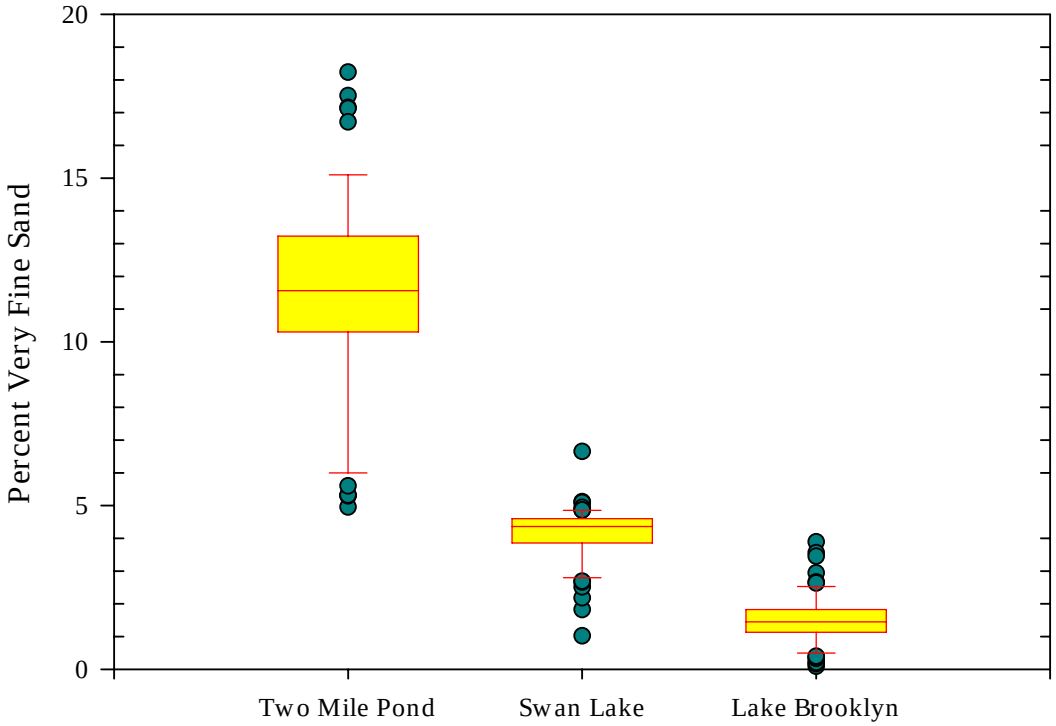

Figure 27. Comparison of percent very fine sand among lakes

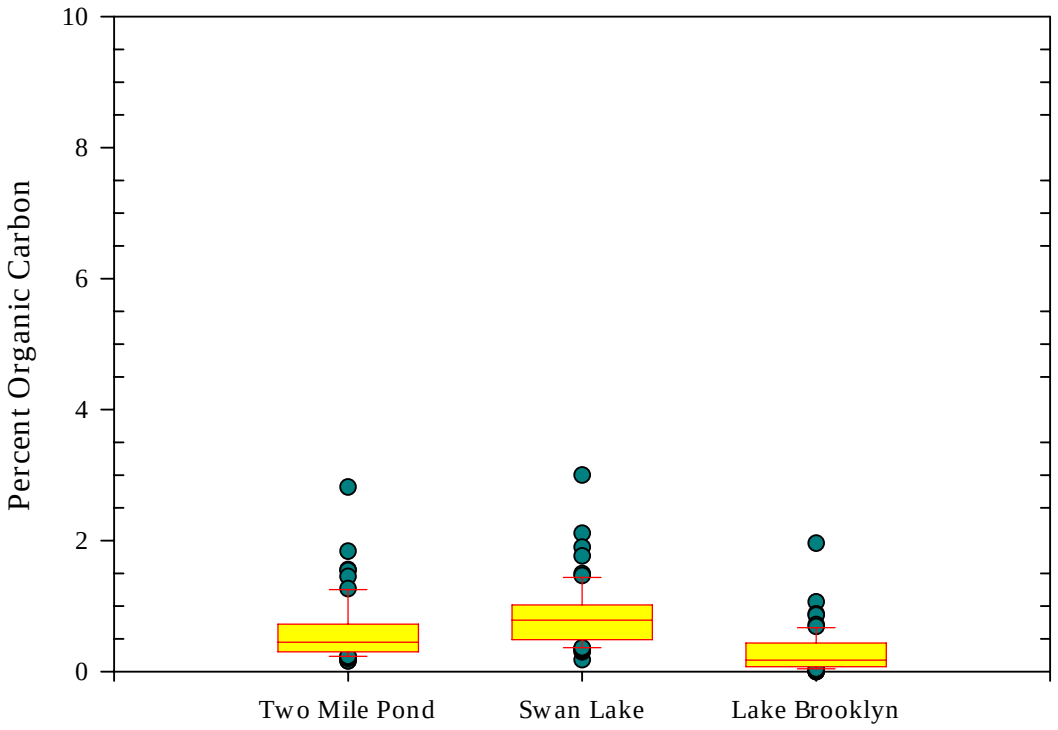

Figure 28. Comparison of percent organic carbon among lakes

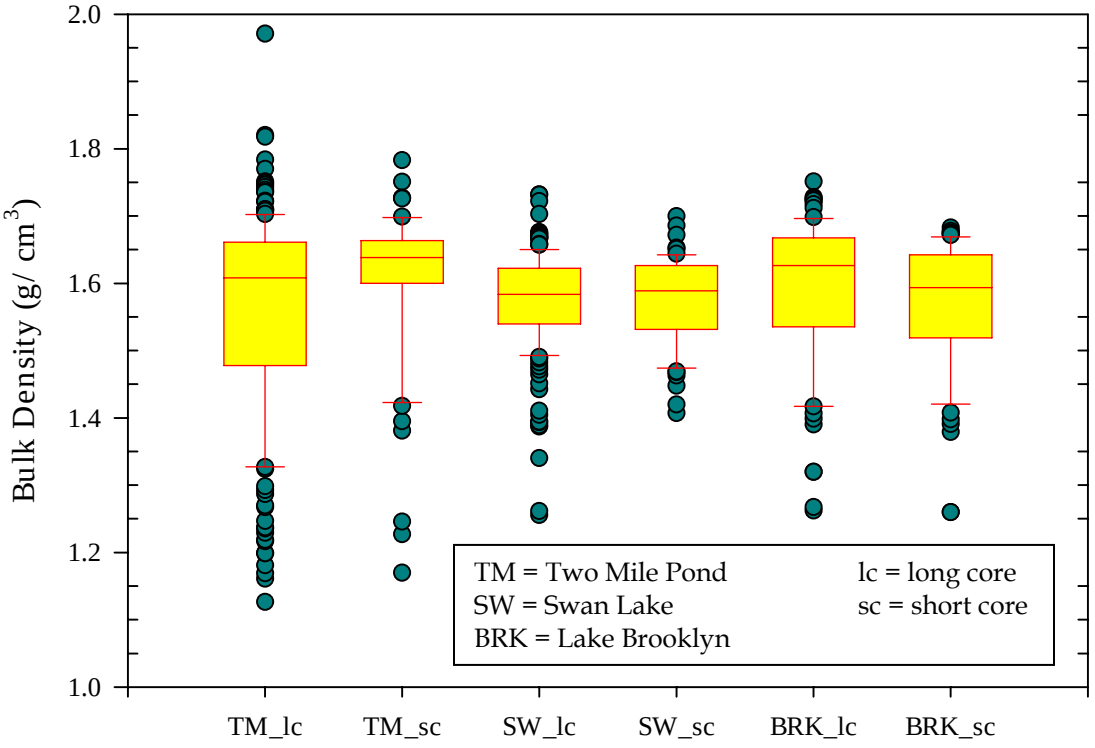

Figure 29. Comparison of bulk density between long and short cores among lakes

Despite overall similarities between each of the physical soil characteristics among lakes, statistically significant differences were commonly observed between soil characteristic means for 3-cm segments from FH and FL sampling locations among lakes. Percent sand, silt, and clay; and percent very coarse, coarse, medium, fine, and very fine sand fractions were normally distributed (α=0.05, p>0.05). A significant difference between 3-cm segment means was observed for each of these physical characteristics (except coarse sand), between at least two lakes (p<0.001, Table 10). Determining which lakes were significantly different with respect to the particle-size classes was not critical information and was not determined.

Particle-size classes were determined with a high degree of precision and were expected to have less than 2% error (Gee and Bauder, 1986), because the settling times were corrected for the viscosity of the solution (5g SMP/L of DI water) and the particle density of the mineral fraction of the soils was expected to be within ± 0.05 g/cm^3 of 2.65 g/cm^3. The precision to which the particle-size distribution was measured and the statistically significant differences observed between particle-size classes among lakes provides further support for the qualitative observations made with PCA (Figure 19). A measurable difference in particle-size classes among lakes was necessary for the development of predictive models of the CFH, HAC, and AEVs, based on the physical soil characteristics.

Table 10. Summary of Type III ANOVA F values for differences in particle-size distribution among lakes

Particle-size class	F Value	p
Sand	59.52	<0.0001
Silt	54.58	<0.0001
Clay	58.64	<0.0001
Very coarse sand	232.75	<0.0001
Coarse sand	0.08	0.9189[a]
Medium sand	514.58	<0.0001
Fine sand	505.77	<0.0001
Very fine sand	1331.37	<0.0001

[a]Not statistically significant at $\alpha/2$=0.05

Note – all others are statistically significant at $\alpha/2$=0.05

Sandhill lakes are dominated by sandy surface materials, but they occur across a range of elevations and were expected to have a range in particle-size distribution and thus a range in pore-size distribution. The range in particle-size distribution is narrow with respect to variability (Figures 20 – 27), but based on the statistical differences of particle-size classes among lakes, it appears that at least a portion of the textural range for sandhill

lakes was sampled. The significant differences for variables among lakes should provide sufficient differences in the pore-size distribution to develop a predictive model of the CFH, HAC, and AEVs from the physical soil characteristics.

If there was an insufficient difference in pore-size distribution, then little or no difference in CFH, HAC, and AEVs would be observed for samples among lakes. The resulting conclusion would be to apply the same value for CFH and HAC as a threshold for minimum levels determinations for all sandhill lakes. However, differences observed for particle-size distribution allowed for development of predictive models of CFH, HAC, and AEVs. The predictive models of CFH and HAC are intended to enable prediction of site-specific values of CFH and HAC from physical soil characteristics.

OBJECTIVE 1: DETERMINE IF A CAPILLARY FRINGE (CF) EXISTS IN SOILS WHERE HIGH AND LOW LAKE STAGE INDICATORS (LSIS) HAVE BEEN IDENTIFIED

The CF was clearly observed in long cores where the water table was set at 6, 12, 18, and 24 cm below the soil surface (Figures 30, 31, 32, and 33). The degree of saturation in each of these cores remained relatively constant for some distance above the water table, this is the CF. The CFH was estimated graphically as the distance between the water table and the point where the regression line fit to the data points where the degree of saturation (s) began to decrease within the core segments intersected the calculated mean degree of saturation for all soil samples taken below the water table (s_b, Figure 34).

The extent of the CFH could not clearly be determined for long cores when the water table was established at 6 or 12 cm below the soil surface (Figures 30 and 31). This was due to the CF extending to the soil surface in all cases when the water table was at 6 cm and frequently when the water table was at 12 cm (Figure 35).

The CFH typically ranged between 6 and 12 cm above the water table in the long cores when water tables were set at 18 and 24 cm. The CFHs determined herein are similar to the CFHs determined for various sands (1-60 cm) by Gillham (1984), Keihn (1992), Nkedi-Kizza and Richardson (2005), Mausbach (1990), and Richardson et al. (2001). In addition, the CFHs determined herein are similar to AEVs for the wetting SMRCs determined in several studies (3-35 cm) by Gillham (1984), Haverkamp and Parlange (1986), Klute and Wilkinson (1958), Lehman et al. (1998), and Tokunaga et al. (2004).

A clear decline in the degree of saturation was evident above the CF in the long cores with water tables set at 18 and 24 cm (Figures 32 and 33). The water table was seldom established at 24 cm and the extent of the CF could not be determined with the water table set at 6 or 12 cm because the CF extended to the soil surface, therefore the CFHs for all analyses were estimated from the long cores with a water table at 18 cm. The degree of saturation for each 3-cm segment was determined for at least one long core from each lake and each FH/FL level with the water table established at 18 cm (except for Two Mile Pond FH1, where the water table was set at 20 cm and segments were normalized to 3-cm segments). This provided consistency across all lakes and levels for subsequent comparisons.

The water table was initially established at 5, 10, 15, 20, and 25 cm from the soil surface in replicate soil cores at the Two Mile Pond FH1 site and in subsequent cores at 6, 12, 18, and 24 cm to determine if the CFH differed depending on the water table depth. The CFH showed no trend with water table depth, based on a regression through the CFHs estimated from long cores with water tables greater than 12 cm (Figure 36). The CFHs from long cores with water tables of 12 cm or less were excluded because the extent of the CF frequently could not be determined. The results suggested that the soils at a site were not different enough with depth to substantially affect the height of the CF.

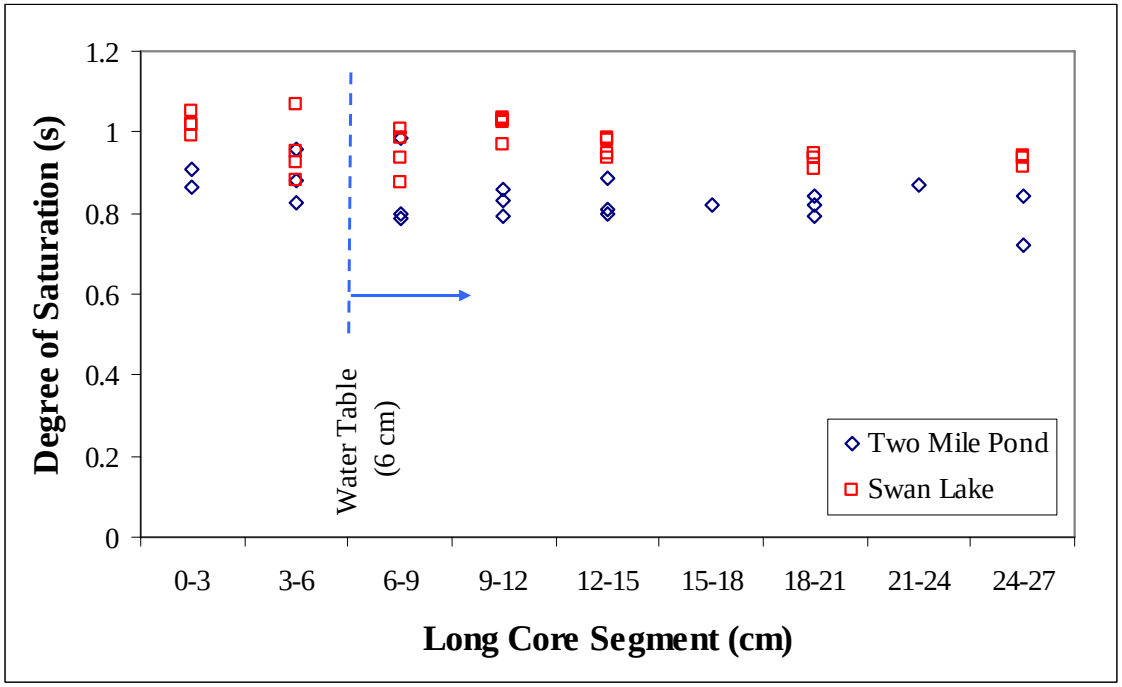

Figure 30. Degree of saturation in long cores with a water table at 6 cm as a function of depth

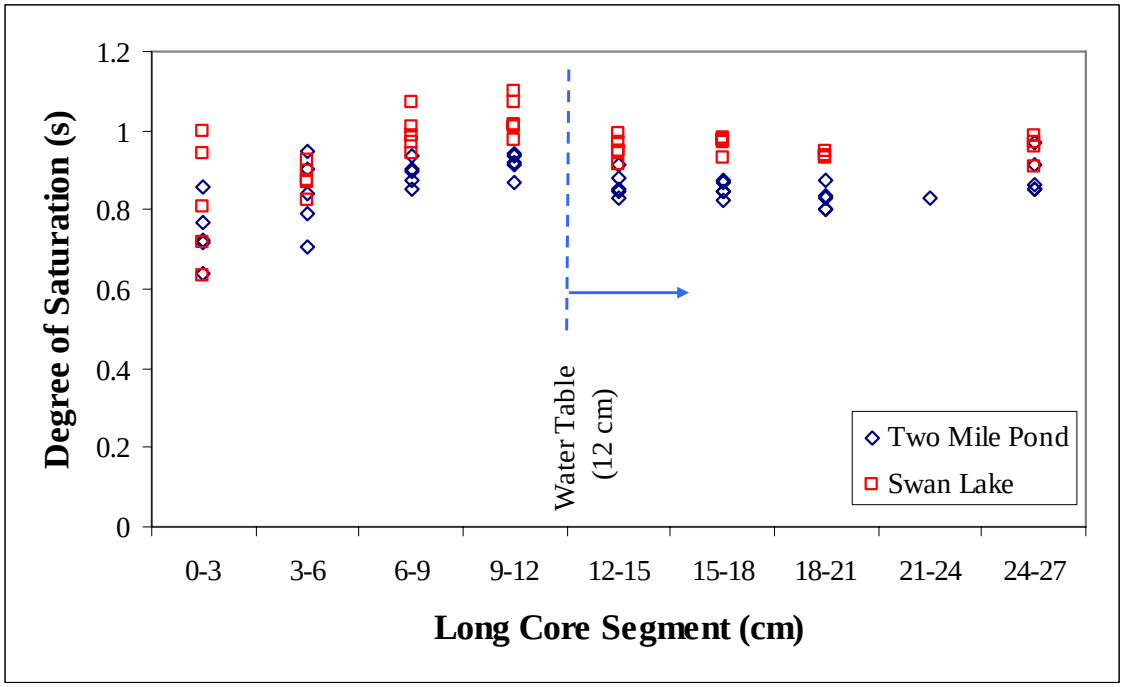

Figure 31. Degree of saturation in long cores with a water table at 12 cm as a function of depth

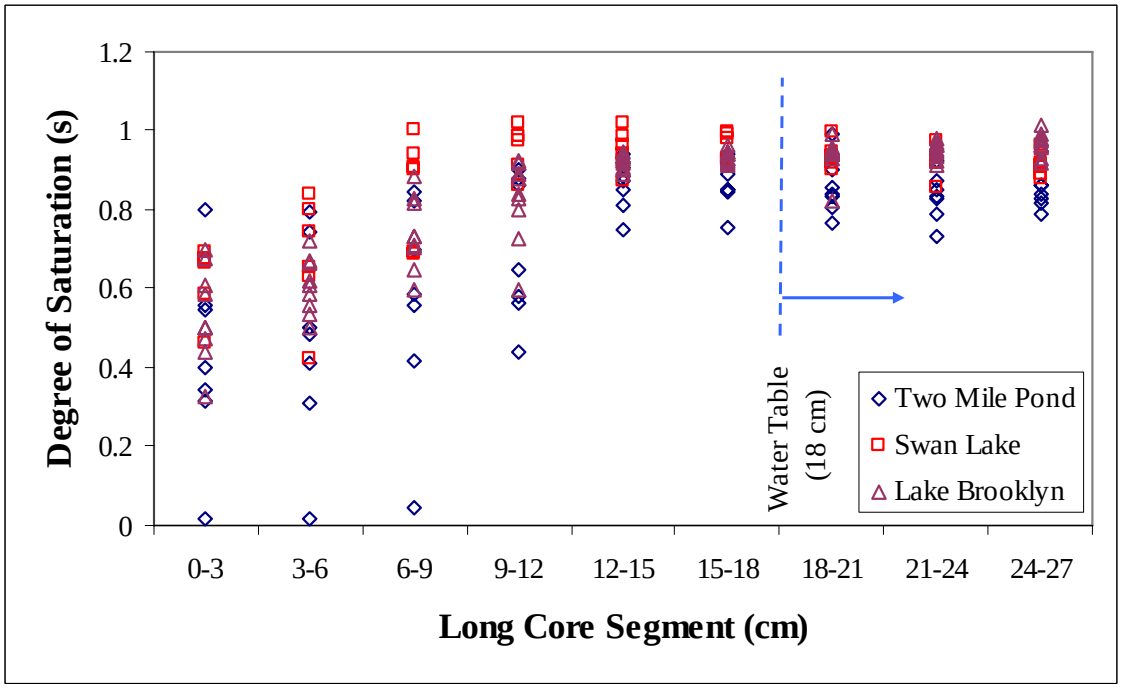

Figure 32. Degree of saturation in long cores with a water table at 18 cm as a function of depth

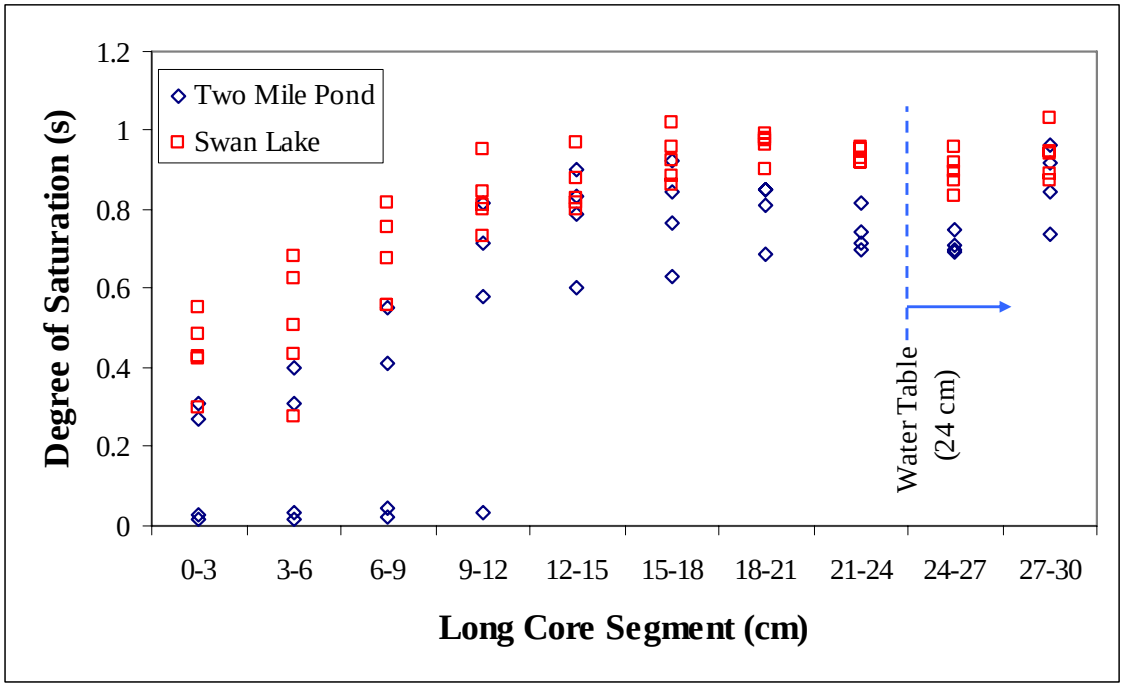

Figure 33. Degree of saturation in long cores with a water table at 24 cm as a function of depth

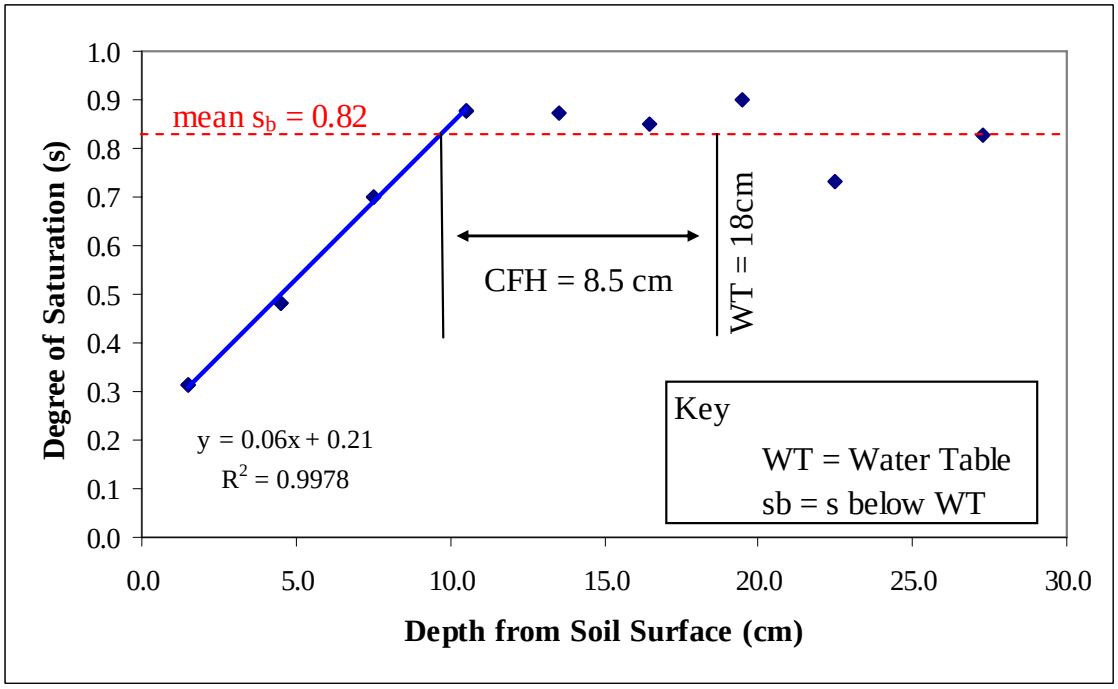

Figure 34. Determination of the capillary fringe height (CFH) from degree of saturation with depth

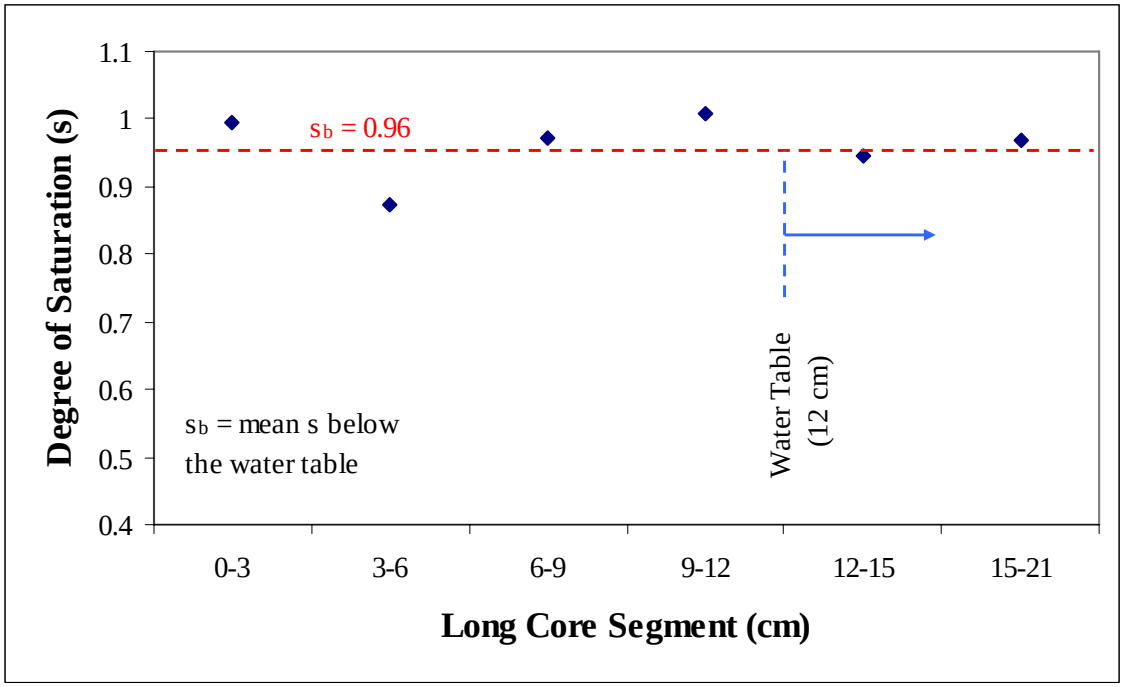

Figure 35. Example of the capillary fringe (CF) extending to the soil surface

The CFH above a water table was consistently identified, with a mean degree of saturation of 0.88 and a standard deviation of ± 0.05. The minimum and maximum degree of saturation at the upper extent of the CF was 0.93 and 0.76, respectively. The CFHs are smallest at Two Mile Pond and Lake Brooklyn, and largest at Swan Lake (Table 11). The results demonstrated that slight differences in texture and thus pore-size distribution may be detected in the CFHs.

Sources of error in the CFHs arise primarily from the determination of the degree of saturation. The most susceptible step for error in measuring the degree of saturation gravimetrically was the measurement of the long core segment length. Upon cutting the long cores into 3-cm segments, each segment length was measured to the nearest 0.5 mm. A 1 mm error in the segment results in approximately a 10% error in the degree of saturation (for 3-cm segments). The error in the determination of the degree of saturation does not appear to be severe based on the consistency of the degree of saturation determined for adjacent soil segments (Figures 30 – 33). This source of error was also minimized because the degree of saturation from multiple segments were averaged in the method to estimate the CFH.

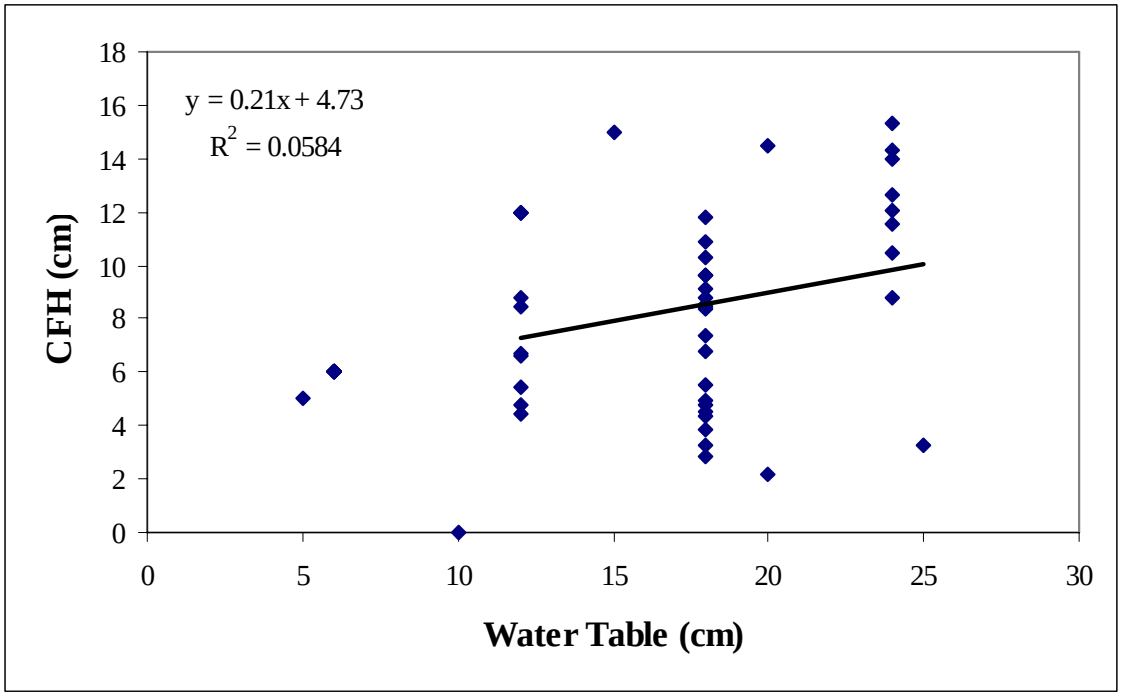

Figure 36. Capillary fringe height (CFH) displays no significant trend with water table depth for water tables greater than 12 cm

Table 11. Summary of capillary fringe height (CFH), height of anaerobic conditions (HAC), and air entry values (AEVs)

Lake	Lake Stage Indicator Location	CFH (cm)	HAC (cm)	AEV (cm)
Swan Lake	FH	9.7 – 11.8	12.4 – 15.8	13.3 – 14.5
	FL	6.8 – 10.3	10.1 – 13.9	12.8 – 15.3
Two Mile Pond	FH	4.6 – 9.1	5.8 – 16.5	8.8 – 13.3
	FL	4.4 – 8.5	5.4 – 10.0	10.2 – 12.3
Lake Brooklyn	FH	6.8 – 7.4	10.4 – 11.2	3.8 – 8.4
	FL	3.3 – 6.2	6.2 – 11.5	6.7 – 8.5

Additional error in the measurement of degree of saturation may have occurred from freezing the long cores prior to sectioning them into 3 cm segments. The volume of a 3-cm long core segment is approximately 53 cm^3. If the soil porosity was 0.5 and all pores were filled with water that expanded by approximately 2.5 cm^3 upon freezing, then the volume would increase by approximately 9%. However, the zones with lower

water content would freeze first and the long core would freeze from outside to inside, due to the heat capacity of water. Therefore, the movement of water due to expansion was expected to be minimized and not substantially affect the water content distribution.

A conservative estimate of the CFH is provided by wetting a soil core because water moving upward through the soil is restricted by the largest pore diameters. Drainage of a saturated sample provides the least conservative estimate of the CFH (i.e., the AEV) because water draining from a saturated soil is restricted by the smallest pore diameters (i.e., hysteresis). Pore-size distribution has greater variability in natural soils due to the greater variability in particle-size distribution. CF estimates based on drainage in natural soils can result in a CFH about twice as large as that determined from wetting a soil (Haines, 1927). AEVs can be determined by optimization of curve fitting to suction and moisture content data with power functions (e.g., Brooks and Corey equation, see pg 42, Equations 16 and 17, Figure 37). This process fits data from saturation at 0 cm suction to residual water content at a suction of up to 15 bars. The Brooks and Corey equation is composed of two functions (Equations 16 and 17). The first is an exponential function that fits the suction/moisture content data at suctions greater than the AEV. The second is a linear function that produces the curve from 0 cm suction and saturation to the AEV. Because the AEVs were of primary interest, AEVs were calculated with the second function of the Brooks and Corey equation (see pg 42, Equations 17 and 18, Figure 38) rather than optimizing fitted curves. Calculation of the AEVs with this method (Figure 38) enables rapid determination of the AEVs and subsequent comparison of the CFH based on wetting and drainage (i.e., AEV).

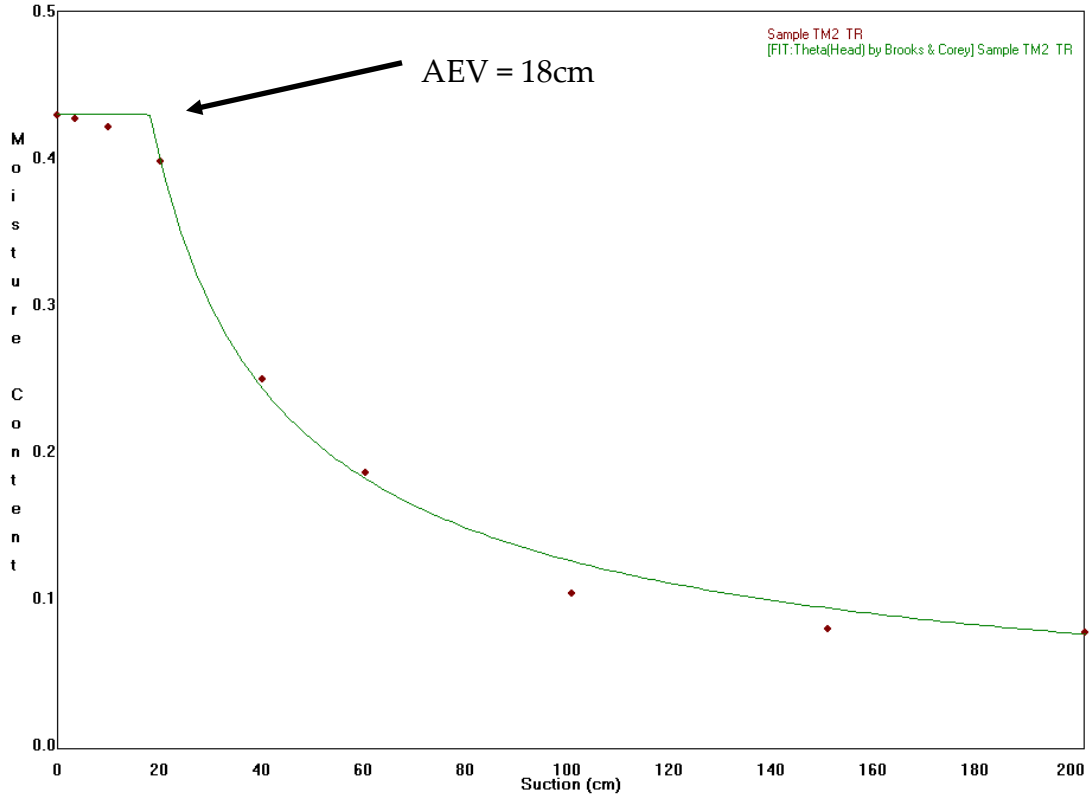

Figure 37. Example of soil moisture release curve and the air entry value (AEV)

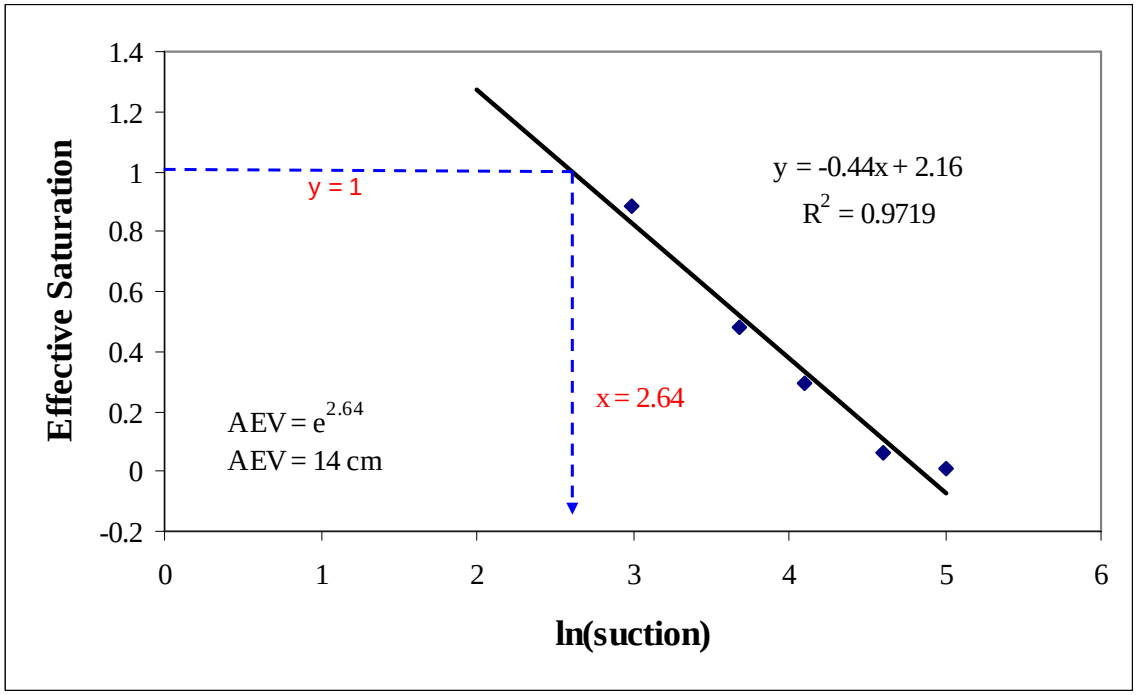

Figure 38. Determination of the air entry value (AEV) from linearization of soil moisture tension data plotted against effective saturation

OBJECTIVE 2: DETERMINE IF ANAEROBIC CONDITIONS DEVELOP WITHIN THE CAPILLARY FRINGE (CF)

The HAC was estimated based on the relationship between ORP and degree of saturation. The degree of saturation where a regression line through the ORP data intersected 0 mV was 0.73 (Figure 39). The HAC was then determined for each of the long cores in which the CFH was estimated, at the point above the water table where the degree of saturation was 0.73. The HAC exists within and slightly above the CFH (Table 11).

Oxidation-reduction potential (ORP) was measured in one FH and one FL long core from each lake (n=6). The FL long core from Two Mile Pond (TM 6-10) was removed from all analyses involving ORP because this long core developed a hydrophobic layer and water was forced into the core to wet it. A hydrophobic layer was observed in several FL cores from Two Mile Pond and likely resulted from excessive drying of the soil after collection and prior to rewetting the core. Forcing water into the core to overcome the hydrophobic layer resulted in biased ORP measurements.

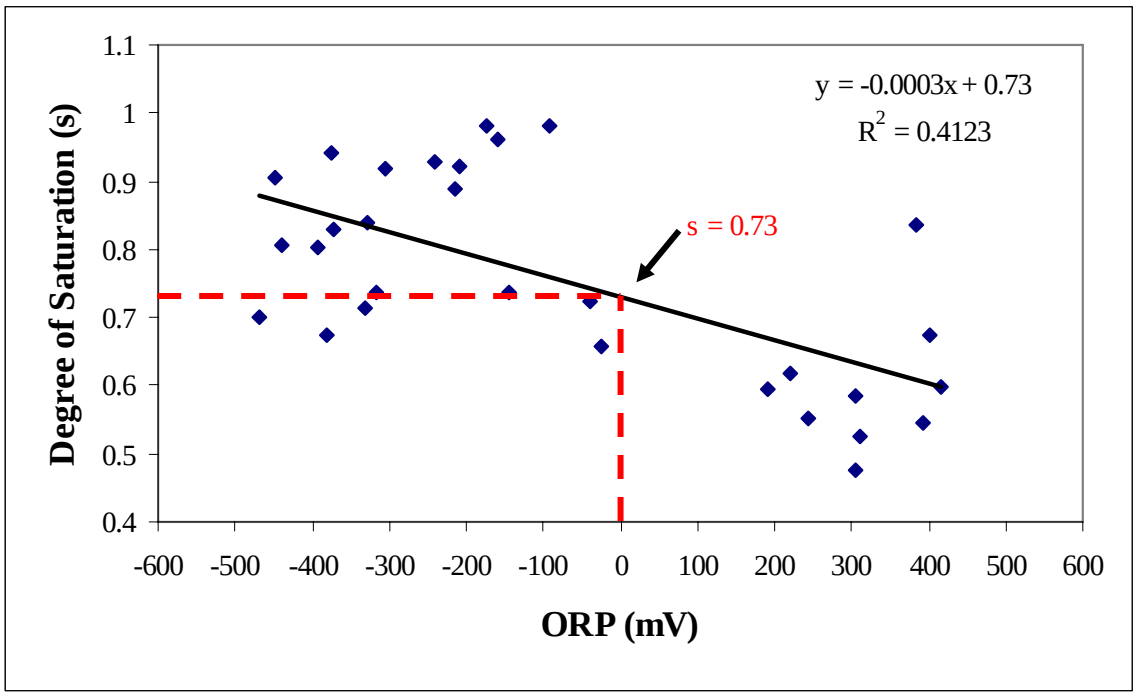

Figure 39. Estimation of the degree of saturation above which oxidation-reduction potentials (ORPs) less than 0 mV are dominant

An ORP of 0 mV was selected as the break point between aerobic and anaerobic conditions because facultative microbes are tolerant of

moderately reduced conditions, but below the zone of Mn^{4+} reduction most redox reactions are performed by obligate anaerobes (Schlesinger 1997). The soils herein have a pH of 4-5. The Eh of a particular redox reaction increases by 59 mV for each pH unit decrease from a pH of 7 (Schlesinger 1997). Based on the observed pH range, 0 mV should be in the ORP range where iron is reduced, ensuring anaerobic conditions and a microbial community dominated by obligate anaerobes.

The HAC followed a similar trend to the CFHs in that, the HAC were largest for Swan Lake and slightly smaller for Lake Brooklyn and Two Mile Pond (Table 11). This was expected, because the HACs were estimated based on the degree of saturation in the same long soil cores from which the CFHs were determined.

A higher degree of saturation was expected for anaerobic conditions to be present. The lower than expected ORP measurements may be the result of heterogeneous pore-size distributions that caused films of water to saturate pore throats (i.e., narrow areas) while air pockets in the pore bodies (i.e., wide areas) were still present. This prevented a connection between entrapped air and the atmosphere that resulted in anaerobic conditions at water contents less than saturation.

The primary source of error in the estimation of the HAC arises from estimation of the degree of saturation at the platinum electrodes from the mean degree of saturation in duplicate soil cores. As can be seen in Figures (31, 32, and 33) the degree of saturation becomes increasingly variable with increasing height above the water table. The degree of saturation was not determined for the long cores in which ORP was measured because removal of some soil during installation of the platinum electrodes results in errors in estimation of the soil volume, which can result in substantial error in the determination of the degree of saturation. In addition, installation of the platinum electrodes alters the soil slightly. It was reasonable to assign the degree of saturation determined from duplicate soil cores from determination of the CFH to the long cores in which ORP was measured because of these potential sources of error.

OBJECTIVES 3: DEVELOP A MODEL TO ESTIMATE THE CAPILLARY FRINGE HEIGHT (CFH) BASED ON THE PHYSICAL PROPERTIES OF SOILS WHERE HIGH AND LOW LAKE STAGE INDICATORS (LSIS) HAVE BEEN IDENTIFIED

CFH Predictive Models Based on Physical Soil Characteristics

Summary of the 0-18-cm segments allowed for comparisons between the physical soil characteristics and the CFH (Appendix B). Segments below 18 cm were not included because these segments were below the water table and did not contribute to the CFH. Scatter plots of the CFH with percent sand, silt, and clay, percent very coarse, coarse, medium, fine, and very fine sand fraction, percent OC, percent LOI, and AEVs are presented in Appendix D. These scatter plots were generated to support the development of a regression model to predict the CFH.

Several of these soil characteristics were strongly related to the CFH with R^2 greater than 0.3. Percent clay had the strongest positive relationship with the CFH (R^2=0.44). As the percent of the smallest particles, clay, silt, OC, and LOI increase, an increase in total porosity and the number of small pores follows and results in an increase in the CFH. Likewise, an increase in the percentage of larger particles (i.e., sand) results in a decrease in total porosity, an increase in the number of large pores, and a corresponding decrease in the CFH. Measure of the individual sand fractions do not consistently follow this relationship, likely because the percent of fine and coarse materials may vary disproportionately, so that an increase in fines (i.e., clays and silts) is masked by an increase in coarse materials and vice versa.

A relationship between the particle-size distribution and the CFH was observed in one study of the literature reviewed. Keihn (1992) developed a relationship between pore pressure (which was converted to CFH) and percent medium sand grains with R^2=0.36. A similar relationship between the CFH and individual soil characteristics (percent clay, sand, very coarse sand, and OC) were determined in this study with R^2=0.44, 0.34, 0.31, and 0.31, respectively (Appendix D). Inclusion of additional particle-size classes results in a better regression model to predict the CFH.

A regression with percent sand (sa), silt (si), and clay (cl) to predict the CFH resulted in the highest degree of fit with the measured CFHs (F=13.87, p=0.0002, and adjusted R^2=0.6943, Equation 22, Figure 40).

$$\text{Predicted CFH} = 23.83(cl) + 23.61(si) + 21.40(sa) - 2140.05 \quad (22)$$

Each of these three variables significantly contributed to the fit with CFH (α=0.05, p=0.0012, 0.0011, and 0.0005, respectively) and the residuals were normally distributed (α=0.05, p=0.1688). The PRESS R^2 (0.5904) implies that the model may be adequate to predict the CFH, based on the relatively small difference between adjusted R^2 and PRESS R^2. Percent sand, silt, and clay would likely account for the pore-size distribution, but application of these three variables results in severe multicollinearity (i.e., the condition when one or more variables are linear functions of other variables, StatSoft, Inc. 2005), with a condition number of 1113. This does not invalidate the model but makes application of the model much less favorable.

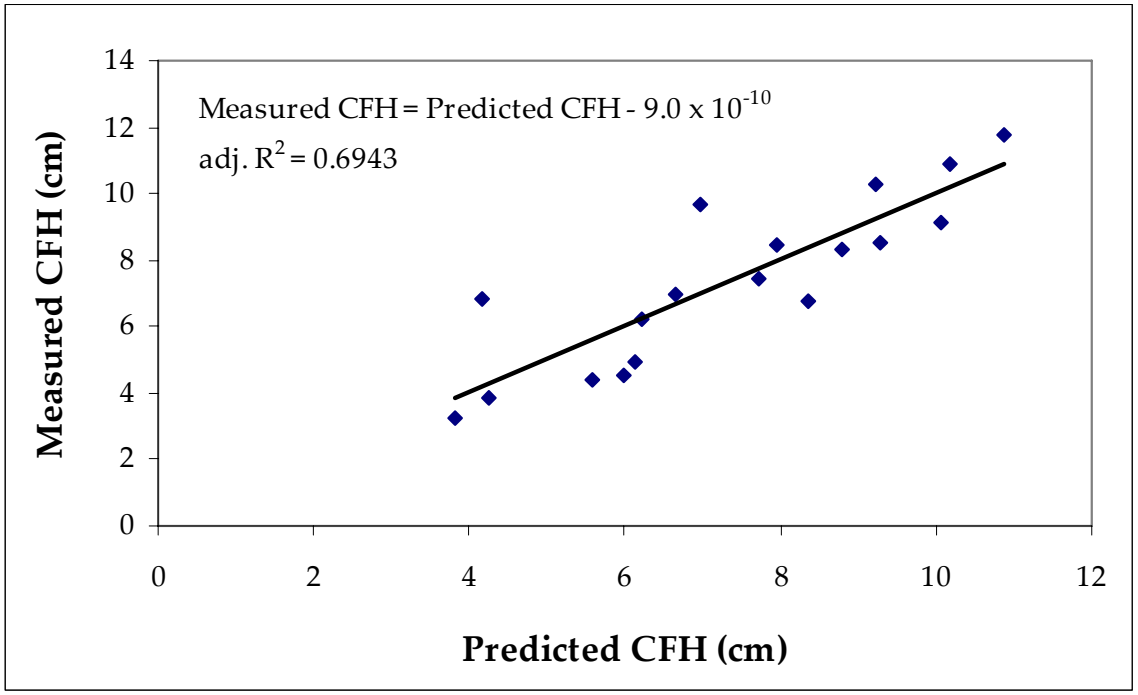

Figure 40. Relationship between the capillary fringe height (CFH) and CFH predicted from percent sand, silt, and clay

A regression with percent clay (cl) and very coarse (vc), coarse (c), fine (fi), and very fine (vf) sand fractions to predict the CFH resulted in a slightly reduced degree of fit (F=15.60, p=0.0033, and adjusted R^2=0.6279, Equation 23, Figure 41), but provides the most robust predictor of CFH determined herein.

$$\text{Predicted CFH} = 2.60(\text{cl}) + 9.22(\text{vc}) - 1.90(\text{c}) - 0.37(\text{fi}) - 0.60(\text{vf}) + 28.15 \quad (23)$$

Each of these five variables significantly contributed to the fit with CFH (α=0.05, p=0.0033, 0.0062, 0.0130, 0.0242, and 0.0092, respectively) and the residuals were normally distributed (α=0.05, p=0.6262). The PRESS R^2 (0.4776) is similar to the adjusted R^2 implying that the model may be adequate to predict the CFH, but the PRESS R^2 and R^2 are different enough to suggest that the model may also be slightly data dependent. Multicollinearity is not a problem in this model with all condition numbers less than 62. Percent clay and percent very coarse, coarse, fine, and very fine sand fractions should account for the pore-size distribution and provide a reasonable estimate of the CFH.

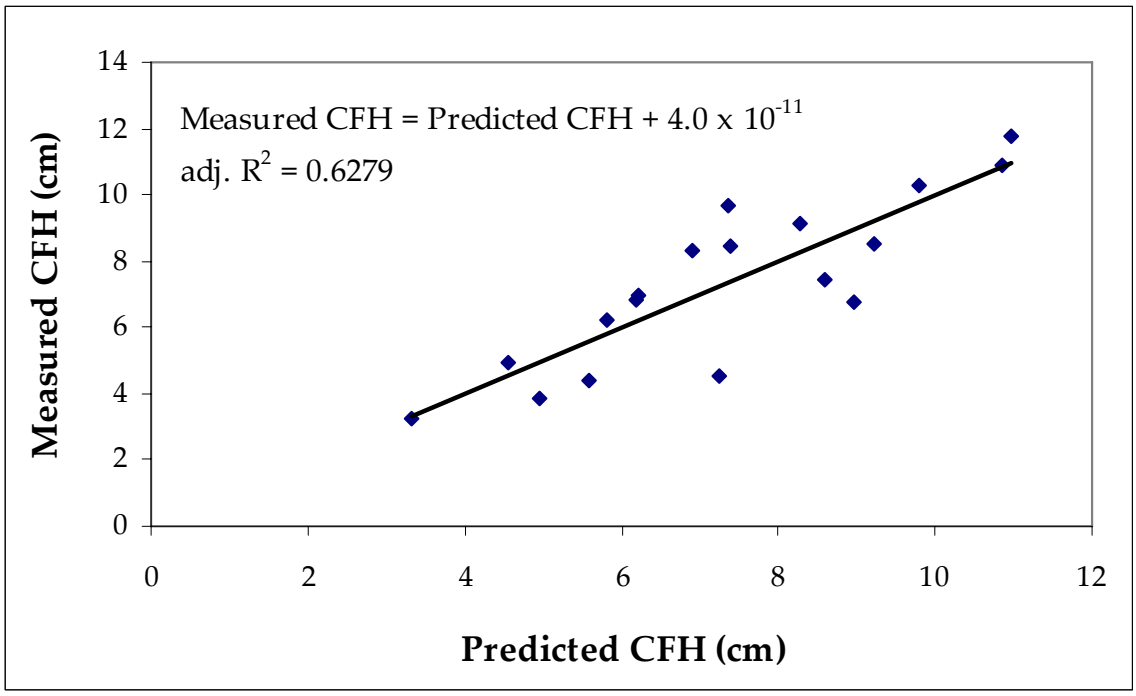

Figure 41. Relationship between the capillary fringe height (CFH) and CFH predicted from percent clay and percent very coarse, coarse, fine, and very fine sand fractions

The PCs of silt and clay (PC1si_cl and PC2si_cl), of very coarse and coarse sand (PC1vc_c and PC2vc_c), and of fine and very fine sand (PC1fi_vf and PC2fi_vf) were generated (Appendix C) from the reduced data set in an effort to decrease the dimensionality of the data and provide a better model to predict the CFH. Each of these soil characteristics was paired based on their expected effect on the CFH. The first PC of each of these pairs accounted for a large percent of the variability in each data set (72.28%, 75.54%, and 66.24%, respectively, Appendix D). A better predictive model of the CFH could not be developed from combinations of these PCs with or without inclusion of the physical soil characteristics. This is in part due to the severe multicollinearity in the regressions when

percent sand was included with the PCs generated from very coarse and coarse sand and fine and very fine sand or when percent silt or clay were included with the PCs generated from silt and clay. In addition, individual soil characteristics frequently did not significantly contribute to the regression models tested with the PCs.

CFH Predictive Model Based on AEVs

A priori, the AEVs were expected to have a strong relationship with the CFH resulting in a good predictive model. The AEVs showed the unanticipated result of poor fit with CFH ($F=5.42$, $p=0.0334$, adjusted $R^2=0.2026$, Equation 24; Figure 42).

$$CFH = 0.38(AEV) + 3.26 \quad (24)$$

The residuals for this regression model were normally distributed ($\alpha=0.05$, $p=0.0937$), but the low adjusted R^2 and the low PRESS R^2 (0.0444) reflect the poor relationship of these variables.

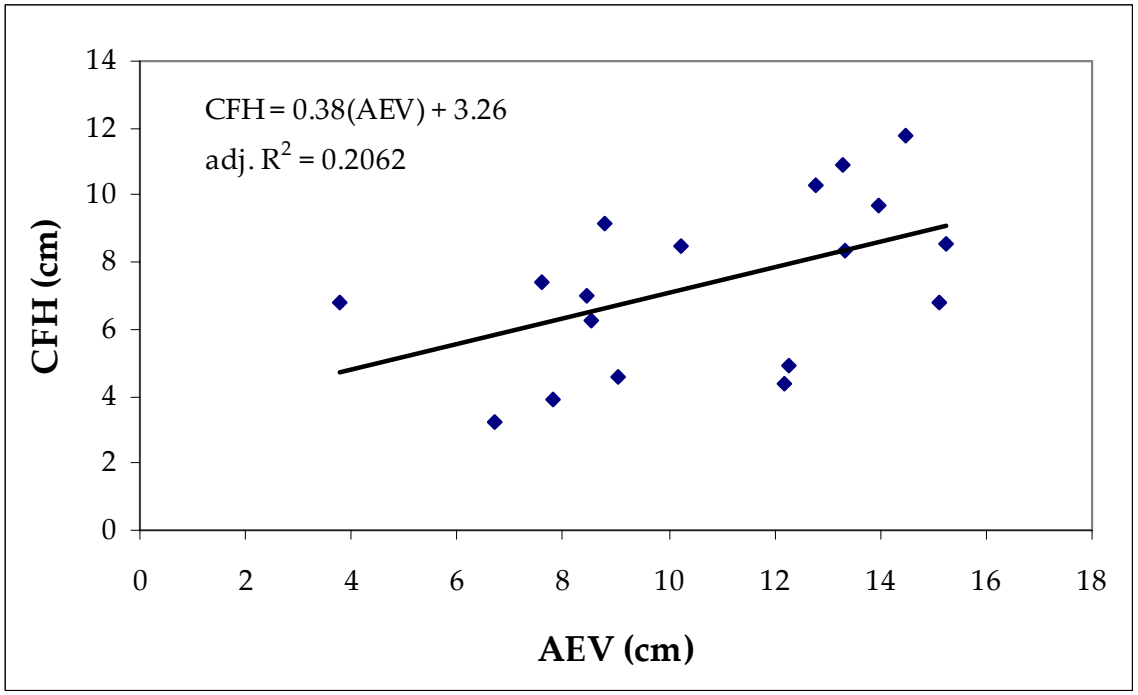

Figure 42. Relationship between capillary fringe height (CFH) and air entry values (AEVs)

Poor fit of the AEVs with the CFH is likely the result of several factors. First, the CFH and AEVs were determined with different methods and differences based on wetting versus drainage may contribute to the poor fit. Also, taking an average of the AEVs from short cores from 0-18 cm

may not adequately represent the pore connectivity in an intact 18-cm core. The AEVs are very similar in magnitude to the CFHs but variability in this narrow data range also contributes to the poor fit (Table 11 and Figure 43).

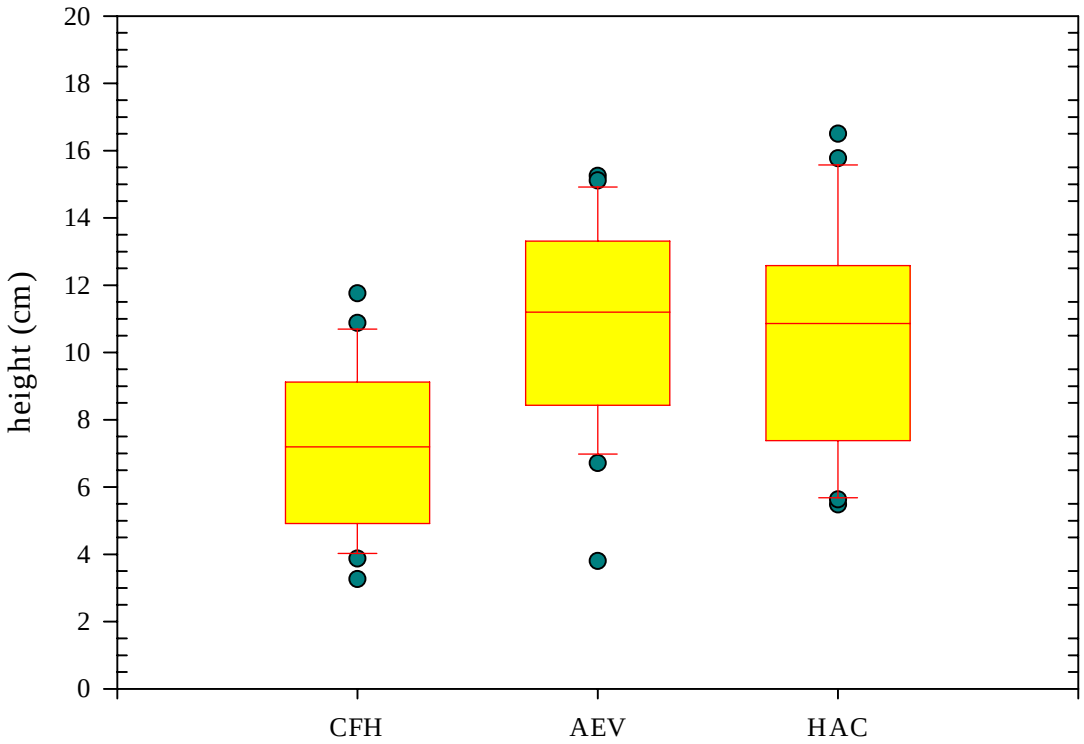

Figure 43. Box plots of the capillary fringe height (CFH), air entry values (AEVs), and height of anaerobic conditions (HAC) for all lakes

AEV Predictive Models Based on Physical Soil Characteristics

Although the AEVs were poor predictors of the CFH determined by wetting a soil, AEVs could be predicted quite reasonably from the physical soil characteristics. A regression with the first PC of percent very coarse and coarse sand (PC1vc_c) and the percent medium (m) sand fraction provided the best predictive model of the AEVs ($F=27.69$, $p<0.0001$, and adjusted $R^2=0.7584$, Equation 25, Figure 44).

$$\text{Predicted AEV} = 1.42(\text{PC1vc\_c}) - 0.23(\text{m}) + 21.53 \quad (25)$$

The first PC of percent very coarse and coarse sand and the percent medium sand significantly contributed to the relationship with the AEVs ($\alpha=0.05$, $p=0.0008$ and 0.0009, respectively) and the residuals were normally distributed ($\alpha=0.05$, $p=0.5857$). The PRESS R^2 (0.6820) is similar

to the adjusted R^2 implying that the model has good predictability and is not data dependent. Multicollinearity is not a problem in this model with all condition numbers less than 3.

Predictive regression models of the AEVs with percent very coarse (vc) sand and with the combination of percent coarse (c) and medium (m) sand also displayed strong relationships ($F=45.90$, $p<0.0001$, adjusted $R^2=0.7254$, Equation 26, Figure 45 and $F=26.88$, $p<0.0001$, adjusted $R^2=0.7528$, Equation 27, Figure 46).

$$AEV = 6.61(vc) + 5.76 \quad (26)$$

$$\text{Predicted AEV} = 1.00(c) - 0.34(m) + 18.86 \quad (27)$$

Percent very coarse sand and the combination of percent coarse and medium sand significantly contribute to the relationship with the AEVs ($\alpha=0.05$, $p<0.0001$ and $p=0.0011$ and $p<0.0001$, respectively) and the residuals for each regression were normally distributed ($\alpha=0.05$, $p=0.9256$ and 0.3385, respectively). The PRESS R^2 (0.6845 and 0.6555, respectively) are similar to the adjusted R^2 implying that the models have good predictability and are not data dependent. Multicollinearity is not a problem in either model with all condition numbers less than 2.

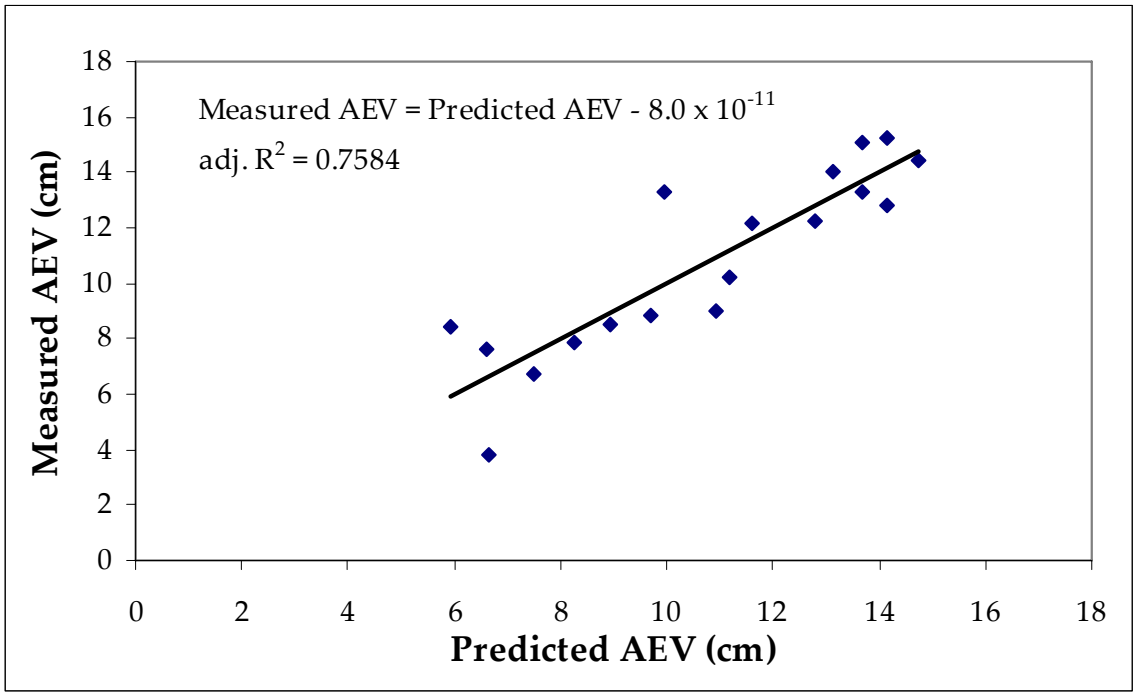

Figure 44. Relationship between air entry values (AEVs) and the predicted AEV from the first principal component of percent very coarse and coarse sand (PC1vc_c) and percent medium (m) sand

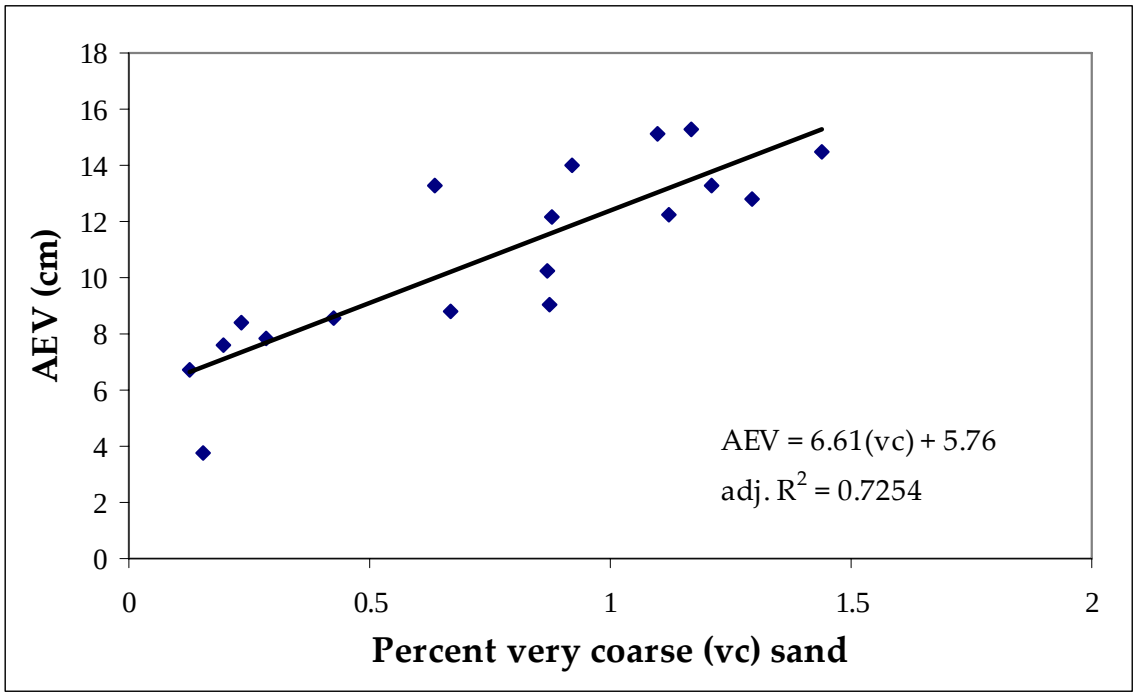

Figure 45. Relationship between air entry values (AEVs) and percent very coarse (vc) sand

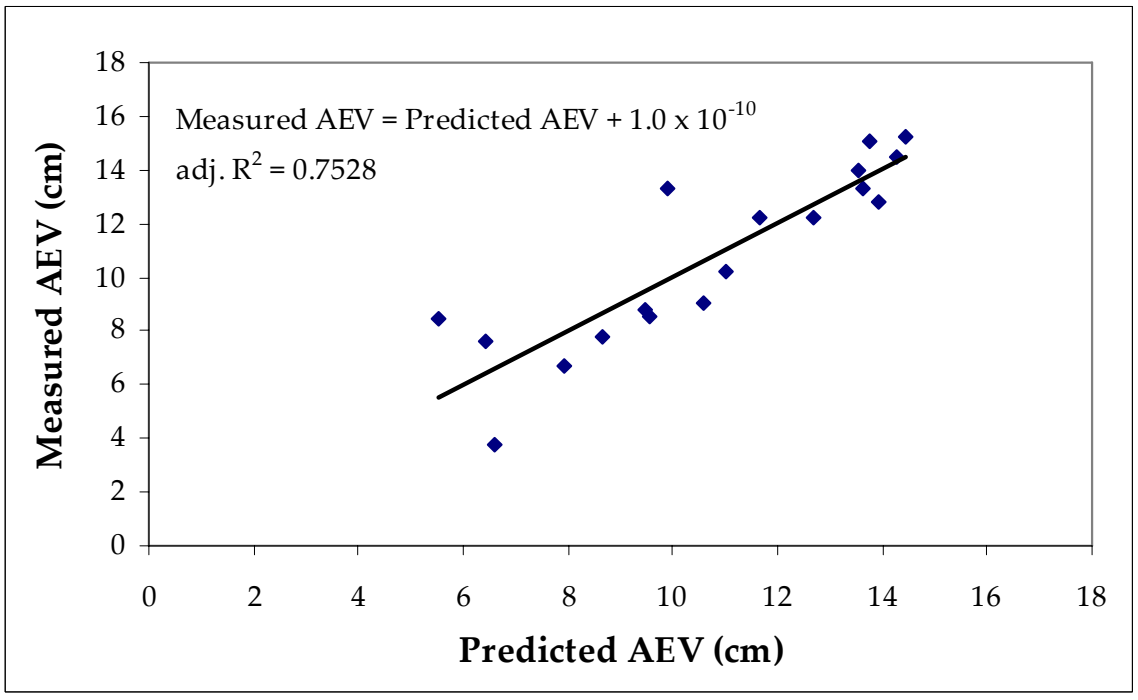

Figure 46. Relationship between measured air entry values (AEVs) and predicted AEVs from percent coarse (c) and medium (m) sand

OBJECTIVES 4: DEVELOP A MODEL TO ESTIMATE THE HEIGHT OF ANAEROBIC CONDITIONS (HAC) ABOVE A FIXED WATER TABLE IN SOILS WHERE HIGH AND LOW LAKE STAGE INDICATORS HAVE BEEN IDENTIFIED

HAC Predictive Model Based on Physical Soil Characteristics

Summary of the 0-18-cm segments also allowed for comparisons between the physical soil characteristics and the HAC (Appendix B). No literature was reviewed that directly related the HAC to the CFH or the physical soil characteristics, though Keihn (1992) noted the need to determine the degree of saturation and the extent of anaerobic conditions within the CF zone. Scatter plots of the HAC with percent sand, silt, and clay; percent very coarse, coarse, medium, fine, and very fine sand fraction; percent OC; percent LOI, and AEVs are presented in Appendix D. These scatter plots were generated to support the development of a regression model to predict the HAC.

Percent clay and the first PC of silt and clay (PC1si_cl) were the only parameters that were strongly related to the HAC with R^2 of 0.36 and 0.27, respectively. As the percent of the smallest particles, (i.e., clay, silt, OC, and LOI) increases, an increase in total porosity and the number of small pores follows and would be expected to result in an increase in the HAC. Likewise, an increase in the percentage of larger particles (i.e., sand) results in a decrease in total porosity, an increase in the number of large pores, and a corresponding decrease in the HAC is expected. Measures of percent sand, silt, and clay follow this relationship; however, the individual sand fractions do not, as discussed for comparisons of these physical soil characteristics with the measured CFH (see pp. 68-69).

The best predictive model of HAC from the physical soil characteristics was developed with percent clay (cl) and very coarse (vc), coarse (c), fine (fi), and very fine (vf) sand fractions ($F=3.90$, $p=0.0249$, and adjusted $R^2=0.4601$, Equation 28, Figure 47).

$$\text{Predicted HAC} = 4.20(\text{cl}) + 9.57(\text{vc}) - 2.51(\text{c}) - 0.46(\text{fi}) - 0.82(\text{vf}) + 37.79 \quad (28)$$

The very coarse and fine sand fractions do not significantly contributed to the fit with HAC ($\alpha=0.05$, $p=0.0042$, 0.0635, 0.0415, 0.0796, and 0.0260, respectively). The residuals were normally distributed ($\alpha=0.05$, $p=0.8513$) and multicollinearity was not a problem in this model with all condition numbers less than 62. The relatively large difference between the PRESS

R^2 (0.0792) and the adjusted R^2, implies that this model is data dependent and is likely inadequate to predict the HAC. Percent clay and percent very coarse, coarse, fine, and very fine sand fractions should account for the pore-size distribution as they provide a reasonable estimate of the CFH, but appear to be inadequate predictors of the HAC.

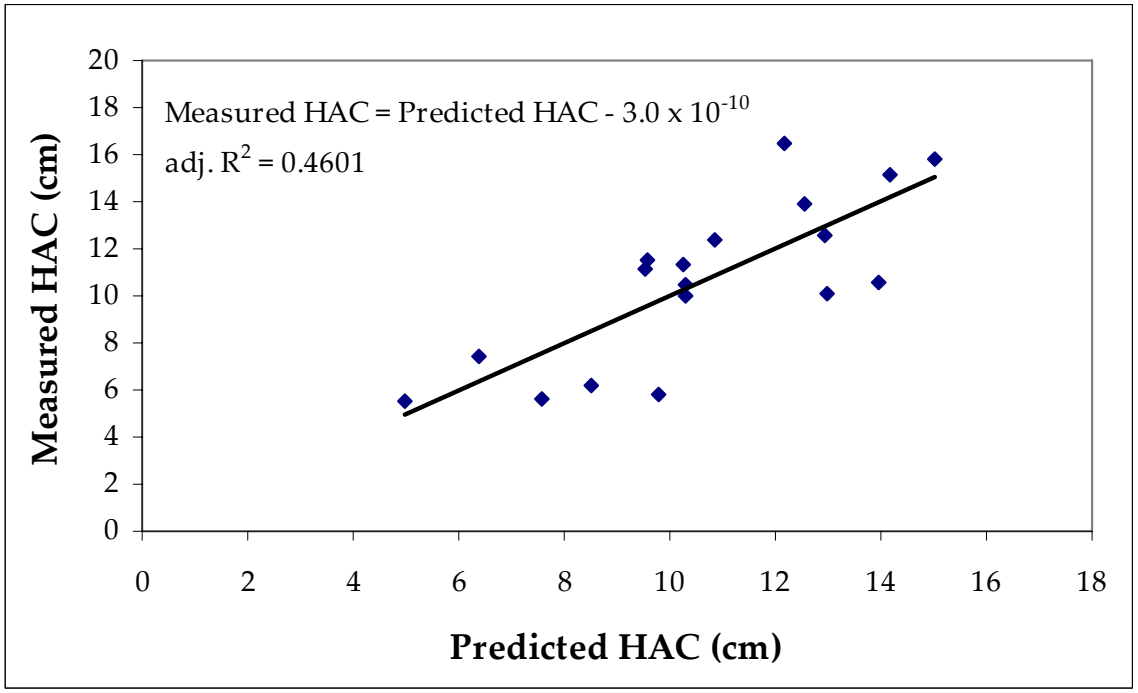

Figure 47. Relationship between the measured height of anaerobic conditions (HAC); predicted HAC from percent clay (cl); and percent very coarse (vc), coarse (c), fine (fi), and very fine (vf) sand fractions

HAC Predictive Model Based on PCs

A reasonable predictive model of the HAC could not be developed from combinations of the PCs with or without inclusion of the physical soil characteristics. This is in part due to the severe multicollinearity in the regressions when percent sand was included with the PCs generated from very coarse and coarse sand and fine and very fine sand or when percent silt or clay were included with the PCs generated from silt and clay. In addition, individual soil characteristics frequently did not significantly contribute to the regression models tested with the PCs.

HAC Predictive Model Based on CFH

Regression of CFH with the HAC demonstrated a strong relationship (F=38.29, p<0.0001, adjusted R^2=0.6869, Equation 29, Figure 48).

HAC = 1.17(CFH) + 2.06 (29)

This was expected because the CFH was consistently identified near 88% saturation and the transition from aerobic to anaerobic conditions occurred at approximately 73% saturation. In addition, the HAC was estimated from the same soil cores from which the CFH was determined. The small difference between the PRESS R^2 (0.6414) and the adjusted R^2 implies that the model is adequate to predict the HAC. In addition, the residuals are normally distributed (p=0.2591).

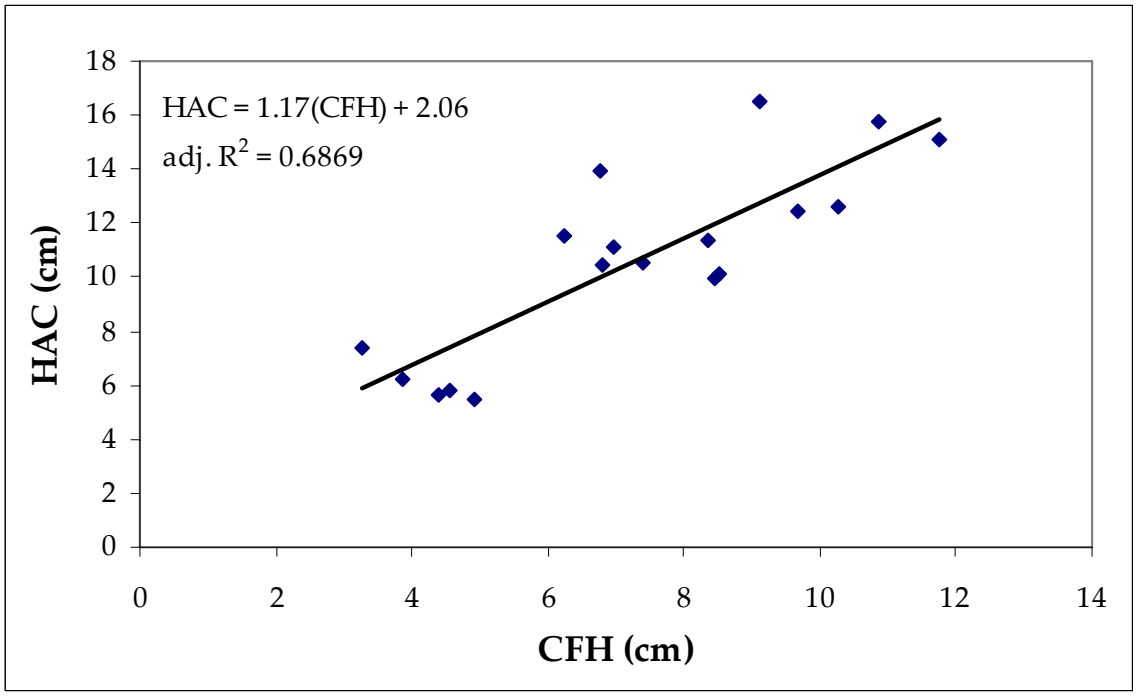

Figure 48. Relationship between the height of anaerobic conditions (HAC) and the capillary fringe height (CFH)

HAC Predictive Model Based on AEVs

The final regressions were between the AEVs and the HAC. Prior to any analyses, the AEVs were expected to have a strong relationship with the HAC, but as determined with CFH, weak relationships existed. AEVs were poorly related to the HAC (F=1.66, p=0.2157, adjusted R^2=0.0375, Equation 30, Figure 49).

$$HAC = 0.32(AEV) + 7.19 \quad (30)$$

Poor fit of the AEVs with the HAC is likely the result of several factors. First, the HAC and AEVs were determined with different methods and differences based on wetting versus drainage may contribute to the poor fit. Also, taking an average of the AEVs from short cores from 0-18 cm may not adequately represent the pore connectivity in an intact 18-cm core. The AEVs are very similar in magnitude to the HACs (Figure 43), but variability for each sampling location due to measurement techniques and the narrow data range also contributes to the poor fit (Figure 43).

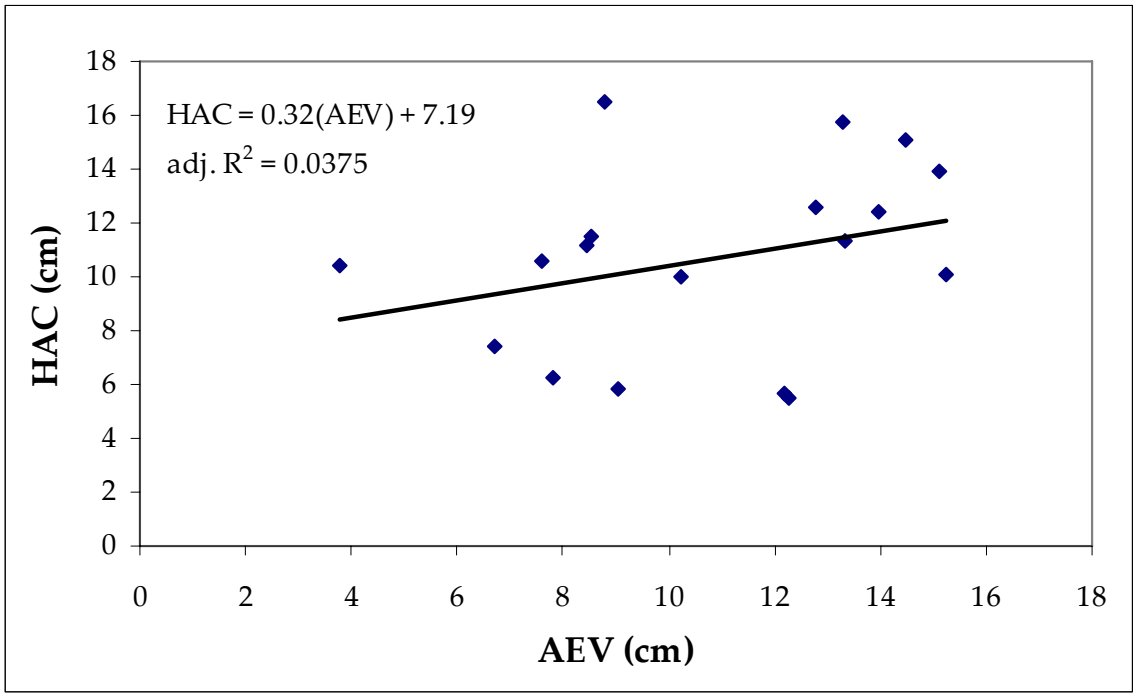

Figure 49. Relationship between the height of anaerobic conditions (HAC) and air entry values (AEV)

APPLICATION TO MINIMUM FLOWS AND LEVELS

The goals of this research were to quantify the CFH and HAC in soils associated with FH and FL LSIs and provide predictive models of the CFH and HAC from easily determined soil characteristics to support the determination of minimum levels at sandhill lakes. The CFH and HAC were recommended as threshold offsets, enabling SJRWMD to allow a small shift in hydrology at sandhill lakes without causing unacceptable impacts to the ecosystem values and functions.

One example of how the HAC may be applied at sandhill lakes to establish minimum levels would be to apply a static threshold offset to the FH and FL LSIs, as recommended by Jones Edmunds (2006). The HAC was estimated at 5.4 to 16.5 cm above a water table, set at 18 cm, in FH and FL soil cores (Figure 43) with a mean of 10.7 cm. The mean HAC for Lake Brooklyn, Swan Lake, and Two Mile Pond was 9.5, 13.3, and 9.1 cm, respectively. No significant differences were detected between the FH and FL soils within a lake; therefore, the same offset can be applied to the FH and FL LSIs in determining minimum levels at a sandhill lake. However, significant differences ($p<0.0001$, Table10) in particle-size distribution, which directly affect the CFH and HAC, were observed among lakes, suggesting that some variability exist among lakes. The observed differences in soil characteristics resulted in a 4.2 cm difference between the largest and smallest mean HAC for the three systems studied.

Another example of how the CFH and HAC may be applied at sandhill lakes to establish minimum levels follows.

1. The FH and FL LSIs would be identified at multiple transects at a sandhill lake.
2. A composite soil sample for the 0-18-cm depth would be collected at each LSI to determine the percent sand, silt, and clay; and percent very coarse, coarse, medium, fine, and very fine sand fractions.
3. The CFH and HAC would then be estimated with Equations. 23 and 29 for each soil sample.

The mean HAC for the FH LSI soil samples provides the offset from the mean elevation of the FH LSIs. This enables calculation of the elevation component of the minimum frequent high level (mean elevation of FH LSI – mean HAC = elevation component of the minimum frequent high level). The mean HAC for the FL LSI soil samples provide the offset from the mean elevation of the FL LSIs. This enables calculation of the elevation component of the minimum frequent low level (mean elevation of FL LSI – mean HAC = elevation component of the minimum frequent low level).

The minimum levels are completed by assigning the appropriate duration and return interval of flooding or dewatering to the FH and FL LSIs. The hydrologic signatures of FH and FL LSIs (Figures 50 and 51) are critical components for developing minimum levels at sandhill lakes and need to be determined for numerous relatively undisturbed sandhill lake systems with long-term hydrologic records or calibrated hydrologic models. This would provide a range of signatures. The minimum levels would allow for a small change in magnitude from historic hydrology and maintain the

duration and return interval of flooding and dewatering on the dry side but within the natural variation of the hydrologic signatures observed (Figures 50 & 51).

For example, the return interval of flooding events should not be made so infrequent that the duration/return interval pair lies to the right of the observed signatures (Figure 50). Likewise, the return interval of dewatering events should not be made so frequent that the duration/return interval pair lies to the left of the observed signatures (Figure 51). In the examples provided a 90-day duration flooding event with a return interval of 1:3 years (33% exceedance or 33:100 years) on average over the long-term would be reasonable for the minimum frequent high level (Figure 50) and a 270-day duration dewatering event with a return interval of 1:5 years (20:100 years) on average over the long-term would be reasonable for the minimum frequent low level (Figure 51). This provides minimum frequent high and minimum frequent low levels with magnitude, duration, and return interval components.

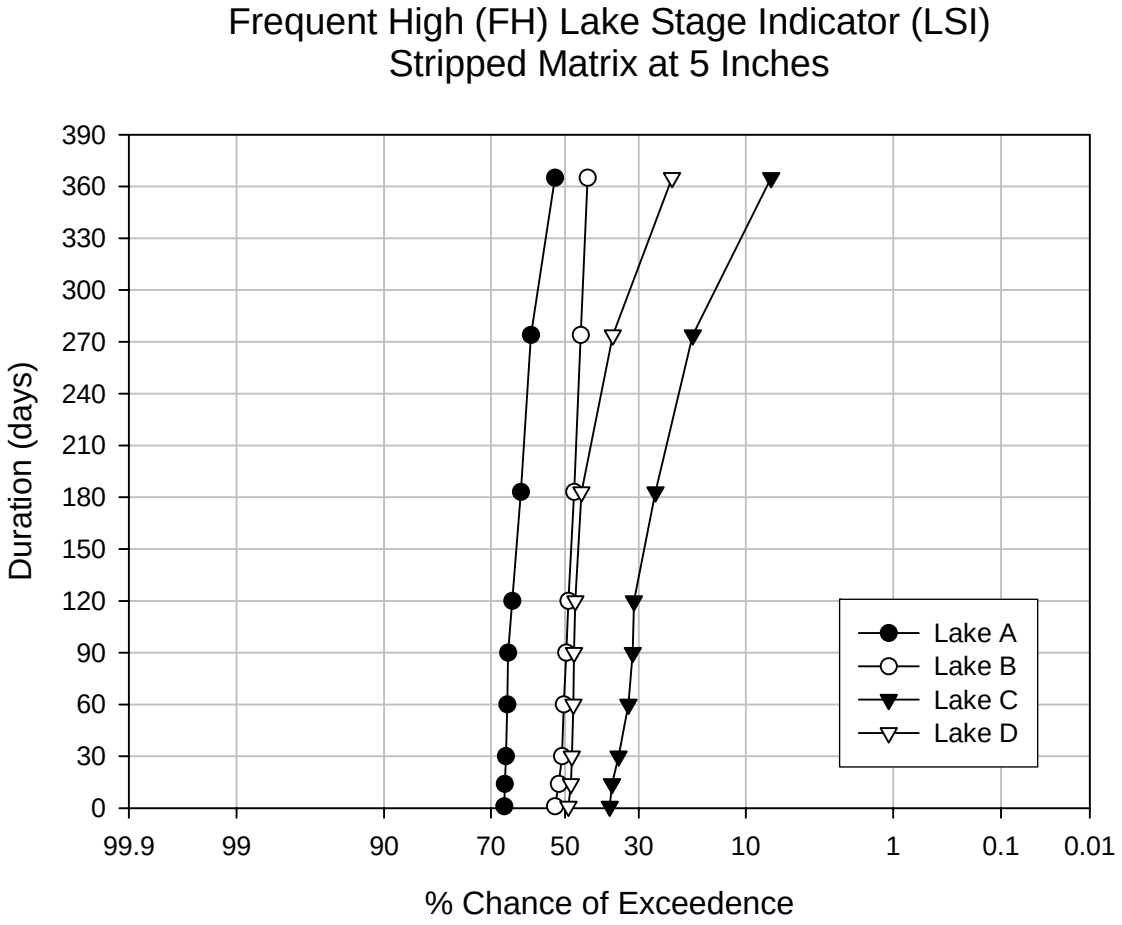

Figure 50. Hypothetical example of hydrologic signatures for the frequent high

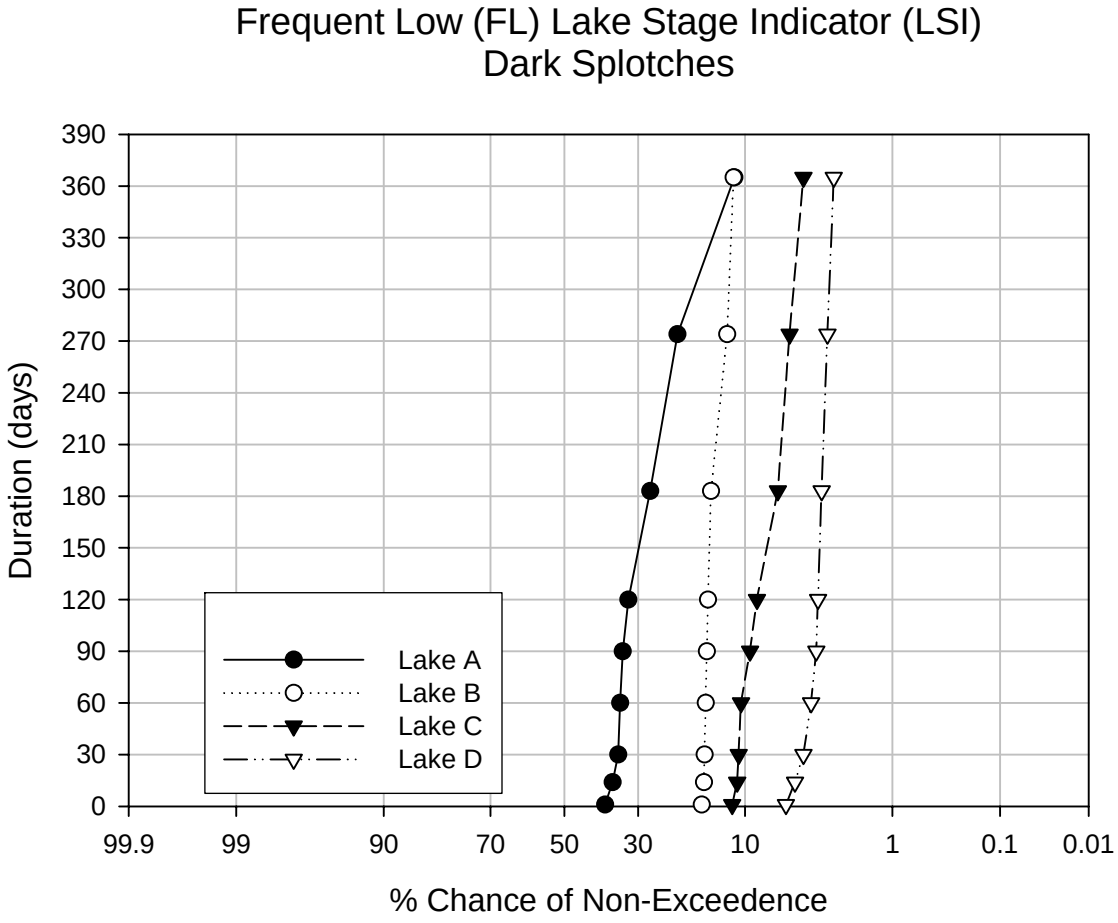

(FH) lake stage indicator (LSI) at four lakes

Figure 51. Hypothetical example of hydrologic signatures for the frequent low (FL) lake stage indicator (LSI) at four lakes

CONCLUSIONS

The goals of this study were to quantify the CFH and HAC in soil samples collected near the FH and FL LSIs at three sandhill lakes and develop models to estimate the CFH and HAC from the physical soil characteristics. In addition to these goals, the CFH and HAC were related to the AEVs, models were developed to estimate the AEVs from the physical soil characteristics, and examples of how this research might be applied to determine minimum levels was presented.

The CF was evident and typically extended 3.3 – 11.8 cm above the water table set at 18 cm in long cores (30 cm length). Anaerobic conditions persisted through and slightly above the upper extent of the CF ranging from 5.4 – 16.5 cm above the water table. Multiple regressions were developed to estimate the CFH and HAC from easily determined physical soil characteristics (e.g., particle-size distribution, bulk density, particle density, etc.), as well as more integrative but costly and time-consuming soil characteristic determinations (e.g., AEVs).

The CFH was best predicted by the particle-size classes percent sand, silt, and clay (adjusted R^2=0.6943). However, due to extreme multicollinearity this model was not recommended for use. A more robust regression model to estimate the CFH incorporates percent clay (cl), very coarse (vc), coarse (c), fine (fi), and very fine (vf) sand (Equation 23, adjusted R^2=0.6279).

$$\text{Predicted CFH} = 2.60(\text{cl}) + 9.22(\text{vc}) - 1.90(\text{c}) - 0.37(\text{fi}) - 0.60(\text{vf}) + 28.15 \quad (23)$$

Errors associated with the determination of the CFH and the physical soil characteristics incorporated into the regression model were small. Sources of error were considered because differences in the CFH were observed and attributed to the small differences in texture among the lakes sampled. The regression model would likely lose its predictive ability if errors in the measurement of the CFH or the parameters incorporated into the predictive model were too large.

The largest source of error in the determination of the CFH was the measurement of the long core segment lengths. Long core segments were measured to the nearest 0.5 mm, but a 0.1 mm error in the measurement of the segment length is equivalent to approximately a 1% error in the degree of saturation determined for that segment. This error was minimized by

careful measurement of the long core segment lengths and by averaging adjacent data points when estimating the CFH.

Errors associated with the particle-size analysis were also minimal because the viscosity of the DI/SMP solution in the 1 L graduated cylinder was accounted for and the particle densities of the mineral component of the soils sampled were very near 2.65 g/cm^3, both of which were accounted for in the settling times associated with the pipette method. This results in less than 2% error in the particle-size distribution measurements. In addition, the data for each particle size class was averaged for 3-cm segments from 0-18 cm reducing the variability of individual measurements. By minimizing errors in the measurement of the CFH and particle-size distribution, the predictive model of CFH is valid across the range of soil textures studied.

The best predictive model of HAC from the physical soil characteristics was developed with percent clay (cl) and percent very coarse (vc), coarse (c), fine (fi), and very fine (vf) sand fractions (adjusted R^2=0.4601). Because of the relatively low adjusted R^2, additional regression models were investigated to provide a better estimate of the HAC. The best predictor of the HAC was the CFH (Equation 29, adjusted R^2=0.6869).

$$HAC = 1.17(CFH) + 2.06 \quad (29)$$

The CFH is a measure of the near saturated zone above the water table and was expected to provide a better estimate of the HAC over a larger range of sandhill lake soils.

Neither the CFH nor the HAC were strongly related to the AEVs. Poor fit of the AEVs with the CFH and HAC was likely the result of several factors. First, the CFH, HAC, and AEVs were determined with different methods and differences based on wetting versus drainage may contribute to the poor fit. Also, taking an average of the AEVs from short cores from 0-18 cm may not adequately represent the pore connectivity in an intact 18 cm core. The AEVs are very similar in magnitude to the CFH and HAC but variability in this narrow data range also likely contributes to the poor fit. The AEVs however, were well correlated with soil texture parameters (Equations 25, 26, and 27; adjusted R=0.7584, 0.7254, and 0.7528, respectively).

$$\text{Predicted AEV} = 1.42(PC1vc\_c) - 0.23(m) + 21.53 \quad (25)$$

$$AEV = 6.61(vc) + 5.76 \quad (26)$$

Predicted AEV = 1.00(c) – 0.34(m) + 18.86 (27)

The CFH and HAC provide the corner stone for application of LSIs to determine minimum levels at sandhill lakes. Two threshold offsets were developed, a static threshold offset and a site-specific threshold offset. The static threshold offset, 10.7 cm, is the mean HAC measured in FH and FL soil cores from Lake Brooklyn, Swan Lake, and Two Mile Pond. The static threshold, 10.7 cm, can be deducted from the elevation of the FH and FL LSIs to establish the minimum levels.

Alternatively, site-specific threshold offsets can be developed based on the physical soil characteristics at a site. Significant differences in particle-size distribution, which directly affect the CFH and HAC, were observed among lakes. The CFH and thus the HAC at individual sandhill lakes can be estimated with the regression equations developed herein, based on the particle-size distribution data at LSIs identified at that particular lake. The HAC can then be applied as the threshold offset from the LSIs to determine the elevations of the minimum levels at a sandhill lake.

Because the regression equations to estimate the CFH and HAC from particle-size distribution data were developed from data on only three lakes and because the observed differences in soil characteristics resulted in only a 4.2 cm difference between the largest and smallest mean HAC for the three systems studied, it is recommended that application of a static threshold to determine minimum levels at sandhill lakes may be the optimal approach at this time. If additional data are collected and provide further support for the regression equations presented to estimate the CFH and HAC then the site-specific approach will become more robust.

The regression equations presented herein were developed in soils with greater than 92% sand and less than 4.2% clay, 4.1% silt, and 3% OC; and may not be applicable in finer textured soils. The regression equations to predict the CFH and HAC are based on a small data set due to the time and level of effort required to determine the CFH and HAC by wetting soil columns. These regression equations should be revised as additional data are collected. Data collection can be expedited by applying only one water table that fully captures the CF and not excessively air drying the soil cores (resulting in long wetting times) prior to use.

LITERATURE

Achtnich, C., F. Bak, and R. Conrad. 1995. Competition for electron donors among nitrate reducers, ferric iron reducers, sulfate reducers, and methanogens in anoxic paddy soil. Biol. Fertil. Soils 19:65-72.

Affek, H.P., D. Ronen, and D. Yakir. 1998. About production of CO2 in the capillary fringe of a deep phreatic aquifer. Water Resour. Res. 34:989-996.

Berkowitz, B., S. E. Silliman, and A. M. Dunn. 2004. Impact of the capillary fringe on local flow, chemical migration, and microbiology. Vadose Zone J. 3:534-548.

Blake, G.R., and K.H. Hartge. 1986. Particle density. p. 377-382. *In* A. Klute (ed.) Methods of Soil Analysis: Physical and Mineralogical Methods. 1986. American Society of Agronomy, Inc.; Soil Science Society of America, Inc., Madison, WI.

Blodau, C., N. Basiliko, and T. Moore. 2004. Carbon turnover in peatland mesocosms exposed to different water tables. Biogeochemistry 67:331-351.

Bovan, M.J., A.L. Endres, D.L. Rudolph and G. Parkin. 2003. The non-invasive characterization of pumping-induced dewatering using ground penetrating radar. J. Hydrol. 281:55-69.

Boufadel, M.C., M.T. Suidan, A.D. Venosa, and M.T. Bowers. 1999. Steady seepage in trenches and dams: Effect of capillary flow. J. Hydraulic Engineering 125(3):286-295.

Brady, N.C. and R.R. Weil. 2002. *The Nature and Properties of Soils, Thirteenth Edition.* pp. 960. Prentice Hall, Upper Saddle River, New Jersey.

Brooks, H.K. 1982. Guide to the Physiographic Divisions of Florida; compendium to the map Physiographic Divisions of Florida 8-5M-82. Cooperative Extension Service, University of Florida, Institute of Food and Agricultural Sciences. Gainesville, FL.

Brooks, R.H. and A.T. Corey. 1964. Hydraulic properties of porous media. Hydrology paper 3. Colorado St. Univ., Fort Collins, Co.

Browder, J.A. and B.G. Volk. 1978. Systems model of carbon transformations in soil subsidence. Ecol. Modell. 5:269-292.

Bumb, A.C., C.L. Murphy, and L.G. Everett. 1992. A comparison of three function forms for representing soil moisture characteristics. Ground Water 30(2):177-185.

Cebrian, J. 2004. Role of first-order consumers in ecosystem carbon flow. Ecology Letters 7:232-240.

Cirmo, C. and J. McDonnell. 1997. Linking the hydrologic and biogeochemical controls of nitrogen transport in near stream zones of temperate forested catchments: A Review. J. Hydrol. 199:88-120.

Conti, R.S. and P.R. Gunther. 1984. Relations of the phenology and seed germination to the distribution of dominant plants in the Okefenokee Swamp. p. 144-167. *In* The Okefenokee Swamp: Its natural history, geology, and geochemistry. Wetland Surveys. Los Alamos, NM.

David, P.G. 1996. Changes in plant communities relative to hydrologic conditions in the Florida Everglades. Wetlands 16(1):15-23.

Day, P.R. 1965. Particle fractionation and particle-size analysis. p. 545-567. *In* C.A. Black et al. (ed.) Methods of soil analysis, Part I. Agronomy 9:545-567.

Delaune, R.D. and K.R. Reddy. 2004. Redox Potential. p. 2200. *In* D. Hillel (ed). Encyclopedia of Soils in the Environment. 2004. Academic Press.

Duever, M.J. 1988. Hydrologic processes for models of freshwater wetlands. p. 9-39. *In* Mitsch, W., M. Straskroba, and S. Jorgensen (ed.) Wetland Modeling: Developments in Environmental Modeling. Elsevier, Amsterdam.

Ellis, L.R. 2002. Investigation of hydric and sub-aqueous soil morphologies to determine Florida sandhill lake stage fluctuations. Thesis. University of Florida, Gainesville, Florida.

Faulkner, S.P., W.H. Patrick, and R.P. Gambrell. 1989. Field techniques for measuring wetland soil parameters. Soil Sci. Soc. Am. J. 53:883-890.

[FNAI and DNR] Florida Natural Areas Inventory and Florida Department of Natural Resource. 1990. Guide to the natural communities of Florida. http://www.fnai.org/PDF/Natural_Communities_Guide.pdf

Gee, G.W. and J.W. Bauder. 1986. Particle-size analysis. p. 383-409. *In* A. Klute (ed) Methods of Soil Analysis, Part 1: Physical and Mineralogical Methods. 1986. American Society of Agronomy, Inc. and Soil Science Society of America, Inc., Madison, WI.

Gerla, P.J. 1992. The relationship of water-table changes to the capillary fringe, evapotranspiration, and precipitation in intermittent wetlands. Wetlands 12(2):91-98.

Gillham, R.W. 1984. The capillary fringe and its effect on water-table response. J. Hydrol. 67:307-324.

Hagenbuck, W.W., R. Thompson, and D.P. Rodgers. 1974. A preliminary investigation of the effects of water levels on vegetative communities of Loxahatchee National Wildlife Refuge, Florida. South Florida Environmental Project, Ecological Report DI-SFEP-74-20. Department of the Interior, Bureau of Sport Fisheries and Wildlife, Atlanta, Georgia.

Haines, W.B. 1927. Studies in the physical properties of soils. J. Agric. Sci. 17:264-290.

Haverkamp, R. and J.Y. Parlange. 1986. Predicting the water-retention curve from particle-size distribution: 1. Sandy soils without organic matter. Soil Sci. 142(6):325-339.

Heuperman, A. 1999. Hydraulic gradient reversal by trees in shallow water table areas and repercussions for the sustainability of tree growing systems. Agricult. Wat. Manag. 39:153-167.

Hillel, D. 1998. *Environmental Soil Physics*. pp. 771. Academic Press, New York.

Hintze, J. 2004. NCSS and PASS. Number Cruncher Statistical Systems. Kaysville, Utah.

Howard, P.J.A. and D.M. Howard. 1990. Use of organic carbon and loss-on-ignition to estimate soil organic matter in different soil types and horizons. Biol. Fertil. Soils 9:306-310.

Hunt, R.J., J.F. Walker, and D.P. Krabbenhoft. 1999. Characterizing hydrology and the importance of ground-water discharge in natural and constructed wetlands. Wetlands 19(2):458-472.

Hurt, G.W., F.C. Watts, and V.W. Carlisle. 2000. Using soil morphology for the identification of seasonal high saturation. p. 51-54. *In* V.W. Carlisle and G.W. Hurt (ed.) Hydric Soils of Florida Handbook. 3rd Edition. 2000. Florida Association of Environmental Soil Scientists, Gainesville, Florida.

Ingebritsen, S.E., C. McVoy, B. Glaz and W. Park. 1999. Florida Everglades. p. 95-106. *In* D. Galloway, D.R. Jones, and S.E. Ingebritsen (ed.) Land subsidence in the United States Circular 1182. U.S. Geological Survey, Denver, CO.

Jellali, S, H. Benremita, P. Muntzer, O. Razakarisoa, and G. Schafer. 2003. A large-scale experiment on mass transfer of Trichloroethylene from the unsaturated zone of a sandy aquifer and its interfaces. J. Contam. Hydrol. 60:31-53.

Jones Edmunds. 2006. Sandhill Lakes: Minimum Flows and Levels – Values, functions, criteria, and thresholds for establishing and supporting minimum levels (Draft Report). Jones, Edmunds, and Associates, Inc. Gainesville, Florida.

Kacimov, A.R. 2004. Capillary fringe and unsaturated flow in a porous reservoir bank. J. Irrig. Drain. Eng. 130(5):403-409.

Keihn, J.D. 1992. Analysis of capillary fringe dynamics in sandy, non-swelling soils. Thesis. George Mason University, Fairfax, VA.

Kim, Y. and E. Eltahir. 2004. Role of topography in facilitating coexistence of trees and grasses within savannas. Water Resour. Res. 40(7):WO7505.

Kinser, P. 1996. Wetland vegetation classification system. Unpublished document. St. Johns River Water Management District, Palatka, FL.

Klenk, I.D. and P. Grathwohl. 2002. Transverse vertical dispersion in groundwater and the capillary fringe. J. Contam. Hydrol. 58:111-128.

Klute, A. and G.E. Wilkinson. 1958. Some tests of the similar media concept of capillary flow: I. Reduced capillary conductivity and moisture characteristic data. Soil Sci. Soc. Am. Proc. 22:278-281.

Kushlan, J.A. 1990. Freshwater marshes. p. 324-363. *In* R.L. Myers and J.J. Ewel (ed.) Ecosystems of Florida. University of Central Florida Press, Orlando, FL.

Lehmann, P., F. Stauffer, C. Hinz, O. Dury, and H. Fluhler. 1998. Efffects of hysteresis on water water flow in a sand column with a fluctuating capillary fringe. J. Contam. Hydrol. 33:122-133.

Lockaby, B.G., R.S. Wheat and R.G. Clawson. 1996. Influence of hydroperiod on litter conversion to soil organic matter in a floodplain forest. Soil Sci. Soc. Am. J. 60:1989-1993.

Marrin, D., and J. Adriany. 1999. C2 and C3 hydrocarbon gases associated with highly reducing conditions in groundwater. Biogeochemistry 47:15-23.

Mausbach, M.J. 1990. Soil survey interpretations for wet soils. p. 176-178. *In* Proc. of the Eighth International Soil Correlation Meeting (VIII ISCOM): Characterization, classification, and utilization of wet soils. Louisiana and Texas. October 6-21, 1990 (Printed March 1992).

Miller, C.D., D.S. Durnford and A.B. Fowler. 2004. Equilibrium nonaqueous phase liquid pool geometry in coarse soils with discrete textural interfaces. J. Contam. Hydrol. 71:239-260.

Morris, D.R, B. Glaz and S.H. Daroub. 2004. Organic soil oxidation potential due to periodic flood and drainage depth under sugarcane. Soil Scientist 169:600-608.

Motz, L.H. and J.P. Heaney. 1991. Upper Etonia Creek Hydrologic Study Phase I Final Report. Special Publication: SJ 91-SP5. St. Johns River Water Management District. Palatka, FL.

Nachabe, M.H., C. Masek, and J. Obeysekera. 2004. Observations and modeling of profile soil water storage above a shallow water table. Soil Sci. Soc. Am. J. 68:719-724.

Nelson, D.W. and L.E. Sommers. 1986. Total carbon, organic carbon, and organic matter. p. 539-579 *In* A. Klute (ed) Methods of Soil Analysis, Part II: Chemical Methods of Soil Analysis. 1986. American Society of Agronomy, Inc. and Soil Science Society of America, Inc., Madison, WI.

Nelson, D.W. and L.E. Sommers. 1996. Total carbon, organic carbon, and organic matter. p. 961-1010. *In* D.L. Sparks, A.L. Page, P.A. Helmke, R.H. Loeppert, P.N. Soltanpour, M.A. Tabatabai, C.T. Johnston, and M.E. Sumner (ed.) Methods of Soil Analysis, Part 3: Chemical Methods. 1996. American Society of Agronomy, Inc. and Soil Science Society of America, Inc., Madison, WI.

Nkedi-Kizza, P. and T.C. Richardson. 2005. Minimum Flows and Levels: Sandhill Lake Criteria Development. Prepared for St. Johns River Water Management District, Contract No. PO 37419. St. Johns River Water Management District, Palatka, FL.

Novakowski, K.S. and R.W. Gillham. 1988. Field investigations of the nature of water-table response to precipitation in shallow water-table environments. J. Hydrol. 97:23-32.

Patrick, W.H. and A. Jugsujinda. 1992. Sequential reduction and oxidation of inorganic nitrogen, manganese, and iron in flooded soil. Soil Sci. Soc. Am. J. 56:1071-1073.

Peech, M., L.A. Dean, and J. Reed. 1947. Methods of soil analysis for soil fertility investigation. USDA Circ. 757. U.S. Gov. Print. Office, Washington, DC.

Peters, V. and R. Conrad. 1996. Sequential reduction processes and initiation of CH4 production upon flooding of oxic upland soils. Soil Biol. Biochem. 28:371-382.

Ponnamperuma, F.N. 1972. The chemistry of submerged soils. Adv. Agron. 24:29-96.

Price J.S., L. Rochefort, and S. Campeau. 2002. Use of shallow basins to restore cutover peatlands: Hydrology. Restoration Ecology 10(2):259-266.

Purdum, E.D., L.C. Burney, and T.M. Swihart. 1998. History of water management. p. 156-159. *In* E.A. Fernald and E.D. Purdum (ed.) Water Resources Atlas of Florida. 1998. Institute of Science and Public Affairs, Florida State University, Tallahassee, FL.

Rao, D.V., S.A. Jenab, and D.A. Clapp. 1990. Rainfall analysis for Northeast Florida Part V: Frequency analysis of wet season and dry season rainfall. Technical Publication SJ 90-3. St. Johns River Water Management District. Palatka, FL.

Rawls, W.J., D.L. Brakensiek, and K.E. Saxton. 1982. Estimation of soil water properties. Trans. ASAE 25:1316-1320, 1328.

Reddy, K.R. and E.M. D'Angelo. 1994. Soil processes regulating water quality in wetlands. p 309-324. *In* W. Mitsch (ed.) Global Wetlands – Old World and New. 1994. Elsevier Pub, New York.

Richards, L.A. 1928. The usefulness of capillary potential to soil-moisture and plant investigators. J. Agric. Res. 37(12):719-742.

Richardson, J.L., J.L. Arndt, and J.A. Montgomery. 2001. Hydrology of wetland and related soils. p. 35-84. *In* J.L. Richardson and M.J. Vepraskas (ed.) Wetland Soils: Genesis, Hydrology, Landscapes, and Classification. 2001. Lewis Publishers, Boca Raton, FL.

Ronen, D., H. Scher, and M. Blunt. 2000. Field observations of a capillary fringe before and after a rainy season. J. Contam. Hydrol. 44:103-118.

Rosenberry, D.O. and T.C. Winter. 1997. Dynamics of water-table fluctuations in an upland between two prairie-pothole wetlands in North Dakota. J. Hydrol. 191:266-289.

SAS Institute, Inc. 2003. Version 9.1.3. Servic Pack 3. Cary, NC.

Saxton, K.E., W.J. Rawls, J.S. Romberger, and R.I. Papendick. 1986. Estimating generalized soil-water characteristics from texture. Soil Sci. Soc. Am. J. 50:1031-1036.

Schlesinger, W.H. 1997. Biogeochemistry in freshwater wetlands and lakes. p. 224-260. *In* Biogeochemistry: An analysis of global change. 1997. Academic Press, New York.

Schothorst, C.J. 1977. Subsidence of low moor peat soils in the western Netherlands. Geoderma 17:265-291.

Schroth, M.H., S.J. Ahearn, J.S. Selker, and J.D. Istok. 1996. Characterization of Miller-similar sands for laboratory hydrologic studies. Soil Sci. Soc. Am. J. 60:1331-1339.

Schulte, E.E. and B.G. Hopkins. 1996. Estimation of soil organic matter by weight loss-on-ignition. p. 21-31. *In* F.R. Magdoff, M.A. Tabatabai, and E.A. Hanlon, Jr. (ed.) Soil Organic Matter: Analysis and Interpretation. SSSA Special Publication no. 46. Soil Science Society of America, Inc., Madison, WI.

Silliman, S.E., B. Berkowitz, J. Simunek, and M. Th. Van Genuchten. 2002. Fluid flow and chemical migration within the capillary fringe. Ground Water 40:76-84.

Simmons, C., M. Pierini, and J. Hutson. 2002. Laboratory investigation of variable-density flow and solute transport in unsaturated-saturated porous media. Trans. Porous Media 47:215-244.

Sinke, A.J. C., O. Dury, and J. Zobrist. 1998. Effects of a fluctuating water table: Column study on redox dynamics and fate of some organic pollutants. J. Contam. Hydrol. 33:231-246.

SJRWMD (St. Johns River Water Management District). 2006a. Methodology to predict frequent high and frequent low water levels in Florida sandhill lakes using soil morphology. Draft Report. T.C. Richardson, D.S. Segal, G.W. Hurt, G.B. Hall, R.J. Epting, and B.L. Skulnick (ed.). St. Johns River Water Management District. Palatka, FL.

SJRWMD (St. Johns River Water Management District). 2006b. Minimum Flows and Levels Methods Manual (draft). Hall, G.B., C. Neubauer, and P. Robison (eds.). St. Johns River Water Management District, Palatka, Florida.

Slaymaker, O. 2000. Research developments in the hydrological sciences in Canada (1995-1998): Surface Water—Quantity, Quality, and Ecology. Hydrological Processes 14:1539-1550.

Soil Survey Staff. 1999. Soil Taxonomy: A basic system of soil classification for making and interpreting soil surveys. Second Edition. United Stated Department of Agriculture, Natural Resources Conservation Service. Handbook No. 436. U.S. Government Printing Office, Washington DC.

StatSoft, Inc. 2005. The Statistics Homepage. (accessed March 8, 2007). www.statsoft.com/textbook/stathome.html

Stephens, J.C. 1984. Subsidence of organic soils in the Florida Everglades--A review and update. p. 375-384. *In* P.J. Gleason (ed.) Environments of South Florida Present and Past II. 1984. Miami Geologic Society, Coral Gables, FL.

Tokunaga, T.K., K.R. Olson, and J. Wan. 2004. Conditions necessary for capillary hysteresis in porous media: Tests of grain size and surface tension influences. Water Resour. Res. 40:WO5111.

USDA. 1992. Soil Survey Laboratory Methods Manual. p. 14. U.S. Department of Agriculture, Washington, DC.

USDA, NRCS. 2002. Field Indicators of Hydric Soils in the United States, Version 5.0. G.W. Hurt, P.M. Whited, and R.F. Pringle (eds.). USDA, NRCS in cooperation with the National Technical Committee for Hydric Soils, Forth Worth, Texas.

USDA, NRCS. 2006. Soil Survey Staff, Official Soil Series Descriptions. Available URL: http://soils.usda.gov [Accessed September 17, 2006]

USDA Soil Conservation Service. 1989. Soil Survey of Clay County, Florida. p. 207. U. S. Department of Agriculture, Washington, DC.

USDA Soil Conservation Service. 1990. Soil Survey of Putnam County, Florida. p. 224. U. S. Department of Agriculture, Washington, DC.

Van der Valk, A.G. 1981. Succession in wetlands: A Gleasonian approach. Ecology 62:688-696.

Veneklaas, E.J. and P. Poot. 2003. Seasonal patterns in water use and leaf turnover of different plant functional types in a species-rich woodland, south-western Australia. Plant and Soil 257:295-304.

Vepraskas, M.J. 2001. Morphological features of seasonally reduced soils. p. 163-182. *In* J.L. Richardson and M.J. Vepraskas (ed.) Wetland Soils: Genesis, Hydrology, Landscapes, and Classification. Lewis Publishers. Boca Raton, FL.

Walkey A., and Black I. A. 1934. An examination of the digestion method for determining soil organic matter and a proposed modification of the chromic acid titration method. Soil Sci. 37:29-38.

Williams, A.G., J.F. Dowd and E.W. Meyles. 2002. A new interpretation of kinematics stormflow generation. Hydrological Processes 16:2791-2803.

Zilberbrand, M., E. Rosenthal, and E. Schachnai. 2001. Impact of urbanization on hydrochemical evolution of groundwater and on unsaturated zone gas composition in the coastal city of Tel Aviv, Israel. J. Contam. Hydrol. 50:175-208.

APPENDIX A – PRINCIPLES OF THE MARIOTTE DEVICE

The Mariotte device was used to apply a constant head (cm), for purposes such as determining saturated hydraulic conductivity or establishing a stable water table. The Mariotte device schematic shown in Figure A1 differs from the Mariotte devices utilized in this research. The schematic facilitates explanation of the device and the principles are the same for both designs. The Mariotte device in Figure A1 was constructed from a burette and was modified with a valve at the top (C), an open glass tube extended from the top to near the bottom of the burette, and an exit valve (D). Four additional valves, I, II, III, and IV, were added along the length of the burette above the air entry point (A) to facilitate an explanation of the principles behind the device.

When valve C is open and valve D is closed the entire system is at atmospheric pressure and the water level in the tubes from Valves I, II, III, and IV are all equal to the water level (X) in the Mariotte device and in the glass tube. When valve C is closed and valve D is open water begins to flow out of valve D. This creates a vacuum (P) above the water level, which in turn simultaneously draws air down the glass tube and draws a portion of the water from the tubes connected to valves I – IV into the device. If valve D remains open, air bubbles will enter from point A to reduce the suction at P and allow water to exit through valve D.

To explain the Mariotte device, assume that valve C is closed and that valve D is open long enough to create a vacuum and allow air to reach point A, at which point valve D is closed. At this point the air remains at point A (atmospheric pressure) because the vacuum is maintained at P, above the water surface. This means that all of the water above point A is exactly counteracted by the suction P, otherwise water would rise in the glass tube above point A. This also means that there is suction applied at valves I – IV. When the water is above a valve the suction at that valve is equal to the difference between the suction at P and the length from the water surface to that valve based on the equations (B-1, B-2, B-3, B-4, and B-5), where A = atmospheric pressure; P =suction in vacuum; X = height of water above the air entry point (bubble); L = distance of valve above air entry point (A). Atmospheric pressure (A) is taken to be 0.

Pressure (h) at air bubble	$A = P + X$	(B-1)
Since	$A = 0$	(B-2)
	$P = -X$ cm	(B-3)
At any valve the pressure is	$h = X-L + P$	(B-4)
	$h = -L$ cm	(B-5)

For example, if the water is (X = 51 cm) above point A, then the suction at P equals 51 cm. For valve I (L = 41 cm) above point A, so there is 10 cm of water above it. This means that the suction at P (51 cm) is only holding up 10 cm of water at valve I, resulting in 41 cm of suction at that valve (Equations B-1 to B-5). Likewise, this results in 30 cm, 19 cm, and 8 cm of suction at valves II, III, and IV respectively. The end result is that the suction at valves I – IV are equal to their height above point A. When the water level is allowed to drop below a valve, the suction at that valve is equivalent to the suction at

point P. Once the water falls below point A the system is open to the atmosphere and no longer provides a constant head.

In summary, the water above the air entry point exerts a pressure towards valve D, but this pressure is balanced by an equal negative pressure (i.e., suction), at point P, above the water level. Therefore, the water above the air entry point acts a source of water for, but does not influence the magnitude of, the constant head. The constant head is only that portion of the water below the air entry point. The head is equal to the vertical distance between point A and the open end of the tube connected to valve D. The constant head as shown in Figure A1 is equal to 27 cm. If the open end of the tube connected to valve D was raised to the same height as point A, no water would exit the tube. The Mariotte device provides a constant head until the water level drops below point A, at which point the entire system goes to equilibrium with the atmosphere.

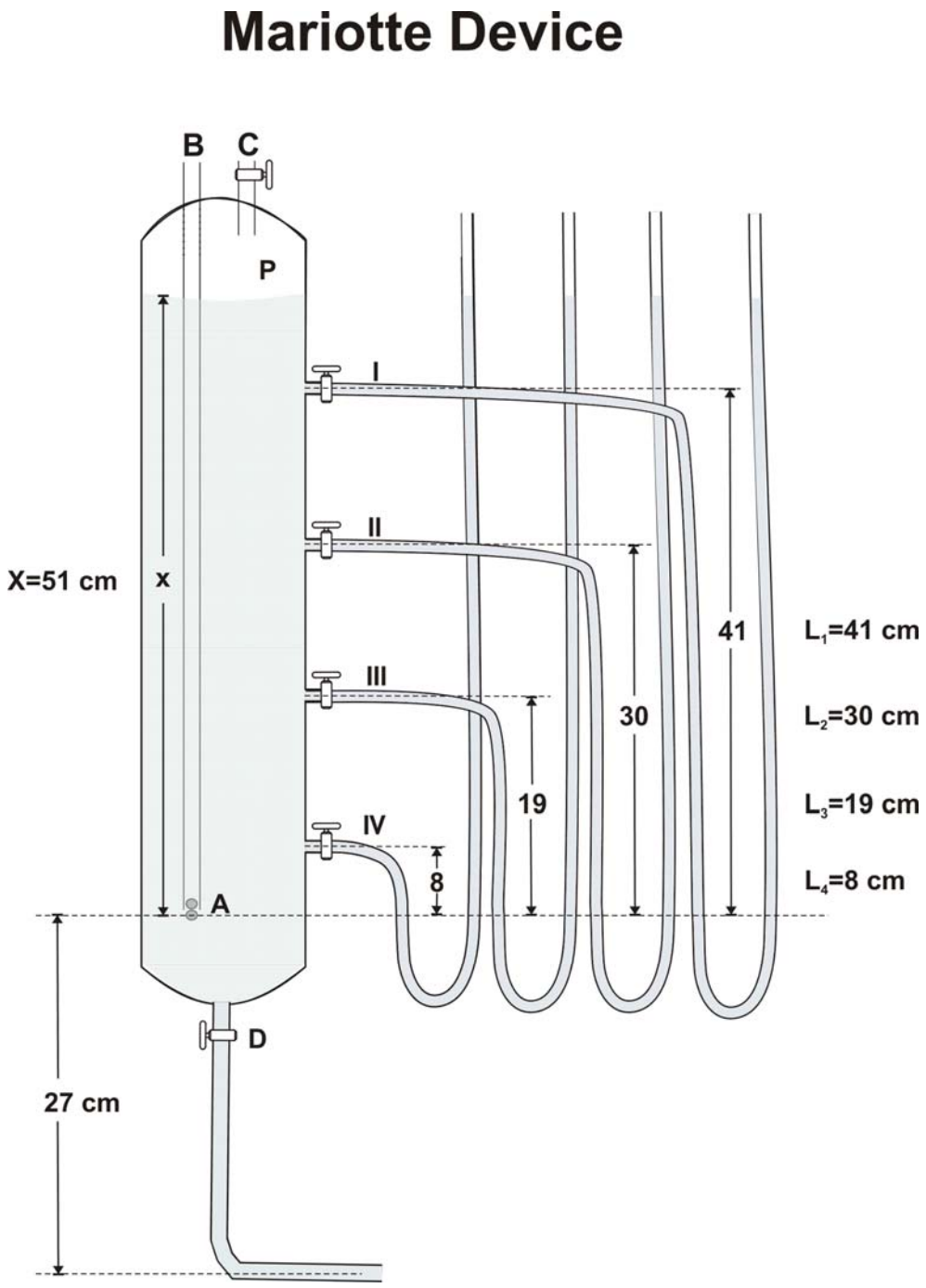

Figure A1. Schematic of a Mariotte Device

APPENDIX B – SUMMARY OF SOIL CORE DATA FOR COMPARISON WITH CAPILLARY FRINGE

Table B1. Soil parameter means for soil core segments from 0-18 cm

lk	loc	wt	cl	sa	si	vc	c	m	fi	vf	sa_tot	loi	oc
BR	FH1	18	1.964	96.635	1.400	0.196	5.755	53.400	38.396	2.267	100.014	1.769	0.878
BR	FH2	18	0.697	99.501	0.037	0.236	7.855	62.250	28.958	0.512	99.811	0.399	0.100
BR	FH3	18	1.082	98.189	0.733	0.155	5.287	51.522	41.121	1.653	99.737	0.431	0.116
BR	FL1	18	1.282	98.142	0.576	0.283	6.615	49.375	41.731	1.940	99.944	0.737	0.291
BR	FL2	18	0.662	98.266	1.073	0.127	5.158	47.301	45.393	1.956	99.934	0.914	0.391
BR	FL3	18	2.099	97.323	0.579	0.423	10.831	59.194	28.184	1.152	99.784	1.129	0.514
SW	FH1	18	2.034	97.757	0.448	1.441	7.913	36.695	49.873	3.842	99.764	1.076	0.484
SW	FH2	18	1.988	96.981	1.031	0.922	6.165	33.778	55.125	4.027	100.017	2.058	1.043
SW	FH3	18	2.785	95.602	1.613	1.208	9.258	42.523	43.563	3.365	99.918	2.275	1.166
SW	FL1	18	2.174	97.519	0.414	1.099	6.723	34.767	52.772	4.580	99.941	1.403	0.670
SW	FL2	18	2.065	95.961	1.973	1.293	8.391	39.182	47.176	3.834	99.876	2.553	1.325
SW	FL3	18	2.738	96.183	1.097	1.168	9.535	40.907	44.647	3.684	99.940	1.796	0.894
TM	FH1	20	2.161	96.173	1.666	0.636	6.475	45.283	34.960	12.648	100.002	1.356	0.631
TM	FH2	18	2.318	95.607	2.075	0.668	6.826	47.683	33.643	11.166	99.987	1.790	1.087
TM	FH3	18	1.610	97.380	1.009	0.873	7.397	46.063	35.785	9.864	99.983	0.924	0.715
TM	FL1	18	1.752	97.587	0.661	0.877	8.489	46.065	32.696	11.761	99.888	1.223	0.397
TM	FL2	18	2.067	96.535	1.398	0.868	8.078	46.716	33.808	10.554	100.025	1.670	0.774
TM	FL3	18	0.756	98.231	1.107	1.121	9.834	46.968	33.440	8.112	99.476	1.515	0.794

Table B1. Continued

lk	loc	wt	vwc	lc_bd	lc_pd	lc_f	lc_sat	sc_bd	sc_pd	sc_f	CFH	cf_sat	HAC	aev
BR	FH1	18	0.38	1.39	2.60	0.27	0.38	1.40	2.52	0.44	7.41	0.88	10.57	7.61
BR	FH2	18	0.30	1.57	2.60	0.19	0.30	1.53	2.62	0.42	6.97	0.90	11.15	8.43
BR	FH3	18	0.29	1.58	2.60	0.19	0.29	1.57	2.66	0.41	6.82	0.89	10.44	3.80
BR	FL1	18	0.28	1.54	2.62	0.18	0.28	1.52	2.62	0.42	3.87	0.92	6.21	7.83
BR	FL2	18	0.31	1.49	2.62	0.21	0.31	1.58	2.61	0.39	3.26	0.91	7.38	6.71
BR	FL3	18	0.30	1.61	2.62	0.19	0.30	1.62	2.63	0.39	6.24	0.90	11.53	8.53
SW	FH1	18	0.33	1.59	2.57	0.21	0.33	1.55	2.60	0.40	11.76	0.92	15.11	14.47
SW	FH2	18	0.33	1.55	2.57	0.21	0.33	1.52	2.59	0.41	9.66	0.91	12.42	13.99
SW	FH3	18	0.36	1.54	2.57	0.23	0.36	1.60	2.49	0.36	10.88	0.93	15.77	13.31
SW	FL1	18	0.31	1.55	2.55	0.20	0.31	1.62	2.60	0.38	6.77	0.89	13.92	15.11
SW	FL2	18	0.33	1.56	2.55	0.21	0.33	1.49	2.51	0.41	10.27	0.92	12.58	12.79
SW	FL3	18	0.30	1.52	2.55	0.20	0.30	1.56	2.53	0.38	8.52	0.88	10.12	15.25
TM	FH1	20	0.30	1.45	2.56	0.20	0.30	1.53	2.58	0.41	8.34	0.76	11.35	13.31
TM	FH2	18	0.31	1.63	2.56	0.19	0.31	1.51	2.34	0.35	9.12	0.85	16.50	8.80
TM	FH3	18	0.26	1.51	2.56	0.17	0.26	1.48	2.54	0.42	4.56	0.84	5.81	9.03
TM	FL1	18	0.21	1.59	2.59	0.13	0.21	1.66	2.61	0.36	4.39	0.91	5.63	12.19
TM	FL2	18	0.27	1.55	2.59	0.17	0.27	1.65	2.49	0.33	8.46	0.82	9.98	10.21
TM	FL3	18	0.15	1.58	2.59	0.09	0.15	1.64	2.32	0.29	4.92	0.78	5.48	12.26

Table B2. Soil parameters and abbreviations

aev	Air entry value calculated based on the Brooks and Corey equation (cm)
c	percent coarse sand
CFH	capillary fringe height (cm)
cf_sat	percent saturation at upper extent of capillary fringe
cl	percent clay
fi	percent fine sand
lc_bd	long core bulk density (g/cm^3)
lc_f	long core porosity
lc_pd	ong core particle density (g/cm^3)
lc_sat	mean degree of saturation in long cores (0-18 cm)
lk	lake name (BR – Brooklyn, SW – Swan, and TM – Two Mile)
loc	location (FH1, FH2, FH3, FL1, FL2, FL3)
loi	percent weight loss on ignition (at 500°C for 3 h)
m	percent medium sand
oc	percent organic carbon
HAC	height of anaerobic conditions (cm)
sa	percent sand
sa_tot	sum of sand fractions
sc_bd	short core bulk density (g/cm^3)
sc_f	short core porosity
sc_pd	short core particle density (g/cm^3)
si	percent silt
vc	percent very coarse sand
vf	percent very fine sand
vwc	volumetric water content
wt	water table (cm)

APPENDIX C – PRINCIPAL COMPONENTS ANALYSIS SUMMARY DATA

Table C1. Correlation matrix for determination of principal components of percent silt (si) and clay (cl)

	si	cl
si	1.000	0.446
cl	0.446	1.000

Table C2. Eigenvectors for determination of principal components of percent silt (si) and clay (cl)

	PC1	PC2
si	0.707	0.707
cl	0.707	-0.707

Table C3. Eigenvalues and proportion of variance accounted for by each principal component of percent silt (si) and clay (cl)

	Eigenvalue	Difference	Proportion	Cumulative
PC1	1.446	0.891	0.723	0.723
PC2	0.554	-	0.277	1.000

Table C4. Correlation matrix for determination of principal components of percent fine (fi) and very fine (vf) sand fractions

	fi	vf
fi	1.000	-0.325
vf	-0.325	1.000

Table C5. Eigenvectors for determination of principal components of percent fine (fi) and very fine (vf) sand fractions

	PC1	PC2
fi	0.707	0.707
vf	-0.707	0.707

Table C6. Eigenvalues and proportion of variance accounted for by each principal component of percent fine (fi) and very fine (vf) sand fractions

	Eigenvalue	Difference	Proportion	Cumulative
PC1	1.325	0.649	0.662	0.662
PC2	0.676	-	0.338	1.000

Table C7. Correlation matrix for determination of principal components of percent very coarse (vc) and coarse (c) sand fractions

	vc	c
vc	1.000	0.511
c	0.511	1.000

Table C8. Eigenvectors for determination of principal components of percent very coarse (vc) and coarse (c) sand fractions

	PC1	PC2
vc	0.707	0.707
c	0.707	-0.707

Table C9. Eigenvalues and proportion of variance accounted for by each principal component of percent very coarse (vc) and coarse (c) sand fractions

	Eigenvalue	Difference	Proportion	Cumulative
PC1	1.511	1.022	0.755	0.755
PC2	0.489	-	0.245	1.000

APPENDIX D – SCATTER PLOTS OF SOIL PARAMETERS WITH THE CAPILLARY FRINGE HEIGHT (CFH) AND THE HEIGHT OF ANAEROBIC CONDITIONS (HAC)

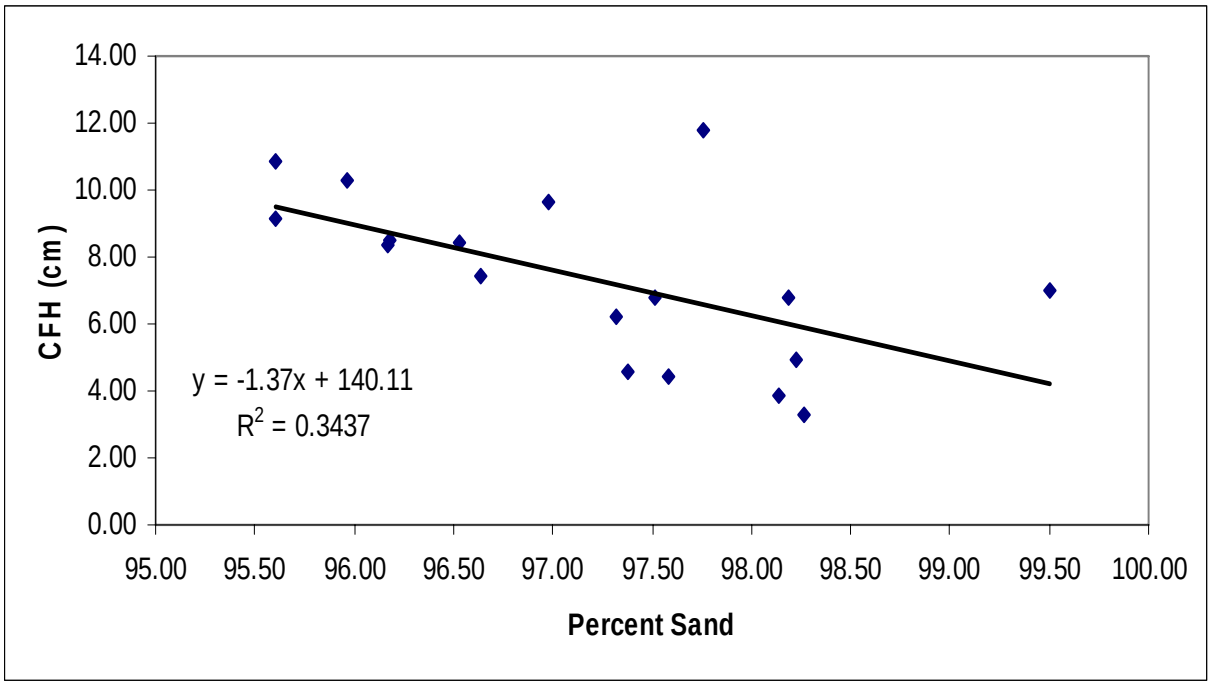

Figure D1. Scatter plot of percent sand with the capillary fringe height (CFH)

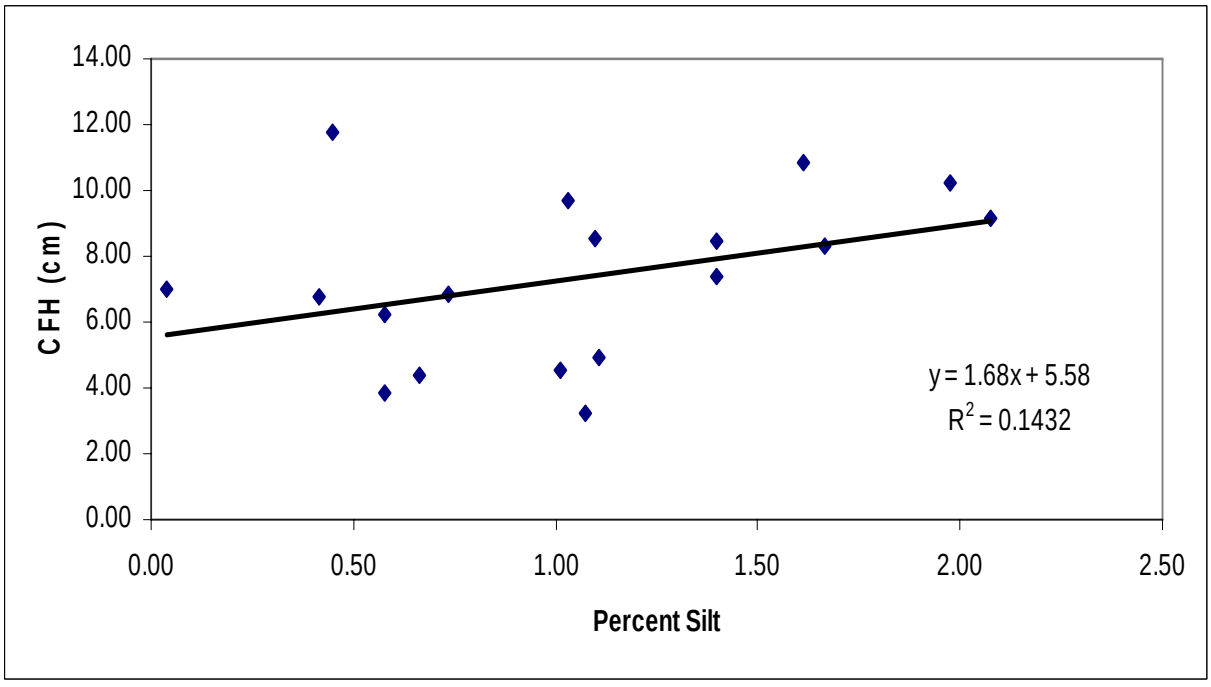

Figure D2. Scatter plot of percent silt with the capillary fringe height (CFH)

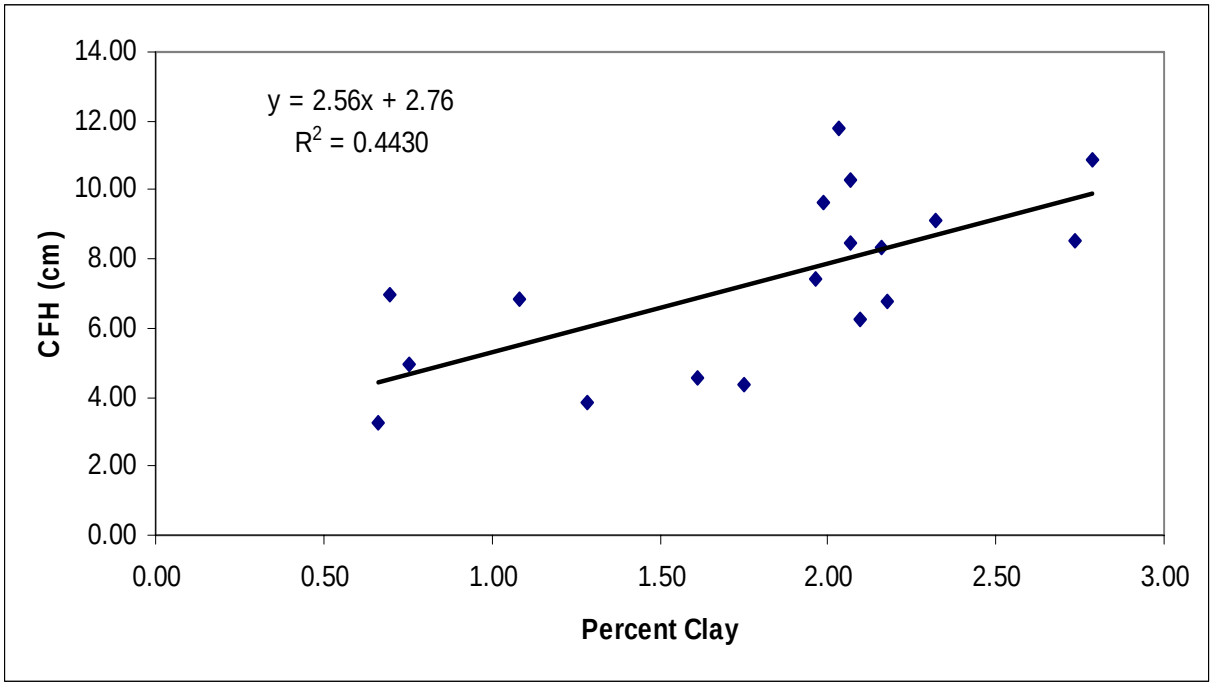

Figure D3. Scatter plot of percent clay with the capillary fringe height (CFH)

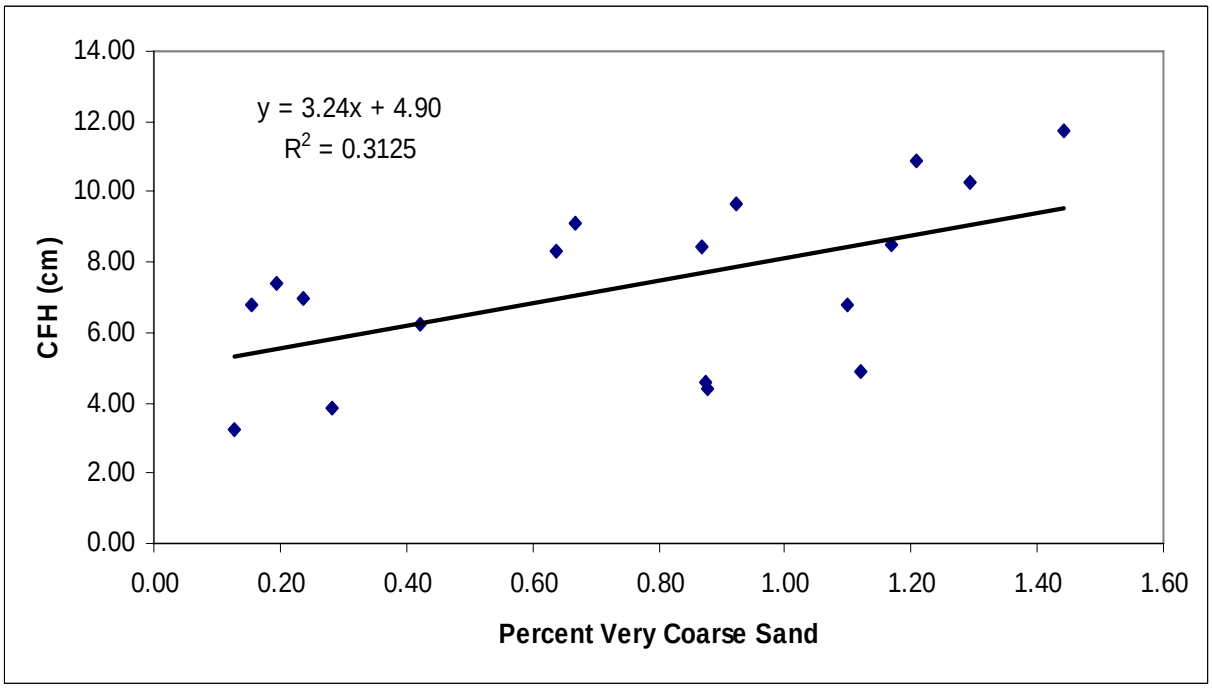

Figure D4. Scatter plot of percent very coarse sand with the capillary fringe height (CFH)

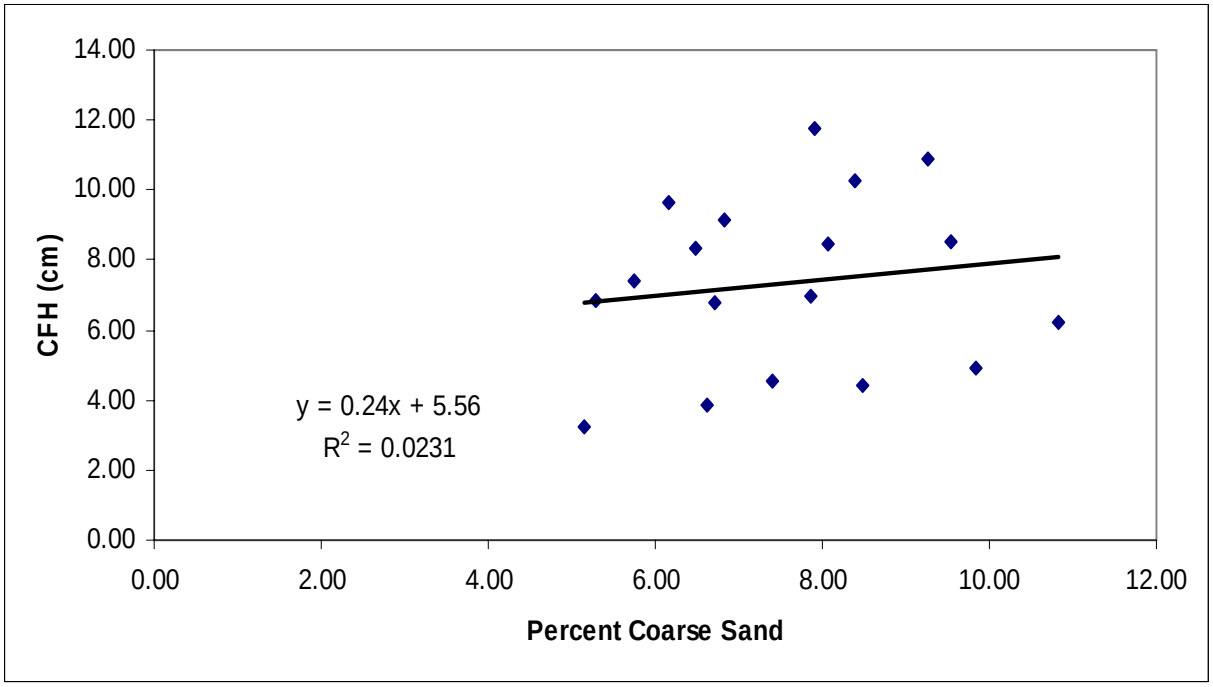

Figure D5. Scatter plot of percent coarse sand with the capillary fringe height (CFH)

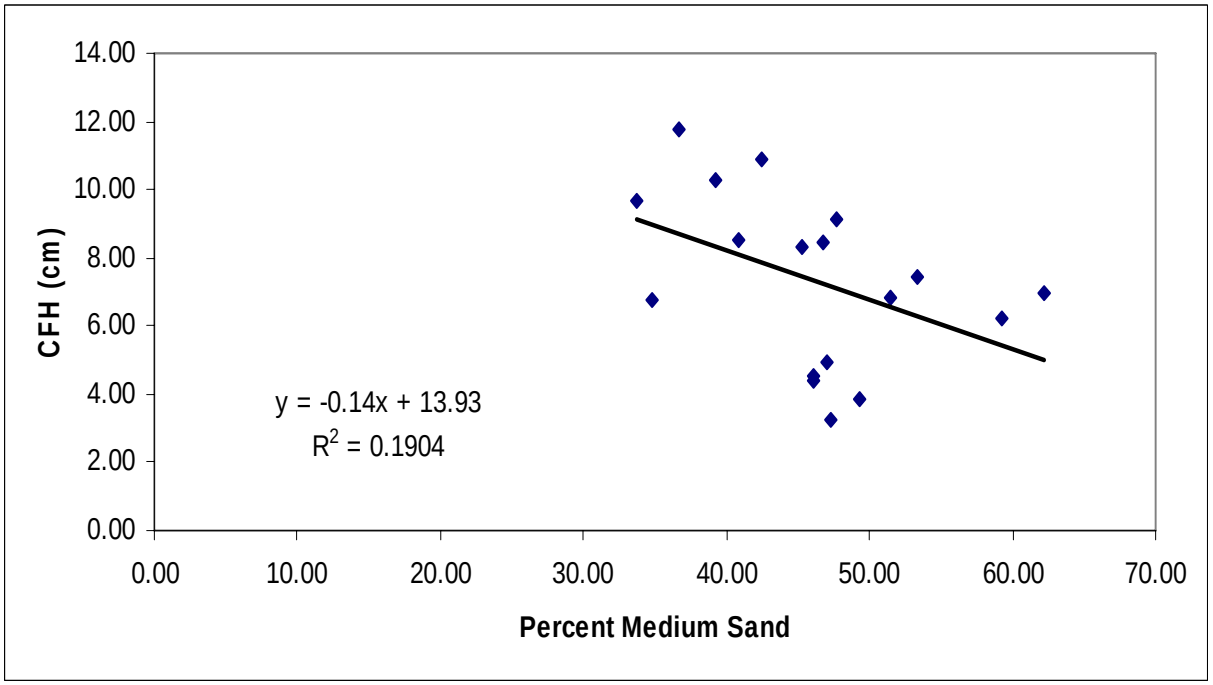

Figure D6. Scatter plot of percent medium sand with the capillary fringe height (CFH)

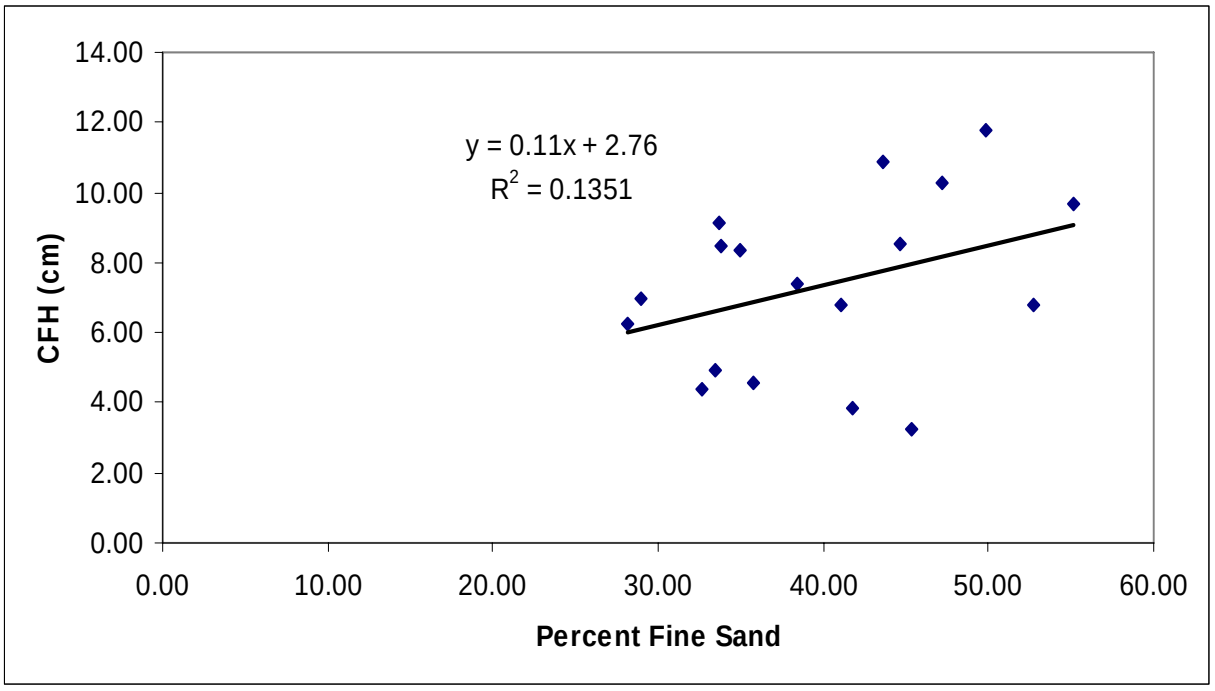

Figure D7. Scatter plot of percent fine sand with the capillary fringe height (CFH)

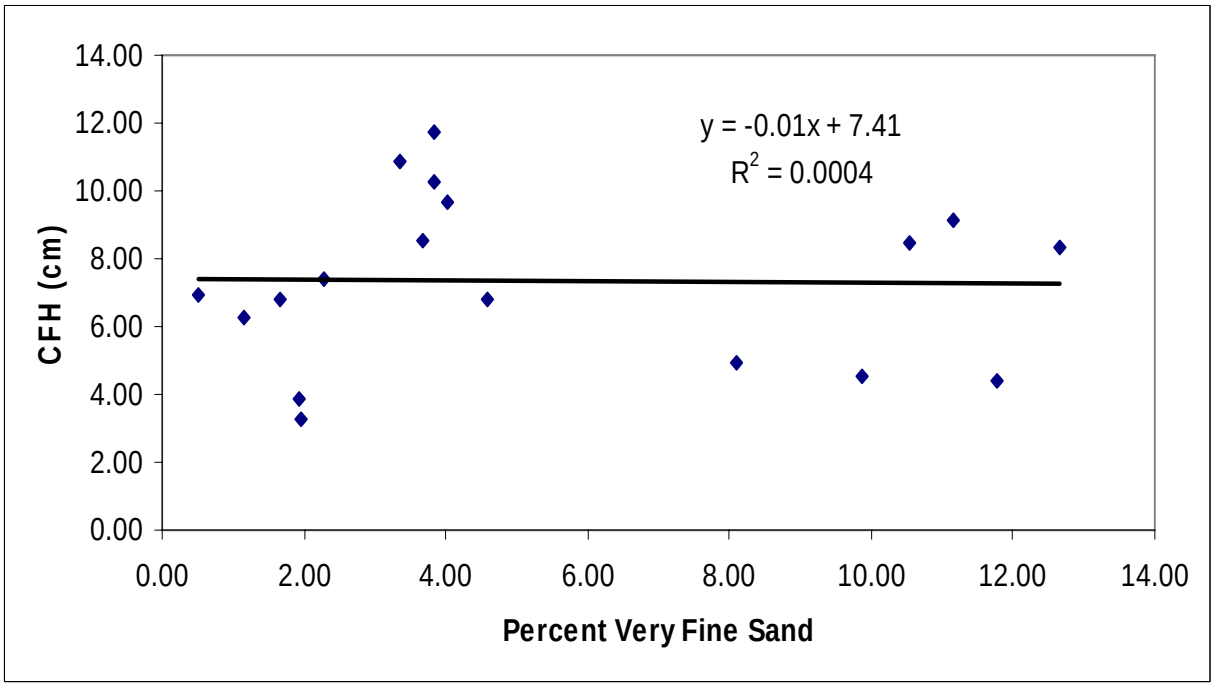

Figure D8. Scatter plot of percent very fine sand with the capillary fringe height (CFH)

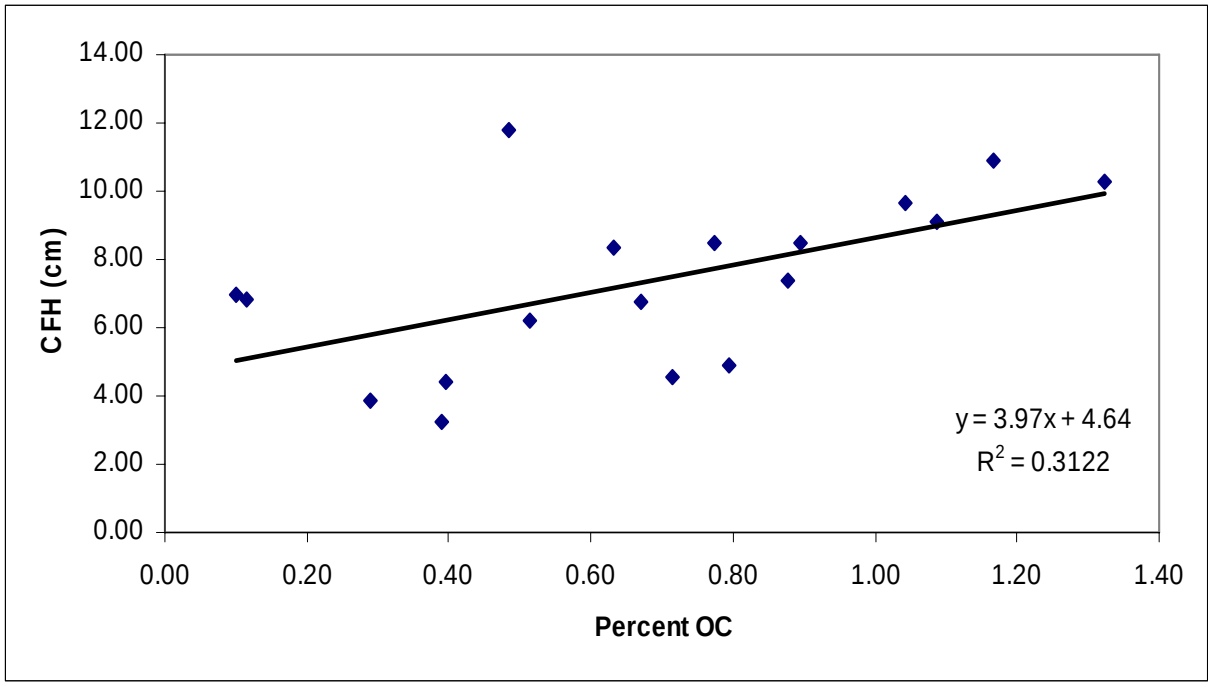

Figure D9. Scatter plot of percent organic carbon (OC) with the capillary fringe height (CFH)

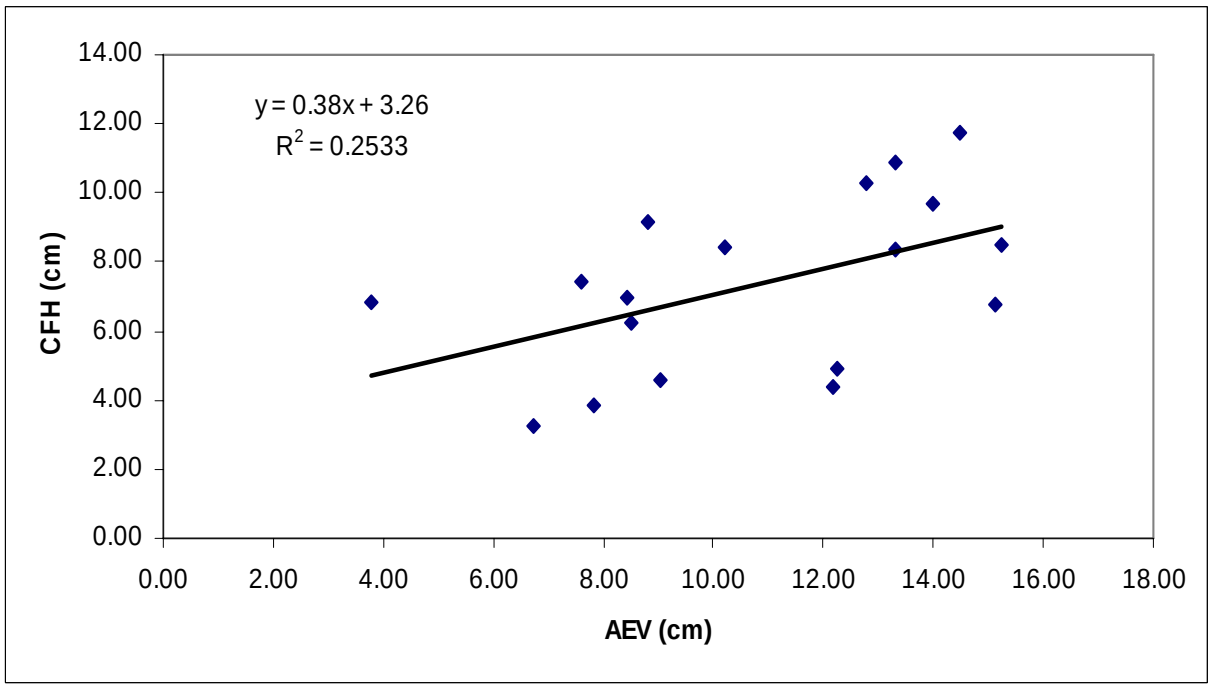

Figure D10. Scatter plot of the air entry values (AEV) with the capillary fringe height (CFH)

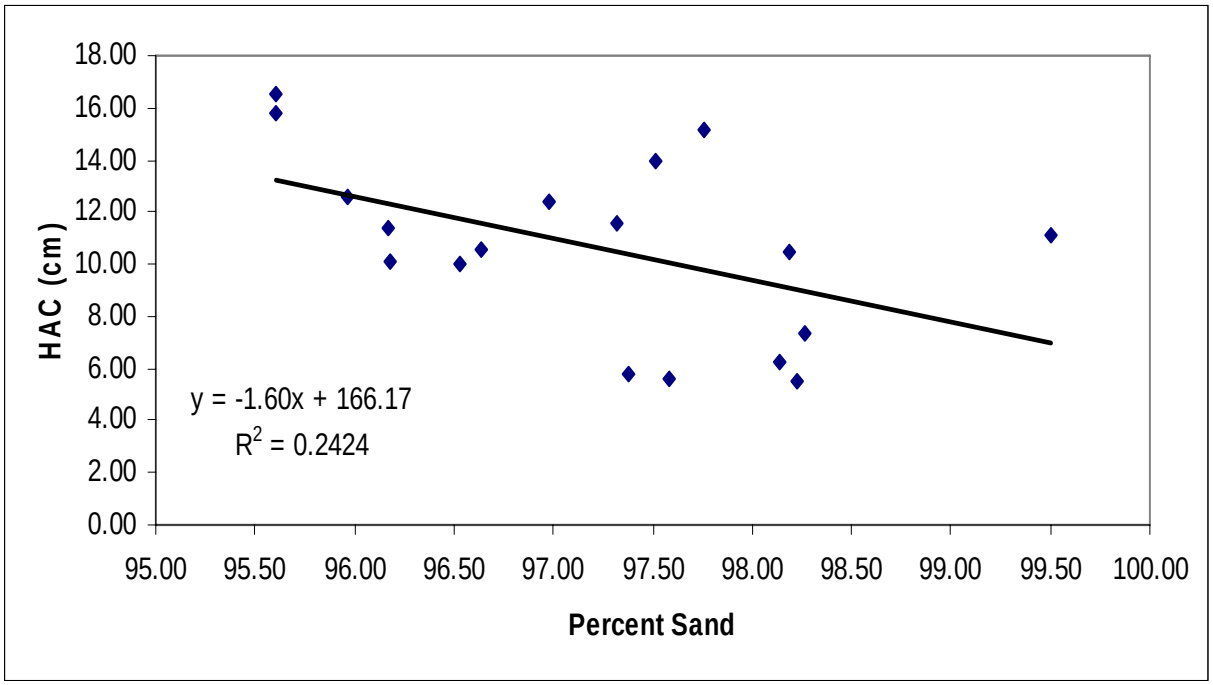

Figure D11. Scatter plot of percent sand with the height of anaerobic conditions (HAC)

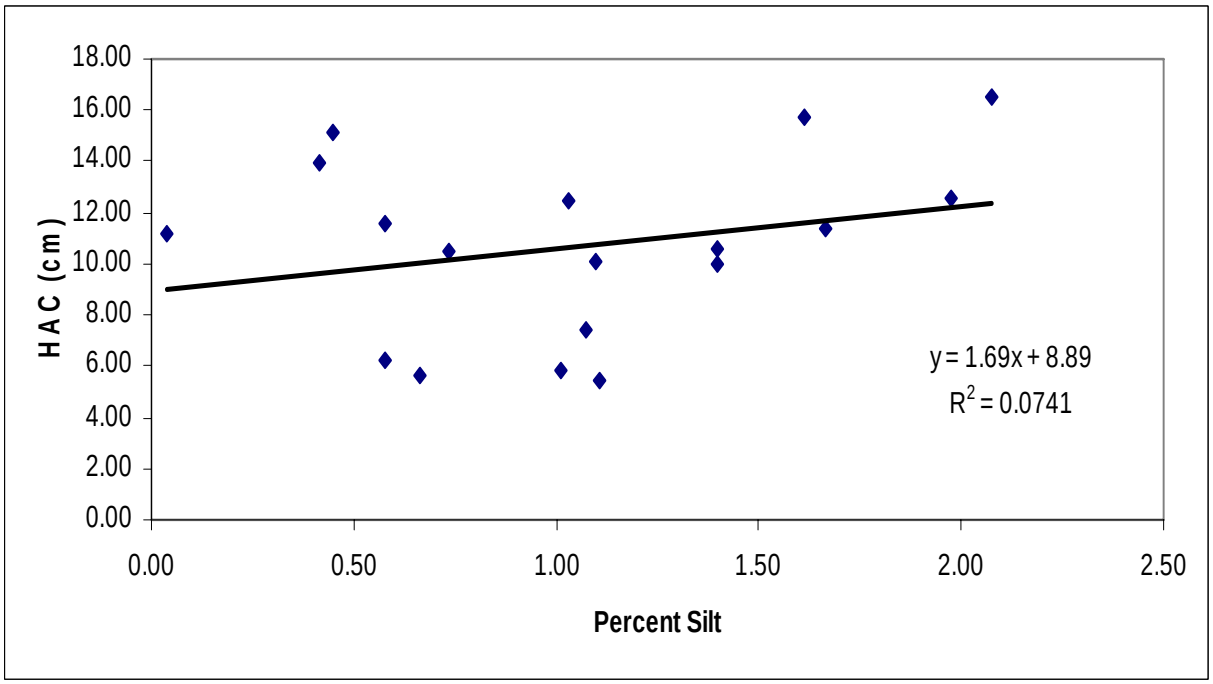

Figure D12. Scatter plot of percent silt with the height of anaerobic conditions (HAC)

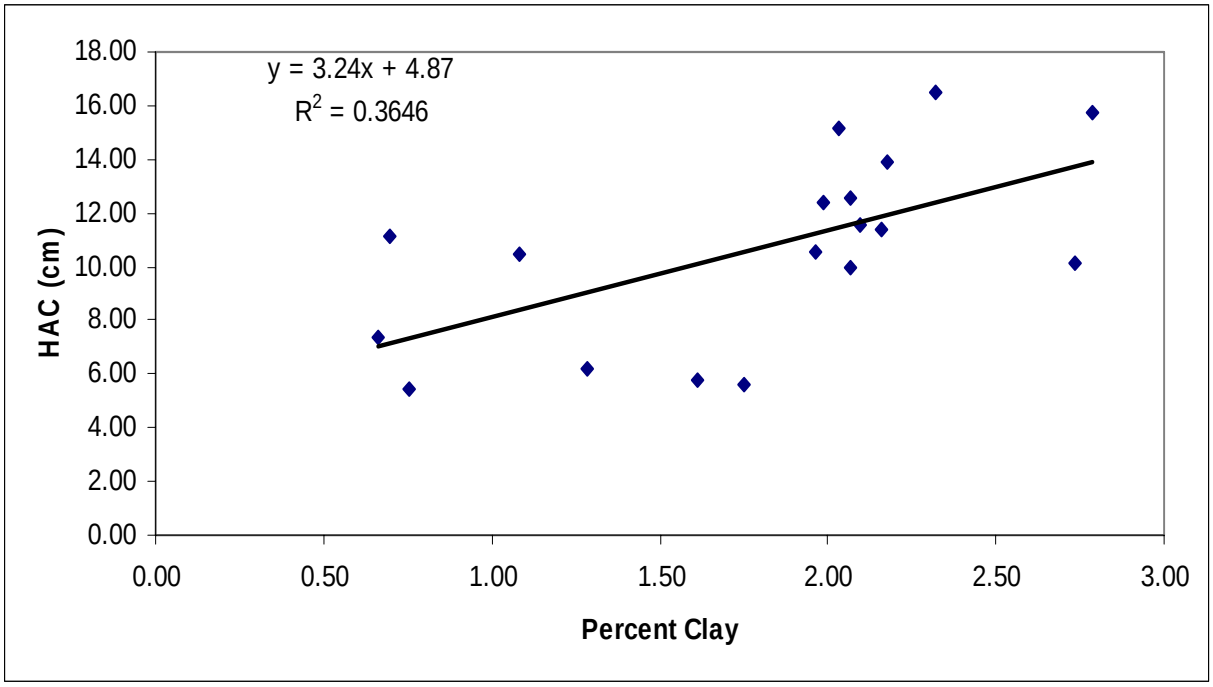

Figure D13. Scatter plot of percent clay with the height of anaerobic conditions (HAC)

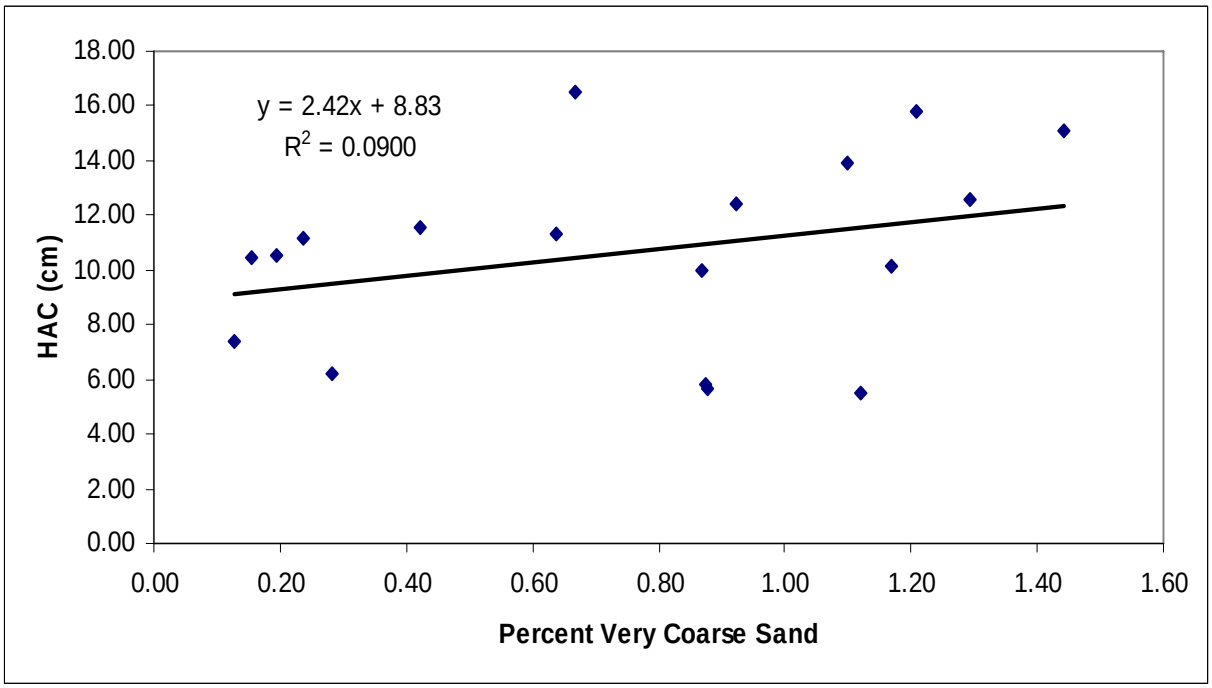

Figure D14. Scatter plot of percent very coarse sand with the height of anaerobic conditions (HAC)

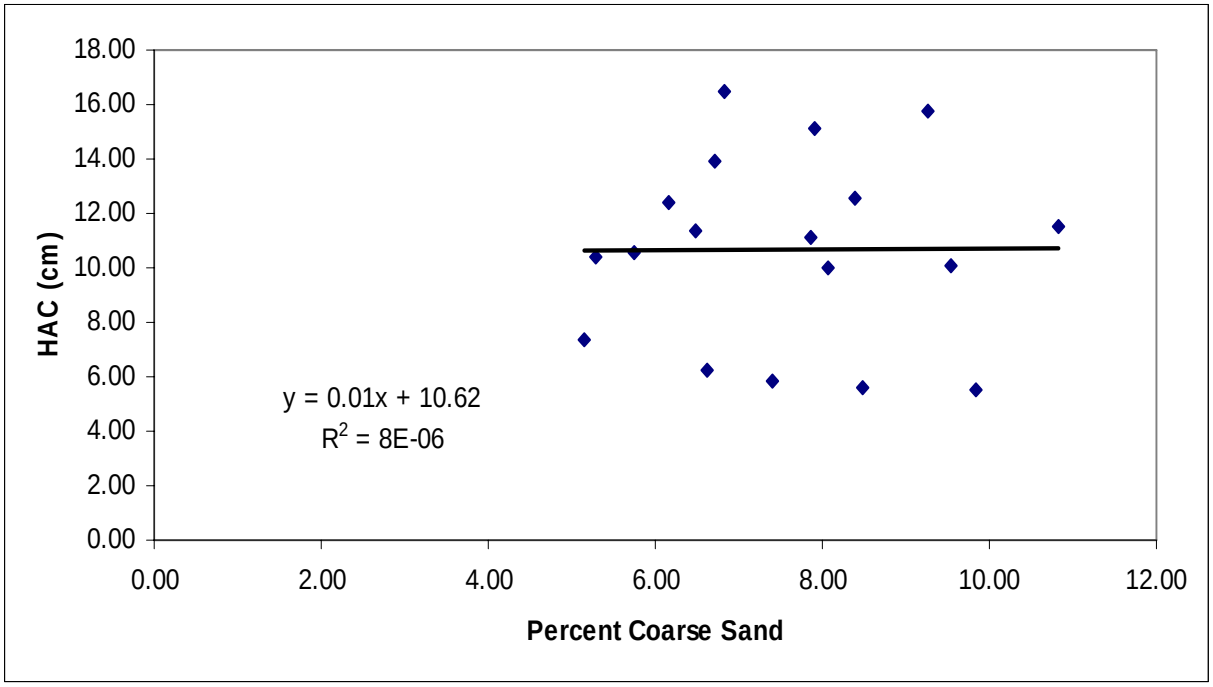

Figure D15. Scatter plot of percent coarse sand with the height of anaerobic conditions (HAC)

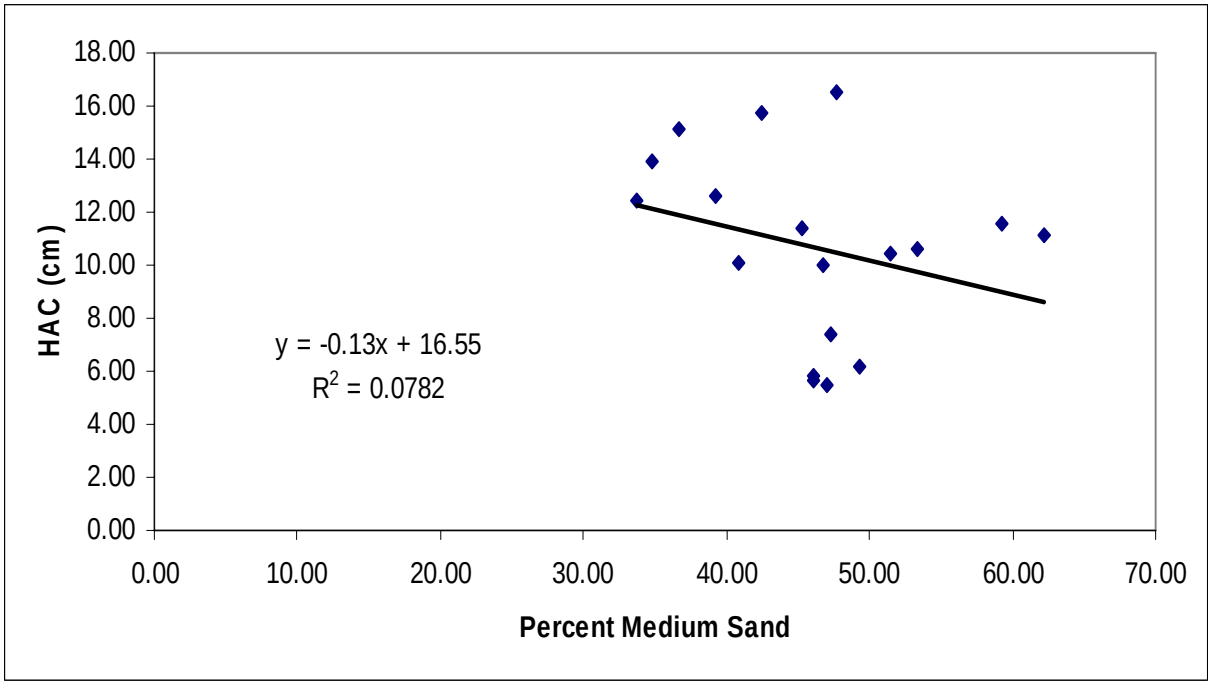

Figure D16. Scatter plot of percent medium sand with the height of anaerobic conditions (HAC)

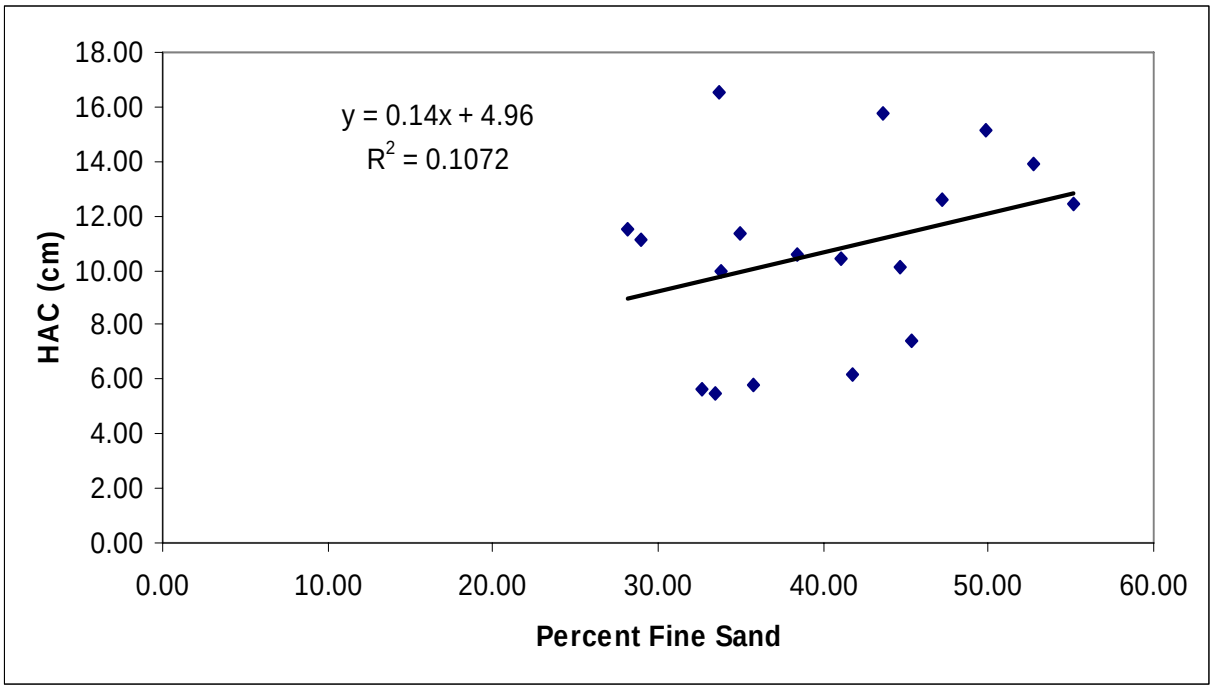

Figure D17. Scatter plot of percent fine sand with the height of anaerobic conditions (HAC)

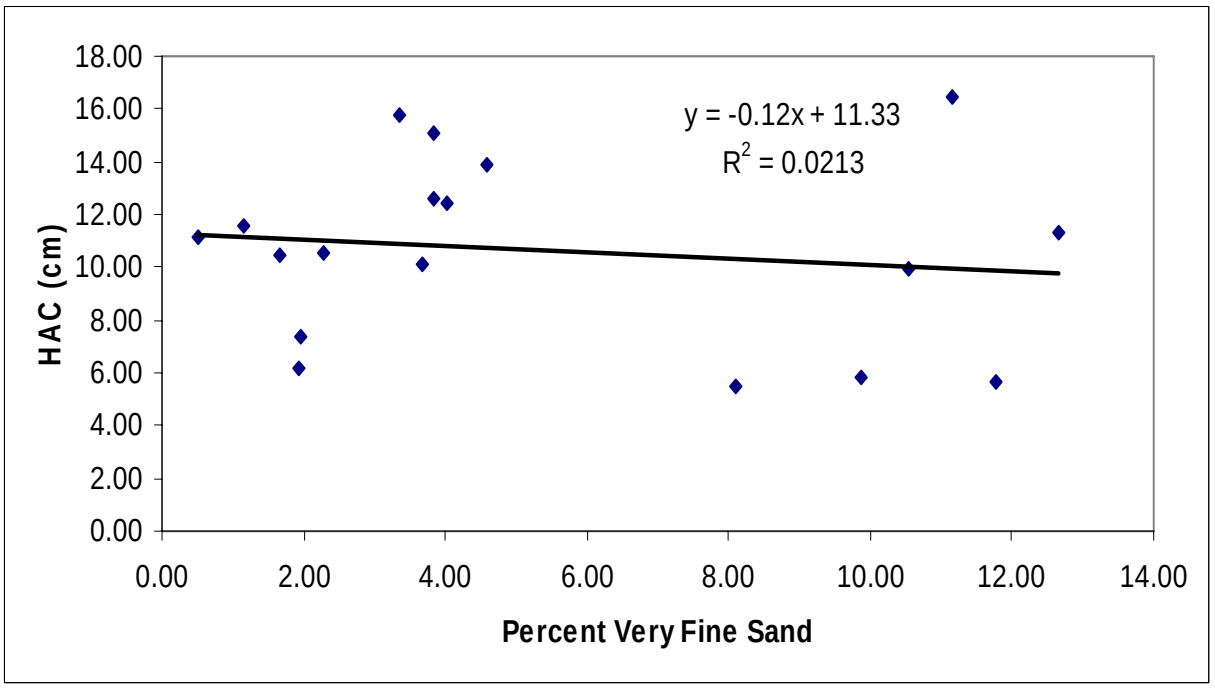

Figure D18. Scatter plot of percent very fine sand with the height of anaerobic conditions (HAC)

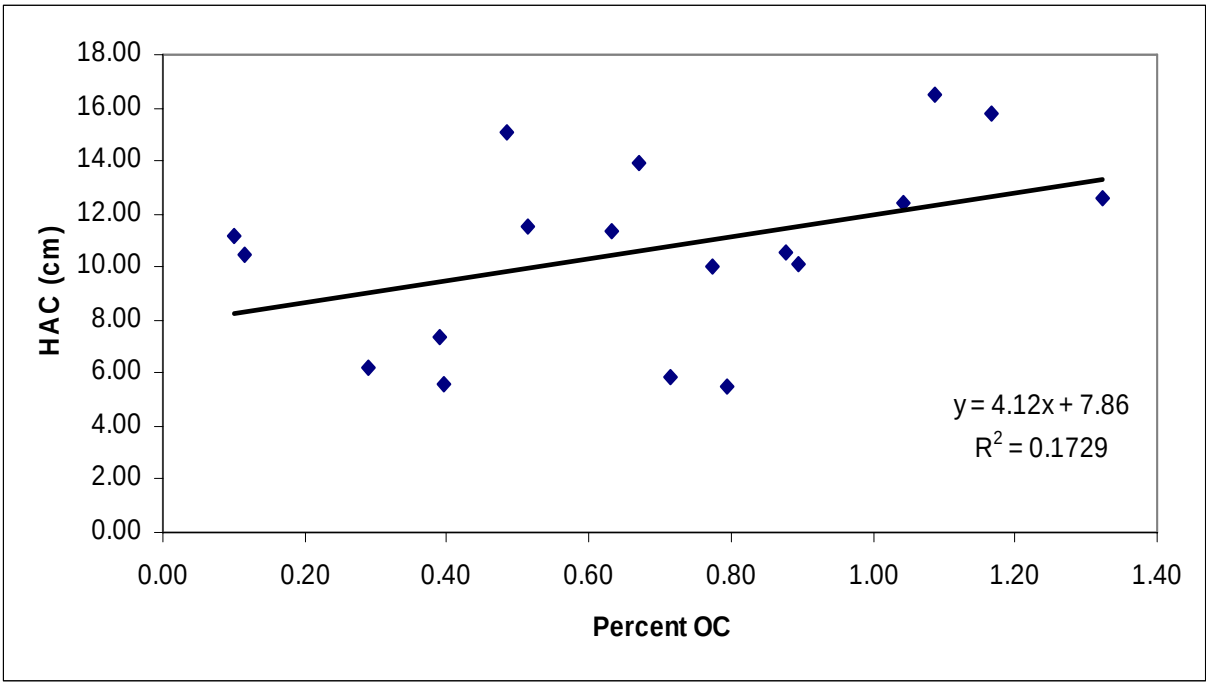

Figure D19. Scatter plot of percent organic carbon (OC) with the height of anaerobic conditions (HAC)

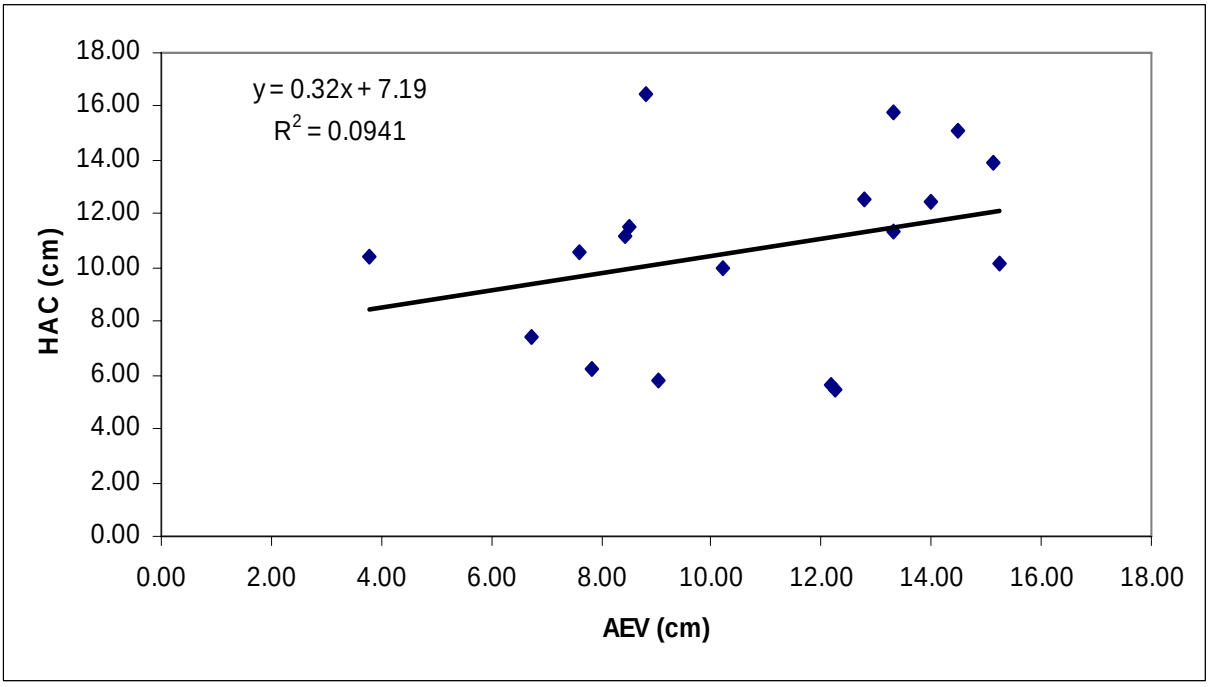

Figure D20. Scatter plot of the air entry values (AEV) with the height of anaerobic conditions (HAC)